JPRS L/8910

7 February 1980

USSR Report

METEOROLOGY AND HYDROLOGY

No. 12, December 1979

FBIS FOREIGN BROADCAST INFORMATION SERVICE

FOR OFFICIAL USE ONLY

APPROVED FOR RELEASE: 2007/02/08: CIA-RDP82-00850R000200050012-1

NOTE

JPRS publications contain information primarily from foreign newspapers, periodicals and books, but also from news agency transmissions and broadcasts. Materials from foreign-language sources are translated; those from English-language sources are transcribed or reprinted, with the original phrasing and other characteristics retained.

Headlines, editorial reports, and material enclosed in brackets [] are supplied by JPRS. Processing indicators such as [Text] or [Excerpt] in the first line of each item, or following the last line of a brief, indicate how the original information was processed. Where no processing indicator is given, the information was summarized or extracted.

Unfamiliar names rendered phonetically or transliterated are enclosed in parentheses. Words or names preceded by a question mark and enclosed in parentheses were not clear in the original but have been supplied as appropriate in context. Other unattributed parenthetical notes within the body of an item originate with the source. Times within items are as given by source.

The contents of this publication in no way represent the policies, views or attitudes of the U.S. Government.

For further information on report content call (703) 351-2938 (economic); 3468 (political, sociological, military); 2726 (life sciences); 2725 (physical sciences).

APPROVED FOR RELEASE: 2007/02/08: CIA-RDP82-00850R000200050012-1

JPRS L/8910

7 February 1980

USSR REPORT

METEOROLOGY AND HYDROLOGY

No 12, December 1979

Selected articles from the Russian-language journal METEOROLOGIYA I GIDROLOGIYA, Moscow.

CONTENTS PAGE

USSR Order of Lenin Hydrometeorological Scientific Research Center Marks its Fiftieth Anniversary
(M. A. Petrosyants)..... 1

Tropospheric Structure Under Tropical Cyclogenesis Conditions
(L. S. Minina and Ye. N. Arabey)..... 28

Peculiarities of Distribution of the Tropopause Over the Earth
(Z. M. Makhover)..... 42

Possibilities of Determining CO and N_2O Profiles from Measurements on Slant Paths in the Microwave Spectral Range
(Yu. M. Timofeyev and V. V. Rozanov)..... 51

Characteristics of Exceeding of a Stipulated Concentration Level in a Stationary Jet
(O. I. Vozzhennikov)..... 63

Vertical Profile of Parameters of Microstructure of Stratus Clouds
(E. L. Aleksandrov and K. B. Yudin)..... 72

Some Peculiarities of the Spatial and Temporal Distribution of Tritium in Precipitation Over the Territory of the USSR
(S. M. Vakulovskiy, et al.)..... 79

Parameterization of the Active Layer in a Model of Large-Scale Interaction Between the Ocean and the Atmosphere
(B. A. Kogan, et al.)..... 86

CONTENTS (Continued) Page

Computations of Runoff Rates and Travel Time of Water from Slopes in Determining Maximum Rain-Induced Discharges for Small Drainage Basins
(I. K. Sribnyy)..... 99

Theoretical Analysis of Dependence of the Soil Water Yield Coefficient on the Rate of Change in Ground Water Level
(I. L. Kalyuzhnyy and K. K. Pavlova).....109

Water Permeability of Frozen Unconsolidated Soils and Analysis of the Dynamics of its Change During the Period of Snow Melting and Thawing
(V. I. Shtykov)..... 119

Method of Moist Convective Adaptation
(A. P. Khain)..... 130

Comparison of Mean Conditional Entropies of Two Coherent Models of the "Atmosphere - Ocean" System
(V. A. Ryasin)..... 137

Meteorological Space Observation System in the United States..... 142

Sixtieth Birthday of Mikhail Aramaisovich Petrosyants..... 158

Sixtieth Birthday of Vasiliy Nikiforovich Babchenko..... 160

Conferences, Meetings and Seminars
(A. P. Zhilyayev, et al.)..... 162

Notes from Abroad
(B. I. Silkin)..... 166

Obituary of Vyacheslav Vyacheslavovich Bykov (1921-1979)..... 168

PUBLICATION DATA

English title	: METEOROLOGY AND HYDROLOGY
Russian title	: METEOROLOGIYA I GIDROLOGIYA
Author (s)	:
Editor (s)	: Ye. I. Tolstikov
Publishing House	: Gidrometeoizdat
Place of Publication	: Moscow
Date of Publication	: December 1979
Signed to press	: 23 Nov 79
Copies	: 3870
COPYRIGHT	: "Meteorologiya i gidrologiya", 1979

UDC 551.5:006.09

USSR ORDER OF LENIN HYDROMETEOROLOGICAL SCIENTIFIC RESEARCH CENTER MARKS ITS FIFTIETH ANNIVERSARY

Moscow METEOROLOGIYA I GIDROLOGIYA in Russian No 12, Dec 79 pp 5-21

[Article by Professor M. A. Petrosyants, Director of the USSR Hydrometeorological Center, submitted for publication 10 August 1979]

Abstract: The article briefly describes the history of development of the USSR Order of Lenin Hydrometeorological Scientific Research Center during the 50 years of its existence. [The article makes use of materials specially prepared by S. L. Belousov and Ye. G. Popov, to whom the author expresses sincere appreciation.]

[Text] The Order of Lenin Hydrometeorological Scientific Research Center traces its history from the USSR Central Weather Bureau (CWB), which in accordance with a decree of the Presidium of the Central Executive Committee dated 7 August 1929 entitled "Creation of a Unified Hydrometeorological Service" and a decree of the USSR Council of People's Commissars dated 28 August 1929 entitled "Organization of the USSR Hydrometeorological Committee," began its activity on 1 January 1930. The most important motivation for the creation of a central organ of the weather service was the decision of the Soviet Union to assume definite international obligations and to transmit meteorological summaries abroad. The first transmission of meteorological information from the CWB for international use on 1 January 1930 also became the official date of beginning of operation of this agency.

The creation of the CWB was dictated by the increasing needs for meteorological servicing of vigorously developing aviation, railroad, river and sea transport and other branches of the national economy and also the incipient exploitation of regions in the Far North of our contry. The USSR Central Weather Bureau was created on the basis of the Moscow Weather Bureau, existing since 1918, by its combining with the Weather Service Division of the Main Geophysical Observatory at Leningrad, which before this

had performed the functions of the main agency in the weather service. The CWB was headed by Ye. I. Tikhomirov and E. P. Puyshe, who was dispatched from Leningrad to Moscow.

It must be said that by 1930 the weather service in our country during the 58 years of its existence had accumulated much experience in operational activity. An event of the greatest importance for its strengthening was the signing of a decree of the Council of People's Commissars RSFSR dated 21 June 1921 by V. I. Lenin; it was entitled "On Organization of the RSFSR Meteorological Service." A direct consequence of the decree was the restoration and development of the information meteorological network of stations which already from the time of G. I. Vil'd had had excellent traditions in the carrying out of observations, and also activation of investigations initiated even prior to the Revolution by I. B. Shpindler, P. I. Brounov, B. I. Sreznevskiy, M. A. Rykachev, A. M. Shenrok, S. D. Griboyedov, B. P. Mul'tanovskiy, and others [105].

From the first days of its existence the CWB became the conveyor of new ideas and methods: a surface isobaric synoptic method was replaced by frontological analysis with its concepts concerning the structure of fronts, cyclones and anticyclones and the properties of air masses, with use of indirect aerology. The T. Bergeron courses organized on the initiative of the CWB in 1930 in Moscow and in 1932 in Moscow and Pyatigorsk, as well as the introduction of a new synoptic code (1929), exerted a decisive influence on the universal introduction of the progressive frontological analysis of atmospheric processes in the USSR. The success of the courses was facilitated by specialists at the CWB: A. I. Asknaziy, S. P. Khromov, V. A. Samoylova and a specialist at the Irkutsk Weather Bureau B. L. Dzerdzeyevskiy.

A. I. Asknaziy, S. P. Khromov and B. L. Dzerdzeyevskiy acted not only as interpreters, but also as commentators and conveyors of the new ideas and methods. This activity was completed with publication of the book by S. P. Khromov entitled VVEDENIYE V SINOPTICHESKIY ANALIZ (Introduction to Synoptic Analysis) (1934), undoubtedly constituting an epoch in formation of synoptic thought among weather service workers. The importance of frontological analysis was not only that it physically more correctly reflected the weather-forming processes transpiring in the atmosphere, but also that it forced the weatherman to think three-dimensionally. The very introduction of frontological analysis laid the way for the next very important stage in the activity of the CWB -- the introduction of pressure pattern charts into the operational service.

From the time of invention of the radiosonde by P. A. Molchanov less than seven years were required for creation of the first aerological network of stations. This enabled Kh. P. Pogosyan, N. L. Taborovskiy, N. V. Petrenko and others, beginning on 1 December 1937, to prepare, on a regular basis, maps of the absolute pressure pattern of the 700- and 500-mb surfaces

and a map of the relative topography 500 over 1000 mb, which immediately came into use for the servicing of aviation.

Parallel with the vigorous development of short-range forecasting work continued in the field of long-range weather forecasting, initiated even before the Revolution in Petrograd. The Long-Range Forecasting Section was also transferred from the Main Geophysical Observatory to the CWB; prior to the Great Fatherland War it remained territorially in Leningrad. Up to 1938 it was headed by V. P. Mul'tanovskiy, who drew a team of enthusiasts to work in this difficult field: E. S. Lir, G. Ya. Vangengeym, S. T. Pagava, L. A. Vitel's, T. A. Duletov, and others. By this time the techniques for a generalized representation of a sequence of synoptic processes in time had been developed and specialists had formulated the basic ideas concerning centers of action in the atmosphere, natural synoptic periods and seasons, their tendencies, and also concepts concerning the trajectories of movement (axes) of anticyclones as indices of transfer prevailing in the atmosphere, concepts to a certain degree anticipating the concepts of a steering current and blocking anticyclones [35, 71]. Proceeding on the basis of these ideas, B. P. Mul'tanovskiy in 1922, working at Leningrad, began the regular issuance of long-range forecasts, which with the organization of the CWB continued in Moscow.

The position of the Central Weather Bureau as the operational prognostic center obligated it to service the directing national economic agencies not only with meteorological, but also with hydrological and agrometeorological information and forecasts. Accordingly, already in 1930 a section on hydrological information and forecasts was organized in the CWB under the direction of V. L. Nikitin, where such now well-known hydrologists as B. A Apollov, V. D. Komarov, O. T. Mashkevich and V. A. Troitskiy began to work.

The research work of the section on hydrological information and forecasts of the CWB was directed to the development of a method of pertinent levels in short-range forecasts and the use of correlation analysis for determining the dependences between the elements of the hydrological regime and the factors governing them. Among the studies of that time we should mention the PRAKTICHESKOYE RUKOVODSTVO DLYA PROIZVODSTVA GIDROLOGICHESKIKH PROGNOZOV (Practical Manual for Making Hydrological Forecasts) by O. T. Mashkevich (1933), the studies of V. D. Komarov (1936-1939) on investigation of the runoff of rivers of the Oka basin, which served as the beginning for the water balance approach to evaluation of losses of meltwater runoff and prediction of the volume of high waters on the basis of data from snow measuring surveys, and also the studies of B. A. Apollov on the development of methods for the prediction of different elements of the water regime of rivers and a generalization of world experience in the field of hydrological forecasts.

Soon after the organization of the CWB, the "harvest service" was transferred to it from the People's Commissariat of Agriculture RSFSR; this was a service for supplying agricultural organizations with agrometeorological information. The practical work of servicing of developing agriculture in our country required not only current weather conditions information, but also the preparation of agrometeorological forecasts. The first such forecasts, a forecast of the wintering of winter crops, was prepared by G. Z. Ventskevich in 1932, and in 1933 A. A. Shigolev gave a forecast of the times of maturing winter rye in the European territory of the USSR.

If we were to characterize the period from 1930 to 1941 as a whole, it could be said that for the CWB it was a period of development of the techniques and procedures for synoptic analysis, the establishment of methods for hydrometeorological forecasts, in short, a period of organization of a forecasting service in our country.

At the same time, at the Main Geophysical Observatory work continued in the field of theoretical meteorology, so brilliantly initiated by A. A. Fridman. Here a group of talented scientists was formed: L. V. Keller, N. Ye. Kochin, I. A. Kibel', B. I. Izvekov, Ye. N. Blinova, A. A. Dorodnitsyn and M. I. Yudin. Their outstanding investigations constituted the theoretical foundation for subsequent successes in weather forecasting. It is particularly necessary to note the studies of N. Ye. Kochin on general circulation of the atmosphere, important for the subsequent creation of a theory of long-range hydrodynamic weather forecasting by Ye. N. Blinova, and the work of I. A. Kibel' entitled PRILOZHENIYE K METEOROLOGII URAVNENIY MEKHANIKI BAROKLINNOY ZHIDKOSTI (Application of the Mechanics of a Baroclinic Fluid to Meteorology), opening the way to the development of numerical methods for short-range weather forecasting.

During the years of the Great Fatherland War all the activity of the Central Weather Institute, and after 1943 the Central Institute of Forecasts, was subordinated to the tasks of meteorological and hydrological support of military operations of the Red Army. This was a period of exceptionally intense work, when under conditions of limited information it was necessary to solve highly important problems in the description and prediction of meteorological and hydrological conditions. For example, N. A. Aristov headed the Central Institute of Forecasts affiliate on the long-range aviation staff; Ye. I. Gogolev and A. D. Gorshkova carried out meteorological servicing of the Main Administration of the Civil Air Fleet; S. M. Prostyakov at Reykjavik prepared weather forecasts for aircraft ferried from Newfoundland and Murmansk; V. R. Dubentsov and I. G. Pchelko headed work on the preparation of forecasts at the institute itself. S. T. Pagava and his section prepared seasonal and monthly weather forecasts for the theater of military operations. A group of hydrologists under the general direction of G. R. Bregman carried out the hydrological support of operations planned by the High Command and the General Staff of the Soviet Army.

But even in the severe war years the research did not cease: in 1943 Ye. N. Blinova published the work GIDRODINAMICHESKAYA TEORIYA VOLN DAVLENIYA, TEMPERATURNYKH VOLN I TSENTROV DEYSTVIYA ATMOSFERY (Hydrodynamic Theory of Pressure Waves, Temperature Waves and Centers of Action in the Atmosphere), from which under her direction began the creation of a method for the hydrodynamic long-range forecasting of weather. Through the efforts of Ye. N. Blinova, N. A. Bagrov, S. A. Mashkovich, A. S. Monin, G. I. Morskiy, Ya. M. Kheyfets and others, already in 1947-1949 it was possible to prepare the first long-range forecasts by means of solution of a linearized system of equations in hydrodynamics in a quasisolenoidal approximation. Later, but more than 35 years under the direction of Ye. N. Blinova, work is continuing on the development of long-range hydrodynamic forecasting of the mean monthly air temperature and some other elements. Now such forecasts are being prepared routinely 40 days before they are to go into effect and are used as mandatory consultation material in the formulation of the official monthly forecast of the USSR Hydrometeorological Center [12-16].

After the victory over Hitler's Fascism in the Great Fatherland War a restructuring of CWB activity began in accordance with the requirements of the national economy, which was being restored. The section of agrometeorological forecasts was returned to the institute from the People's Commissariat of Agriculture; a section on aviation meteorology was organized under the direction of I. G. Pchelko; work was expanded on the development of methods for hydrological and marine hydrological forecasts.

In the field of short-range weather forecasts, there was, on the one hand, active use of new aerological data, in essence, the creation of truly three-dimensional synoptic forecasting, and on the other hand, unusually intensive development of the theory of hydrodynamic short-range weather forecasting. Work along these lines was headed by an outstanding scientist, Corresponding Member USSR Academy of Sciences I. A. Kibel', who began his activity in the Central Institute of Forecasts in 1943 as the director of the section on dynamic meteorology. Very rapidly a group of talented young people was formed in the section; these included N. N. Buleyev, S. L. Belousov, P. N. Belov, V. V. Bykov, Ye. M. Dobryshman, G. I. Marchuk, S. A. Mashkovich, A. S. Monin, Sh. A. Musayelyan, A. M. Mkhitaryan, V. P. Sadokov, A. S. Sarkisyan, and others. The fact of existence of a small parameter in the equations of atmospheric dynamics, mentioned by I. A. Kibel', enabled him to create the first method for numerical short-range forecasting of pressure and temperature [48]. The testing of this method gave encouraging results and work on its improvement was continued by I. A. Kibel', B. D. Uspenskiy, N. I. Buleyev and others [52]. At the same time, V. A. Bugayev, Kh. P. Pogosyan and N. L. Taborovskiy gave an interpretation of the prognostic formulas and developed qualitative rules for the change in pressure which were used by weathermen for judging the future development of the process [17, 86, 96]. Somewhat later N. I. Buleyev created a simple graphic method for constructing a future map of altitudes of the "mean" level of the troposphere (700 or 500 mb).

At the beginning of the 1950's N. I. Buleyev and G. I. Marchuk took a new and extremely important step in formulating a theory of hydrodynamic short-range forecasting -- they examined a three-dimensional baroclinic model of the atmosphere and gave a solution for the time derivative of geopotential in general form with use of Green's functions [22]. This solution served as a basis for formulating operational forecasting schemes, when with the appearance of electronic computers a new stage began -- the stage of practical use of numerical forecasts of future fields of geopotential and other meteorological elements.

In 1954 S. L. Belousov [9] used an electronic computer for realizing the first barotropic model; then in 1955 S. A. Mashkovich [64] made use of a baroclinic two-level model; and in 1958 P. K. Dushkin and Ye. G. Lomonosov created a three-level model [34]. Numerical forecasts of pressure pattern charts using this model were better than the charts prepared by the synoptic method. This immediately shifted the computations on electronic computers which were made on the machines of other organizations since 1953 from the field of promising experiments into the field of direct operational use. Already by 1961 the director of the Joint Meteorological Computation Center of the Main Administration of the Hydrometeorological Service and the USSR Academy of Sciences (later the World Meteorological Center) P. K. Yevseyev, devoting great forces and energies to outfitting the center with electronic computers, succeeded in having a first-generation electronic computer (the M-20) come into use for the routine computation of forecasts and in 1963 the first technological system for routine numerical forecasting was created. It provided for the use in forecasting of filtered models for a restricted region, and then for the entire northern hemisphere. An objective analysis scheme was formulated on the basis of the optimum interpolation method developed by L. S. Gandin [10] in order to obtain the initial geopotential fields. Later equipment for automated primary processing of initial data and means for the automatic representation of computed prognostic charts were created and included in the work. The created technological system ensured the issuance of forecasts for a limited region (Europe and Western Siberia) for a time up to 36 hours for the geopotential fields at different levels on the basis of the spatial quasigeostrophic model developed by N. I. Buleyev and G. I. Marchuk [22] and forecasts of a number of other parameters (vertical velocities, trajectories of air particles, etc.). The introduction of this system made possible a complete abolition of compilation of prognostic high-level charts by the synoptic method.

Simultaneously with the creation of numerical forecasting methods, which initially had the purpose primarily of prediction of pressure (geopotential), vertical currents and the trajectory of air particles, there was intensive development of methods for computing weather elements: temperature (Ye. M. Orlova, D. A. Ped'), wind (D. A. Chistyakov, N. V. Petrenko), cloud cover (K. G. Abramovich, T. P. Popova, L. S. Minina), precipitation (A. F. Dyubyuk, N. I. Buleyev, N. L. Lebedeva, A. A. Bachurina, B. D. Uspenskiy, Ye. M. Orlova, B. Ye. Peskov), fog and visibility (N. N.

Petrenko), aircraft turbulence (I. G. Pchelko).

This intensive work, undertaken on the initiative and under the direction of the director of the Central Institute of Forecasts Academician Uzbek Academy of Sciences V. A. Bugayev, was completed by the publication in 1964-1965 of the RUKOVODSTVO PO KRATKOSROCHNYM PROGNOZAM POGODY (Manual on Short-Range Weather Forecasting) (Parts I and II), which constitutes the basic instructions for working weathermen even at the present time.

The introduction of pressure pattern charts into weather service practice did not leave long-range weather forecasting to one side. A radical reconsideration of the experience accumulated in the field of long-range forecasting was begun under the direction of S. T. Pagava; this was true of both methods for short-range forecasts for relatively short times in advance (S. T. Pagava, Yu. B. Khrabrov, D. A. Ped', A. L. Kats), and with respect to weather forecasts for a month and a season (S. T. Pagava, L. I. Blyumina, Ye. I. Borisova, O. N. Khazova, V. G. Shishkov -- the rhythm of atmospheric processes and N. A. Bagrov, K. A. Vasyukov, N. I. Zverev, D. A. Ped', S. A. Mashkovich, Kh. Kh. Rafailova, Yu. B. Khrabrov, D. A. Drogaytsev -- similarity of atmospheric processes). In particular, we should note the activity of N. A. Bagrov, who made a major contribution to objectivization of the classification of atmospheric processes and evaluation of forecasts [6-8, 26, 32, 37, 38, 46, 78, 79, 81].

The ever-increasing practical requirements in the servicing of planned agriculture led to the rapid development of the agrometeorological service in the country and agrometeorological investigations in the institute. Methods for agrometeorological observations were created (I. M. Petunin, V. V. Sinel'shchikov, M. S. Kulik, A. A. Okushko, V. A. Moiseychik). Also developed were quantitative methods for evaluating the state and onset of phases of development of different agricultural crops (A. A. Shigolev, A. V. Protserov, Yu. I. Chirkov, T. A. Pobetova, N. Z. Ivanova-Zubkova, M. S. Kulik, Ye. S. Ulanova, and others), methods for computing the moisture reserves under agricultural crops and the anticipated moisture supply (S. A. Verigo, L. A. Razumova, M. S. Kulik, A. V. Protserov, B. N. Ponomarev, N. A. Zubarev, A. S. Kontorshchikov), methods for long-range forecasting of areas of death of winter crops during wintering (I. M. Petunin, V. A. Moiseychik), and finally, and most importantly, methods for the long-range forecasting of the yield of agricultural crops (M. S. Kulik, Ye. S. Ulanova, A. V. Protserov, K. V. Kirilicheva, B. N. Ponomarev, Yu. I. Chirkov, Yu. S. Mel'nik, and others) [28, 29, 55, 56, 70, 100, 101].

Agrometeorological investigations also continued to be developed later, although with the transfer of some of the specialists of the Central Institute of Forecasts to the Institute of Experimental Meteorology (Obninsk) in 1964 it became more difficult to combine operational and research work.

The first post-war decade was characterized by the intensive development of hydrological investigations, which were dictated by the necessity to solve the problems, which had become the order of the day, of long-range

forecasts of the runcff of lowland and mountain rivers, forecasts of the maximum discharges and levels of spring high water and rain-induced high waters, predictions of the levels of navigable rivers, long- and short-range ice forecasts.

During this period specialists developed the theoretical principles for computing absorption and retention of water and surface runoff for lowland river basins and created a physical-statistical method for the long-range forecasting of spring runoff (Ye. G. Popov, V. D. Komarov, V. N. Parshin, M. S. Salov, Ye. S. Zmiyeva, T. I. Velikanova, and others). On the basis of a model of a river basin as a system with a nonuniform distribution of surface capacity and a variable infiltration capacity of the soils it was possible to derive equations for integral runoff and water release of a basin for capacitive and infiltration-capacitive types of water absorption, expressing the general form of water balance dependences for long-range forecasts of the runoff of high water (Ye. G. Popov) [87]. The introduction of nonuniformity of falling and melting of the snow cover and the depth of soil freezing into theory and practical computations of meltwater runoff was of fundamental importance (V. D. Komarov) [53].

A method was created for predicting discharge and the levels of high water and rain-induced high waters along the watershed into the channel network and the water reserves in the channel network, computed on the basis of hydrometric data (G. P. Kalinin); it was applied and developed applicable to different rivers (V. I. Sapozhnikov, A. I. Afanas'yev and others); the principles were laid for a method for predicting the seasonal runoff of the mountain rivers of Central Asia, Siberia and the Caucasus (T. S. Abal'yan, A. N. Vazhnov, N. G. Dmitriyeva, V. N. Parshin, A. A. Kharshan and others); a study was made of the ice regime of rivers and methods were developed for ice forecasts for different times in advance (V. V. Piotrovich, L. G. Shulyakovskiy, S. N. Bulatov, B. M. Ginzburg, Ye. I. Savchenkova and others).

During the subsequent years the development and improvement of practical methods for long-range forecasts of runoff of lowland and mountain rivers, in particular, the inflow of water into the reservoirs of large hydroelectric power stations, for different times in advance occupied an important place in investigations of hydrological forecasts (V. N. Parshin, Ye. S. Zmiyeva, T. S. Abal'yan, V. I. Sapozhnikov, Yu. V. Gorbunov and others). A method for short-range forecasts of the appearance of ice on rivers and reservoirs was developed and widely introduced into practice (L. G. Shulyakovskiy).

In the field of short-range forecasting of the discharges and levels of water great attention was devoted to the development of approximate methods for computing the unsteady motion of water in channels (G. P. Kalinin, P. I. Milyukov, A. P. Zhidikov) and numerical methods for its computation on the basis of the equations of hydrodynamics applicable to individual

reaches of rivers (L. S. Kuchment, V. I. Koren') and reservoirs (Ye. P. Chemerenko) [30].

The results attained to the late 1950's in the field of creation of methods for hydrological forecasts were generalized in the four-volume publication RUKOVODSTVO PO GIDROLOGICHESKIM PROGNOZAM (Manual on Hydrological Forecasts) (1963, 1964).

Immediately after ending of the Great Fatherland War, at the Central Institute of Forecasts there was activation of work on methods for marine hydrological forecasts. This was facilitated to a considerable degree by the experience accumulated during hydrometeorological support of operations of the Navy in different theaters of military operations. Methods were developed for long-range forecasts of ice phases in the nonarctic seas washing the shores of the USSR, forecasts of the ice coverage of seas, short-range ice forecasts, computation of water temperature and position of the ice edge in the open sea, long-range forecasts of water temperature and mean monthly levels, short-range forecasts of levels and currents, mean annual levels of the Caspian Sea (N. A. Belinskiy, G. P. Kalinin, A. I. Karakash, G. S. Ivanov, Ye. M. Sauskan, M. G. Glagoleva, S. I. Kan, Ya. A. Tyutnev, and others [24, 43, 44].

Late in 1965 the Central Institute of Forecasts and the World Meteorological Center were joined together and the USSR Hydrometeorological Scientific Research Center was created on their basis. V. A. Bugayev, Academician Uzbek Academy of Sciences, a leading scientist and outstanding organizer of Soviet hydrometeorological science, was designated director of the USSR Hydrometeorological Center. Many initiatives leading to the restructuring of all scientific and operational activity of the weather services are associated with the name of V. A. Bugayev. Together with the American scientist G. Wexler, V. A. Bugayev was the creator of the plan for the World Weather Watch (WWW). The successive implementation of this plan led to a modern, international, well-organized operational prognostic system with a clear distribution of functions between world, regional and national meteorological centers both in the field of processing of meteorological information and the output of prognostic products, but also in the field of practical servicing of the user with weather forecasts [19, 20, 84].

V. A. Bugayev was an initiator of application of space information in meteorology. Inspired by his enthusiasm, specialists at the USSR Hydrometeorological Center I. P. Vetlov, N. F. Vel'tishchev, L. S. Minina, T. P. Popova, G. N. Isayeva and others carried out methodological, technical and scientific direction of the introduction of satellite information into the practical work of the weather service. K. P. Vasil'yev -- into the practical work of servicing of navigation, and P. N. Belov, A. I. Burtsev, G. I. Morskoy and Sh. A. Musayelyan -- into numerical weather analysis and forecasting [40, 68, 72].

During 1968-1972 the second-generation electronic computers M-220, M-222 and "Vesna" were installed at the USSR Hydrometeorological Center. This made it possible, in addition to numerical forecasts of pressure pattern charts and within the framework of this same system for the processing of information, to introduce hydrodynamic forecasts of continuous precipitation, extremal temperatures and convective phenomena into actual practice, as well as forecasts of the surface pressure fields, on the basis of a synoptic-hydrodynamic scheme, taking into account data on surface pressure tendencies and using hydrodynamic forecasting of AT_{500} charts [4, 67]. A technology was also developed for obtaining forecasts of waves on the basis of numerical hemispheric forecasts of surface pressure fields for a time up to five days using a quasisolenoidal model.

With this the possibilities of the quasigeostrophic and quasisolenoidal prognostic models were exhausted. Their principal shortcoming is the impossibility of predicting rapid restructurings of the pressure field and other transformations associated with considerable deviations of the wind from geostrophic.

With the setting aside of the restrictions of the geostrophic approximation a new stage began in the field of numerical weather forecasts with a changeover to the use of a "full" system of equations [49, 51, 62]. The first prognostic models for a restricted region on the basis of full equations were introduced into practice at the Hydrometeorological Center in 1965. However, as a result of the incompleteness of the initial data employed (lack of initial wind fields), inadequate resolution and due to other limitations during this period the new models did not make it possible to obtain significant refinements in the forecasts for 24-36 hours in comparison with the filtered models. Their known advantage was manifested only in a forecast of the surface chart. Later, also on the basis of the full equations, hemispheric multilevel prognostic schemes were formulated and introduced (1971-1972). Despite the enumerated restrictions, forecasts made using these models found everyday practical application: they were used as consultative material in the preparation of weather forecasts for 3-5 days in advance at the USSR Hydrometeorological Center [23, 27, 41, 49, 50, 88].

The creation of a new system for the processing of meteorological information at the USSR Hydrometeorological Center began with the acquisition of a BESM-6 electronic computer in 1975. Specialists organized support for this computer, supplying it with higher-quality initial information accumulated using "Minsk-32" computers specially designed for these purposes. The means for checking and objective analysis of meteorological information on the BESM-6 were also improved. All this made it possible to introduce into practice the operational calculation of forecasts for a hemisphere using a model based on the full equations of hydrodynamics and generalizing the experience of operational use of the schemes employed earlier. In order to improve information support there was organized preparation of

additional initial data for operational forecasts (in addition to automatically processable observational data). These data are prepared by weathermen for regions with limited observational data on the basis of all available information and professional experience. The data are fed to the electronic computer in the form of "communications" from some fictitious stations. All this determined the advantage of hemispherical forecasts using the new model in comparison with forecasts made using former models (Tables 1, 2) [5, 11, 45, 103].

Together with the development and improvement of prognostic models and methods for objective analysis provision was also made for an increase in the output of prognostic materials for direct use in practical work. Already in the 1960's hemispherical forecasts of surface pressure were used for computing the height and direction of waves in the ocean, serving as a basis for issuance of recommended courses for ship navigation. Later these methods were introduced into the practical work of a number of other centers in charge of meteorological support of merchant marine operations. The last few years, using numerical forecasting of the geopotential and wind fields, for use in civil aviation computations are made of the position of zones of moderate and strong turbulence at the altitude of aircraft flight and computations are made of flight plans along the principal long-distance air routes (about 40 air routes) [21]. The results of these computations in the form of maps and tables in logs with flight plans respectively are sent directly from the Hydrometeorological Center to the subdivisions providing operational meteorological support for aviation. The savings from the introduction of the automated system of navigation computations is several hundred thousand rubles per year.

At the present time at the USSR Hydrometeorological Center provision is made for issuance of the following prognostic materials for use in synoptic practice:
-- Under the program of the World Meteorological Center -- predictions for the northern hemisphere region: predictions of surface pressure and altitudes of different isobaric surfaces (to 100 mb) for from 24 to 84 hours in advance. Nineteen prognostic charts are issued daily: these charts are ready within 9 hours after the time of observations.
-- Under the program of the Regional Meteorological Center -- regional forecasts of the surface pressure fields and the altitudes of six isobaric surfaces (to 200 mb) for from 18 to 72 hours in advance; forecasts of vertical currents, quantity of precipitation and trajectories of air particles, a total of about 50 charts. These materials are ready for use at the Hydrometeorological Center and for facsimile transmission within the limits from 5 to 6 hours after the time of observations.

The numerical forecasts of the pressure (geopotential) field which have now been developed for the time being have not replaced synoptic meteorology -- the formulation of a weather forecast remains and will probably long remain its responsibility. However, numerical forecasts have exerted the

most direct influence not only on increasing the probable success of weather forecasts, but also on the nature of research, whose center of gravity has recently been shifted from a search for rules for predicting the future development of the process (which is now given by numerical forecasts) to the development of objective methods for forecasting (computing) weather phenomena, especially when they attain a dangerous or particularly dangerous intensity.

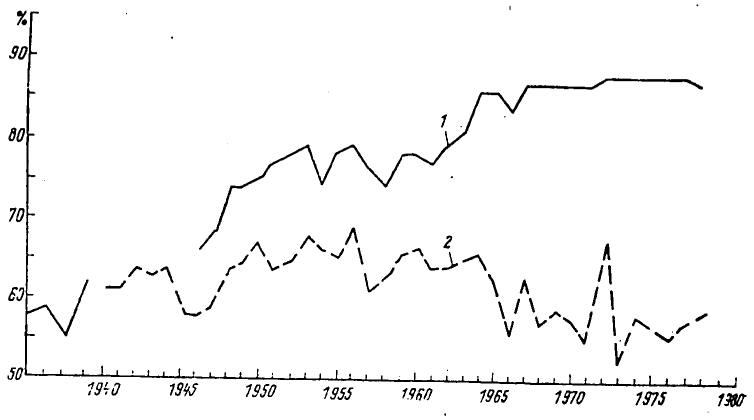

Fig. 1. Probable success (%) of short-range weather forecasts for Moscow. 1) forecasts by the USSR Hydrometeorological Center, 2) inertial forecasts.

In this connection during recent years at the Hydrometeorological Center much attention has been devoted to methods for predicting storm winds, intensive convective phenomena (showers, thunderstorms, squalls), glaze, low clouds and fogs, precipitation, etc. [18, 97, 102]. The results of the combined efforts of hydrodynamicists and forecasters can be seen in the example of the increase in the probable success of weather forecasts for Moscow (Fig. 1).

Progress in numerical methods has also led to a substantial improvement in short-range weather forecasting. The synoptic-statistical method for predicting five- and ten-day temperature and its anomaly, developed by A. L. Kats and his associates and introduced into practical work in 1965, was considerably improved by the use of numerical forecasting of AT_{500} for 72 hours as the basic predictor [25, 47]. The so-called synoptic-hydrodynamic-statistical method for predicting the mean five-day temperature, five-day temperature anomaly and five-day quantity of precipitation, and also the mean ten-day temperature and its anomaly was introduced in 1973. Since that time in the supplement to the YEZHEDNEVNYY GIDROMETEOROLOGICHESKIY BYULLETEN' GIDROMETTSENTRA SSSR (Daily Hydrometeorological Bulletin of the USSR Hydrometeorological Center), which has been published since 1 May

1936, appendices to the bulletin containing the above-mentioned forecasts are published on Mondays, Wednesdays and Fridays.

Table 1

Relative Errors in Operational Forecasts Prepared at the Hydrometeorological Center Using a Regional Quasigeostrophic Model and a Hemispherical Model on the Basis of Full Equations in 1976-1977 (Comparison for Region of the Regional Model)

Прогностическая модель 1	24 ч 2		48 ч		72 ч	
	земля 3	500 мб 4	земля	500 мб	земля	500 мб
5 Региональная квазигеострофическая модель	—	0,70	—	0,76	—	0,88
6 Полушарная модель с полными уравнениями	0,71	0,66	0,81	0,76	0,88	0,82

KEY:

1. Prognostic model
2. hours
3. earth's surface
4. mb
5. Regional quasigeostrophic model
6. Hemispherical model with full equations

During recent years the greatest attention has been devoted to the problem of long-range weather forecasting, the most necessary for the national economy, but the problem which is most difficult to solve, that is, weather forecasting for a month or season in advance. Research is being conducted in different directions. In particular, improvements are being made in the official B. P. Mul'tanovskiy-S. T. Pagava monthly forecasting method, especially with respect to the means employed for automating the selection of analogue-years in the objectivization of the basic points in the method (rhythmic activity, similarity evaluation [2, 8, 39, 80, 82, 83].

The experience accumulated in preparing monthly weather forecasts, both at the USSR Hydrometeorological Center and in other agencies of the weather service, in 1972 was generalized in the RUKOVODSTVO PO MESYACHNYM PROGNOZAM POGODY (Manual on Monthly Weather Forecasts), which is now in use. In addition to the deterministic approach to the description of atmospheric processes, statistical methods are also being employed at the USSR Hydrometeorological Center [94, 95]. The pioneer in the application of these methods in our institute was N. A. Bagrov, who was the first to introduce into meteorological research representations of meteorological fields in the form of

expansion in natural orthogonal components. This method then found extensive application in the development of physical-statistical methods for forecasting the most diversified of meteorological and hydrological parameters [1, 6, 31].

Table 2

Indices of Success of Numerical Operational Forecasts of the Pressure Field Prepared at the Hydrometeorological Center (on 1 June 1979) (According to A. I. Ugryumov)

Прогностическая модель 1	Уровень 2	Срок прогноза, ч 3	4 Показатели успешности ε	r	δ	S_1'
5 Региональные прогнозы						
7 Синоптико-гидродинамическая	земля ground	24	0,70	0,73	3,34	50
		36	0,83	0,60	3,82	62
8 Квазигеострофическая	500 *мб* mb	24	0,67	0,62	3,58	45
		36	0,68	0,62	4,95	52
6 Полушарные прогнозы						
9 Полусферная модель Гидрометцентра	земля	24	0,79	0,64	3,75	55
		48	0,90	0,53	5,81	74
		72	0,95	0,48	7,01	85
	500 *мб*	24	0,75	0,70	3,72	41
		48	0,83	0,61	6,15	57
		72	0,93	0,51	8,08	70

KEY:
1. Prognostic model
2. Level
3. Forecast period
4. Success index
5. Regional forecasts
6. Hemispherical forecasts
7. Synoptic-hydrodynamic
8. Quasigeostrophic
9. Hemispherical model (Hydrometeorological Center)

Note. ε is the relative forecasting error; r is the correlation coefficient between the actual and predicted changes; δ is the absolute forecasting error (mb or dam); S_1 is the index of success in forecasting field gradients (in an ideal forecast $S'_1 = 0$).

In the investigations of recent years a significant place is occupied by numerical modeling of general circulation of the atmosphere: I. V. Trosnikov created a finite-difference and S. A. Mashkovich and I. G. Veyl' created two variants of a spectral model of global circulation which are intended for numerical experiments on general circulation of the atmosphere and for forecasting for periods up to 7-10 days in advance [65, 66, 98, 99].

Table 3

Sample Volume of Hydrometeorological Information Emanating from the USSR Hydrometeorological Center in Course of Year

	Виды информации 1	Количество в год 2	Тираж 3	Всего экз. 4
9	Специальные справки и доклады в руководящие органы	165	30	4950
	5 Метеорологическая информация			
10	Ежедневный гидрометеорологический бюллетень	254	750	190500
11	Прогноз погоды на 5 дней	150	750	110000
12	То же на 10 дней	70	750	525000
13	» на месяц	12	1750	21000
14	» на сезон	6	50	300
15	Предупреждения об особо опасных явлениях	108		
	6 Агрометеорологическая информация			
16	Агрометпрогнозы	36	50	1800
17	Бюллетени	62	300	18600
18	Особенности недели	32	92	2944
	7 Гидрологическая информация			
19	Гидрологические бюллетени	45	340	15300
20	Морские бюллетени	9	370	3330
	8 Радио, телевидение, печать			
21	Радио (5 программ)			
22	дикторское чтение	19000		
23	выступления специалистов	624		
24	Телевидение (6 программ)			
22	дикторское чтение	3960		
23	выступления специалистов	600		
25	Газеты			
26	12 центральных и городских	365		
27	2 еженедельника	52		

Карты погоды регулярно публикуются в газетах «Известия», «Неделя», «Ленинское знамя».

KEY:

1. Type of information
2. Number per year
3. Copies, each
4. Total copies
5. Meteorological information
6. Agrometeorological information
7. Hydrological information
8. Radio, television, press
9. Special summaries and reports to key agencies
10. Daily hydrometeorological bulletin
11. Weather forecast for 5 days
12. Same, for 10 days
13. Same, for month
14. Same, for season
15. Warnings of especially dangerous phenomena
16. Agrometeorological forecasts
17. Bulletins
18. Special weekly events
19. Hydrological bulletins
20. Marine bulletins

KEY TO TABLE 3 (continued)

21. Radio (5 programs)
22. Announcer's reading
23. Presentation by specialists
24. Television (6 programs)
25. Newspapers
26. 12 central and city
27. 2 weeklies

The weather maps are regularly published in the newspapers IZVESTIYA, NEDELYA and LENINSKOYE ZNAMYA.

During the last few years, under the direction of Sh. A. Musayelyan and V. P. Sadokov, work has begun on the practical implementation of the new idea, formulated by Academician G. I. Marchuk, of developing a long-range forecasting method based on integration of the conjugate equations of atmospheric dynamics. Closely related to these studies are investigations of long-range asynchronous physical relationships between processes of a planetary scale in the atmosphere and in the oceans in regions considerably spaced in distance [63, 73, 74, 91, 92].

Equally important are studies having the purpose of improving the official method for seasonal weather forecasting created by S. T. Pagava and its extension to the entire territory of the USSR [3, 33, 93]. It must be noted that ten years of experience in the preparation of seasonal forecasts by the official method, based on the concepts of a natural synoptic season and disruptions-precursors, demonstrated that for the European USSR these forecasts not only have ρ = 0.30-0.40, but also a relative error in summer less than unity. At present this is the only method having such a high probable success. In our opinion this result is of fundamental importance because it shows experimentally that the predictability of large anomalies is quite great and exceeds 14 days.

Weather forecasting is impossible without information on the current and preceding states of the atmosphere and the underlying surface. The longer the period for which a forecast is made, the greater is the area from which information must be received. Information is necessary from the entire earth for long-range weather forecasting. This trivial situation nevertheless continues to persist and at the present time the problem of initial data remains unsolved. At the USSR Hydrometeorological Center great attention has always been devoted to the collection of meteorological information. Publication of the SINOPTICHESKIY BYULLETEN' began in January 1949. This SYNOPTIC BULLETIN contains synoptic and aerological maps of the northern hemisphere. In 1953 V. R. Dubentsov headed work on an analysis of synoptic and aerological charts, first for the northern hemisphere, and then the southern hemisphere and the tropical zone. During this time unique material was accumulated for the study of planetary circulation of the atmosphere. However, considerable gaps in the observation network of the world weather service over the oceans,

in the tropics and in some other regions of the earth served as one of the reasons for the development of the GARP program, in whose planning an active part was taken by V. A. Bugayev, Ye. N. Blinova, and others. In the course of implementation of such GARP experiments as GATE and "Musson-77" ["Monsoon-77"] the Hydrometeorological Center performed the functions of a national coordinator [85, 104]. The USSR Hydrometeorological Center participates with equal activity in the implementation of the First Global Experiment.

In proceeding to studies in the field of hydrological forecasts, it must be noted that in the investigations of the last decade an important place is occupied by the development of mathematical models of formation of rain and melt runoff which is directed to the creation of methods for short-range forecasts of water discharges and levels of lowland and mountain rivers realized with electronic computers. Such methods have been developed for the prediction of discharges of rain-induced high waters [54, 61] and predicting water inflow into Volga reservoirs during the period of spring high water [36], as well as in computations of the runoff of mountain rivers [89].

During recent years work has been done on the development of a two-dimensional model of the formation of rain-induced high waters with use of the equations for a kinematic wave [61, 69], as well as work for creating models for continuous computations of water discharge during the course of the year [69]. The development of the latter models, taking into account all types of inflow, affords a possibility for continuous short-range forecasts of discharges and levels or the inflow of water into reservoirs, which is necessary for automatic systems for control of the water economy.

In the field of marine hydrological forecasts, during the last decade, in addition to physical-statistical methods, there has been development of a hydrodynamic direction, which is headed by P. S. Lineykin. During recent years hydrodynamic short-range forecasting methods have been developed for predicting dangerous levels in the White Sea, Baltic Sea, Sea of Azov, Black Sea and Caspian Sea, the fields of currents and long-range forecasts of thermal characteristics in the active layer of the ocean [42, 57, 58, 59, 60, 75, 76, 77, 90].

During the course of its entire history and at the present time the USSR Hydrometeorological Center in the weather service has represented and represents, in essence, a scientific-production combine in which scientific research work is very closely combined and intertwined with operational prognostic activity. Such a combination has a favorable effect on the development of scientific research, which has always been directed to the solution of prognostic problems. In addition, the needs of prognostic "production" forced much money and personnel into the channel of creating automatic technological lines for the processing of information. For example, there are now four: ASPD - "Minsk-32" for preparing actual weather

charts (82), ASPD - M-222 - BESM-6 and ASPD - "Minsk-32" - BESM-6 -- for computing prognostic charts (70); ASPD - YeS-1022 - YeS-1040 -- for the accumulation of information for the First Global Experiment (level IIa).

On the other hand, only the possibility for the rapid use of the results of scientific research in operational work will enable the USSR Hydrometeorological Center to meet its present-day obligations for servicing the national economy. Table 3 gives some idea about the volume of this work.

The following have particular economic importance:
-- warnings of dangerous and especially dangerous phenomena, as well as specialized weather forecasts, including for the Gas Pipelines Administration and for the Central Dispatcher Administration of the Power Ministry;
-- agrometeorological forecasts of mean oblast yield of winter wheat and rye, spring wheat and barley, corn, buckwheat, sunflower, sugar beets, potatoes, fiber flax, sown and meadow grasses;
-- forecasts of the reserves of productive moisture in the soil, wintering and state of winter grain crops in spring;
-- hydrological forecasts of the water volume in rivers, water inflow into reservoirs, opening-up and freezing-over of water bodies, maximum levels and characteristic monthly levels;
-- forecasts of water temperature in seas and oceans, waves, freezing-over and opening-up of nonarctic seas and navigation conditions in them, convoying of ships on recommended courses and a number of others.

Finally, all the information and prognostic activity of the weather service and the USSR Hydrometeorological Center as its central link is associated with the need for several times a day processing an enormous amount of information, that is, is dependent on the possibilities of modern electronic computers and communication systems. The requirements on productivity of electronic computers are beyond existing possibilities. The productivity and efficiency of electronic computers are now a key factor which governs progress in our work. Accordingly, the technical outfitting of the USSR Hydrometeorological Center always was and remains a highly important condition determining the level of our activity.

With the development of a socialist planned national economy the importance of hydrometeorological and agrometeorological forecasts is continuing to increase. Precisely for this reason in the Resolutions of the 25th Congress CPSU it is stated, in particular, "...implement the further development of methods for forecasting weather and meteorological calamities." These instructions have served as a basis for all the activity of the USSR Hydrometeorological Center, whose personnel arrive at its 50th anniversary full of creative forces and with an intense striving for performance of the tasks assigned by the Communist Party and the Soviet government.

BIBLIOGRAPHY

1. Abuzyarov, Z. K., "Method for Operational Forecasting of Waves in the Northern Part of the Atlantic Ocean," TRUDY GIDROMETTSENTRA SSSR (Transactions of the USSR Hydrometeorological Center), No 127, 1973.

2. Aristov, N. A., Blyumina, L. I., "Development of the Synoptic Method for Long-Range Weather Forecasting of the B. P. Mul'tanovskiy School During 50 Years," TRUDY GIDROMETTSENTRA SSSR, No 43, 1969.

3. Aristov, N. A., Ped', D. A., "Present Status of the Method of Seasonal Weather Forecasts and Prospects for its Development," METEOROLOGIYA I GIDROLOGIYA (Meteorology and Hydrology), No 4, 1979.

4. Bagrov, A. N., "Prediction of Precipitation Using an Electronic Computer," METEOROLOGIYA I GIDROLOGIYA, No 12, 1965.

5. Bagrov, A. N., "Operational Scheme for Objective Analysis of Aerological Information for the Northern Hemisphere Using a BESM-6 Electronic Computer," TRUDY GIDROMETTSENTRA SSSR, No 196, 1978.

6. Bagrov, N. A., "Analytical Representation of a Series of Meteorological Fields Using Natural Orthogonal Components," TRUDY TsIP (Transactions of the Central Institute of Forecasts), No 74, 1959.

7. Bagrov, N. A., Zverev, N. I., Ped', D. A., "The Analogue Principle and its Use in Practical Work," TRUDY TsIP, No 132, 1964.

8. Bagrov, N. A., "Statistical Properties of Some Evaluations of Forecasts," TRUDY MMTs (Transactions of the Moscow Meteorological Center), No 9, 1966.

9. Belousov, S. L., "Short-Range Pressure Forecasting Using an Electronic Computer," TRUDY TsIP, No 60, 1957.

10. Belousov, S. L., Gandin, L. S., Mashkovich, S. A., OBRABOTKA OPERATIVNOY METEOROLOGICHESKOY INFORMATSII S POMOSHCH'YU EVM (Processing of Routine Meteorological Information Using an Electronic Computer), Leningrad, Gidrometeoizdat, 1968.

11. Belousov, S. L., et al., "Operational Model of Numerical Forecasting of Meteorological Elements in the Northern Hemisphere," TRUDY GIDROMETTSENTRA SSSR, No 212, 1978.

12. Blinova, Ye. N., "Hydrodynamic Theory of Pressure Waves, Temperature Waves and Centers of Action in the Atmosphere," DOKLADY AN SSSR (Reports of the USSR Academy of Sciences), Vol 39, No 7, 1943.

13. Blinova, Ye. N., "Studies of Hydrodynamic Long-Range Forecasting Carried Out in the USSR," TRUDY MMTs, No 5, 1965.

14. Blinova, Ye. N., "Status and Prospects of Development of Hydrodynamic Methods for Long-Range Weather Forecasting," METEOROLOGIYA I GIDROLOGIYA, No 10, 1972.

15. Blinova, Ye. N., "Hydrodynamic Long-Range Weather Forecasting," METEOROLOGIYA I GIDROLOGIYA, No 11, 1974.

16. Blinova, Ye. N., "Hydrodynamic (Numerical) Long-Range Forecasting of Pressure, Temperature, Wind and Moisture Content," TRUDY GIDROMETTSENTRA SSSR, No 135, 1976.

17. Bugayev, V. A., "Order of Magnitude of Horizontal Derivatives of the Atmospheric Pressure and Temperature Fields," IZV. AN SSSR, SER. GEOFIZ. (News of the USSR Academy of Sciences, Geophysical Series), No 4, 1952.

18. Bugayev, V. A., Peskov, B. Ye., "On the Status and Prospects of Operational Forecasting of Particularly Dangerous Hydrometeorological Phenomena," METEOROLOGIYA I GIDROLOGIYA, No 6, 1972.

19. Bugayev, V. A., "Weather Forecasting in the Recent Past, at Present and in the Future," METEOROLOGIYA I GIDROLOGIYA, No 9, 1972.

20. Bugayev, V. A., NOVOYE V PROGNOZIROVANII POGODY (New Developments in Weather Forecasting), Leningrad, Gidrometeoizdat, 1972.

21. Buldovskiy, G. S., Bortnikov, S. A., Rubinshteyn, M. V., "Prediction of Zones of Strong Turbulence in the Upper Troposphere," METEOROLOGIYA I GIDROLOGIYA, No 2, 1976.

22. Buleyev, N. I., Marchuk, G. I., "Dynamics of Large-Scale Atmospheric Processes," TRUDY IFA AN SSSR (Transactions of the Institute of Physics of the Atmosphere USSR Academy of Sciences, No 2, 1958.

23. Bykov, V. V., Bortnikov, S. A., Kadyshnikov, V. M., Pressman, D. Ya., "Present Status and Immediate Problems in Hydrodynamic Short-Range Forecasting," TRUDY V VSESOYUZNOGO METEOROLOGICHESKOGO S"YEZDA (Transactions of the Fifth All-Union Meteorological Congress), Vol II, Leningrad, Gidrometeoizdat, 1972.

24. Vasil'yev, K. P., Matushevskiy, G. V., "Marine Hydrological Forecasts," METEOROLOGIYA I GIDROLOGIYA, No 12, 1972.

25. Vasil'yev, P. P., Fedorova, N. G., Borodina, A. V., Kastin, O. M., "Developing an Automated System of Five- and Ten-Day Forecasts of Weather Elements," TRUDY GIDROMETTSENTRA SSSR, No 205, 1978.

26. Vasyukov, K. A., Zverev, N. I., Ped', D. A., "Use of the Analogue Principle in Predicting Synoptic Processes and Weather for Five Days in Advance," TRUDY TsIP (Transactions of the Central Institute of Forecasts), No 116, 1962.

27. Veyl', I. G., "Hydrodynamic Models for Short-Range Weather Forecasting," TRUDY GIDROMETTSENTRA SSSR, No 124, 1973.

28. Verigo, S. A., "Method for Preparing a Forecast of Reserves of Productive Moisture in the Soil and Evaluation of the Moisture Supply of Grain Crops," SBORNIK METODICHESKIKH UKAZANIY PO ANALIZU I OTSENKE AEROMETEOROLOGICHESKIKH USLOVIY (Collection of Systematic Instructions on Analysis and Evaluation of Aerometeorological Conditions), Leningrad, Gidrometeoizdat, 1957.

29. Verigo, S. A., Razumova, L. A., POCHVENNAYA VLAGA (Soil Moisture), Leningrad, Gidrometeoizdat, 1973.

30. GIDROLOGICHESKIYE PROGNOZY: TRUDY VSESOYUZNOGO GIDROLOGICHESKOGO S"YEZDA (Hydrological Forecasts. Transactions of the Fourth All-Union Hydrological Congress), Vol VII, Leningrad, 1976.

31. Glagoleva, M. G., Skriptunova, L. I., PROGNOZ TEMPERATURY VODY V OKEANE (Prediction of Water Temperature in the Ocean), Leningrad, Gidrometeoizdat, 1979.

32. Gromova, G. G., "Characteristics of Zonal and Meridional Processes Over Eastern Siberia and the Adjacent Part of the Pacific Ocean," TRUDY TsIP, No 119, 1962.

33. DOLGOSROCHNYYE PROGNOZY POGODY: TRUDY GIDROMETTSENTRA (Long-Range Weather Forecasts: Transactions of the Hydrometeorological Center), No 202, Moscow, 1978.

34. Dushkin, P. K., Lomonosov, Ye. G., "Results of Prediction of the Pressure Field at Three Levels Using an Electronic Computer," TRUDY TsIP, No 106, 1960.

35. Duletova, T.A., Pagava, S. T., Rozhdestvenskiy, A. A., Shirkina, N. A., OSNOVY SINOPTICHESKOGO METODA DOLGOSROCHNYKH PROGNOZOV POGODY (Principles of the Synoptic Method for Long-Range Weather Forecasts), Leningrad, Gidrometeoizdat, 1940.

36. Zhikikov, A. P., Levin, A. G., Nechayeva, N. S., Popov, Ye. G., METODY RASCHETA I PROGNOZA POLOVOD'YA DLYA KASKADA VODOKHRANILISHCH I RECHNYKH SISTEM (Methods for Computing and Predicting High Water for the Cascades of Reservoirs and River Systems), Leningrad, Gidrometeoizdat, 1977.

37. Zverev, N. I., "Statistical Method for Predicting Precipitation of the Cold Half-Year for 1-3 Days for the Central Region of the European Territory of the USSR," TRUDY TsIP, No 97, 1960.

38. Zverev, N. I., Ped', D. A., "Determination of the Similarity of Fields of Meteorological Elements Using a 'Pogoda' Electronic Computer," METEOROLOGIYA I GIDROLOGIYA, No 10, 1960.

39. Zverev, N. I., "Status and Prospects for Compiling Long-Range Weather Forecasts," TRUDY GIDROMETTSENTRA, No 155, 1974.

40. "Use of Images from Satellites in the Analysis and Forecasting of Weather," TEKHNICHESKAYA ZAPISKA VMO (WMO Technical Note), No 124, Leningrad, Gidrometeoizdat, 1974.

41. Kadyshnikov, V. M., "Use of the Integral Relationships Method in Solving Prognostic Equations," IZV. AN SSSR, SER. GEOFIZ., No 8, 1962.

42. Kalatskiy, V. I., MODELIROVANIYE VERTIKAL'NOY TERMICHESKOY STRUKTURY DEYATEL'NOGO SLOYA OKEANA (Modeling of the Vertical Thermal Structure of the Active Layer in the Ocean), Leningrad, Gidrometeoizdat, 1978.

43. Karakash, A. I., "Method for Predicting Water Temperature in the Barents Sea," TRUDY TsIP, No 57, 1957.

44. Karakash, A. I., "Ice Forecasts in the Nonarctic Seas of the USSR," TRUDY GIDROMETTSENTRA, No 51, 1969.

45. Kastin, O. M., Semendyayev, K. A., "System of Algorithms for the Primary Processing of the Principal Types of Meteorological Information," EKSPRESS-INFORMATSIYA (Express Information), No 3(8), Obninsk, Gidromettsentr SSSR, 1970.

46. Kats, A. L., SEZONNYYE IZMENENIYA OBSHCHEY TSIRKULYATSII ATMOSFERY I DOLGOSROCHNYYE PROGNOZY (Seasonal Changes in General Circulation of the Atmosphere and Long-Range Forecasts), Leningrad, Gidrometeoizdat, 1960.

47. Kats, A. L., "Model of a Synoptic-Hydrodynamic-Statistical Weather Forecast for 3-10 Days," METEOROLOGIYA I GIDROLOGIYA, No 6, 1973.

48. Kibel', I. A., "Application of the Equations of the Mechanics of a Baroclinic Fluid to Meteorology," IZV. AN SSSR, SER. GEOGRAF. I GEOFIZICH. (News of the USSR Academy of Sciences, Geographical and Geophysical Series), No 5, 1940.

49. Kibel', I. A., "Adaptation of Air Motion to Geostrophic Movement," DOKLADY AN SSSR (Reports of the USSR Academy of Sciences), Vol 104, No 1, 1955.

50. Kibel', I. A., "Hydrodynamic (Numerical) Short-Range Forecasting," METEOROLOGIYA I GIDROLOGIYA ZA 50 LET SOVETSKOY VLASTI (Meteorology and Hydrology During 50 Years of Soviet Rule), Leningrad, 1967.

51. Kibel', I. A., "Hydrodynamic Short-Range Forecasting in Problems of Mesometeorology," TRUDY GIDROMETTSENTRA SSSR, No 48, 1970.

52. Kibel', I. A., VVEDENIYE V GIDRODINAMICHESKIYE METODY KRATKOSROCHNOGO PROGNOZA POGODY (Introduction to Hydrodynamic Methods for Short-Range Weather Forecasting), Moscow, 1957.

53. Komarov, V. D., VESENNIY STOK RAVNINNYKH REK YEVROPEYSKOY CHASTI SSSR, USLOVIYA YEGO FORMIROVANIYA I METODY PROGNOZOV (Spring Runoff of Lowland Rivers in the European Part of the USSR, Conditions for its Formation and Forecasting Methods), Leningrad, Gidrometeoizdat, 1959.

54. Koren', V. I., Kuchment, L. S., "Mathematical Model of Formation of Rain-Induced High Waters, Optimization of its Parameters and Use in Hydrological Forecasts," METEOROLOGIYA I GIDROLOGIYA, No 11, 1971.

55. Kulik, M. S., "Criteria for Dry Dessicating Winds," SUKOVEI, IKH PROISKHOZHDENIYE I BOR'BA S NIMI (Hot Dessicating Winds, Their Origin and Contending With Them), Moscow, Izd-vo AN SSSR, 1957.

56. Kulik, M. S., Ulanova, Ye. S., "Development of Methods for Agrometeorological Forecasts," METEOROLOGIYA I GIDROLOGIYA, No 12, 1972.

57. Kutalo, A. A., "Horizontal Circulation of a Baroclinic Layer and Westerly Boundary Currents in the Ocean," OKEANOLOGICHESKIYE ISSLEDOVANIYA (Oceanological Research), No 25, Moscow, Nauka, 1976.

58. Lineykin, P. O., "Theory of the Main Thermocline," OKEANOLOGIYA (Oceanology), Vol 14, No 6, 1974.

59. Lineykin, P. S., "Nonlinear Wave Disturbances in the Main Oceanic Thermocline," DOKLADY AN SSSR, Vol 241, No 6, 1978.

60. Lineykin, P. S., Frolov, A. A., "Nonstationary Two-Parameter Model of the Main Oceanic Thermocline), METEOROLOGIYA I GIDROLOGIYA, No 1, 1979.

61. MATEMATICHESKIYE MODELIROVANIYE PROTSESSOV FORMIROVANIYA STOKA. TRUDY GIDROMETTSENTRA SSSR (Mathematical Modeling of Runoff Formation Processes), No 183, 1977.

62. Marchuk, G. I., CHISLENNYYE METODY V PROGNOZE POGODY (Numerical Methods in Weather Forecasting), Leningrad, Gidrometeoizdat, 1967.

63. Marchuk, G. I., "Hydrodynamic Models in the Dynamics of the Atmosphere and Ocean," PROBLEMY SOVREMENNOY GIDROMETEOROLOGII (Problems in Modern Hydrometeorology), Leningrad, 1977.

64. Mashkovich, S. A., "Prediction of Surface Pressure Using an Electronic Computer," METEOROLOGIYA I GIDROLOGIYA, No 1, 1957.

65. Mashkovich, S. A., Veyl', I. G., "Multilevel Spectral Model for Study of Global Atmospheric Processes," TRUDY GIDROMETTSENTRA SSSR (Transactions of the USSR Hydrometeorological Center), No 145, 1974.

66. Mashkovich, S. A., "Two-Level Global Spectral Model of the Atmosphere With the Use of Full Equations," TRUDY GIDROMETTSENTRA SSSR, No 203, 1978.

67. Mertsalov, A. N., "Numerical Synoptic-Hydrodynamic Forecasts of the Surface Pressure Field for 24 Hours," TRUDY GIDROMETTSENTRA SSSR, No 129, 1974.

68. Minina, L. S., PRAKTIKA NEFANALIZA (Practice of Nephanalysis), Leningrad, Gidrometeoizdat, 1970.

69. "Modeling of Processes of Runoff Formation," TRUDY GIDROMETTSENTRA SSSR, No 218, 1978.

70. Moiseychik, V. A., AGROMETEOROLOGICHESKIYE USLOVIYA I PEREZIMOVKA OZIMYKH KUL'TUR (Agrometeorological Conditions and the Wintering of Winter Crops), Leningrad, Gidrometeoizdat, 1975.

71. Mul'tanovskiy, B. P., OSNOVNYYE POLOZHENIYA SINOPTICHESKOGO METODA DOLGOSROCHNYKH PROGNOZOV POGODY (Principal Points in the Synoptic Method of Long-Range Weather Forecasts), Moscow, GIMIZ, 1933.

72. Musayelyan, Sh. A., "Solution of Some Inverse Problems in Satellite Meteorology Using a Diagnostic Equation of Atmospheric Dynamics," IZV. AN SSSR, FIZIKA ATMOSFERY I OKEANA (News of the USSR Academy of Sciences, Physics of the Atmosphere and Ocean), Vol 3, No 7, 1967.

73. Musayelyan, Sh. A., O PRIRODE NEKOTORYKH SVERKHDLITEL'NYKH ATMOSFERNYKH PROTSESSOV (Nature of Some Superlong Atmospheric Processes), Moscow, Gidrometeoizdat, 1978.

74. Musayelyan, Sh. A., Ugryumov, A. I., Zadorozhnaya, T. N., "On the Problem of Asynchronous Relationships Between Cloud Cover Anomalies Over the Ocean and Air Temperature Anomalies on a Continent," TRUDY GIDROMETTSENTRA SSSR, No 177, 1976.

75. Nesterov, Ye. S., "Numerical Forecasting of the Thermal Characteristics of the Upper Layer of the Ocean in the North Atlantic," TRUDY GIDROMETTSENTRA SSSR, No 200 [year not given].

76. Ovseyenko, S. N., "Numerical Modeling of Ice Drift," IZV. AN SSSR, FIZIKA ATMOSFERY I OKEANA, Vol 12, No 11, 1976.

77. Ovseyenko, S. N., Efroimson, V. O., "On the Theory of Drift of Melting Ice," DOKLADY AN SSSR, Vol 246, No 5, 1979.

78. Pagava, S. T., "Principles of the Synoptic Method for Long-Range Weather Forecasts for a Short Time in Advance," TRUDY NIU GUGMS (Transactions of the Scientific Research Institutes of the Main Administration of the Hydrometeorological Service), Series II, No 20, 1946.

79. Pagava, S. T., "Synoptic Method for Monthly Weather Forecasts," TRUDY TsIP, No 5, 1958.

80. Pagava, S. T., et al., OSNOVY SINOPTICHESKOGO METODA SEZONNYKH PROGNOZOV POGODY (Principles of the Synoptic Method for Seasonal Weather Forecasts), Leningrad, Gidrometeoizdat, 1966.

81. Ped', D. A., "Method for Predicting the Ten-Day Quantity of Precipitation," TRUDY TsIP, No 147, 1966.

82. Ped, D. A., "Seasonal Weather Conditions Associated With the Times of Spring Change in Stratospheric Circulation," TRUDY GIDROMETTSENTRA SSSR SSSR, No 120, 1973.

83. Ped', D. A., Rudicheva, L. M., "Influence of the Duration of Persistence of the Stratospheric Anticyclone on the Weather of Subsequent Months," TRUDY GIDROMETTSENTRA SSSR, No 122, 1973.

84. Petrosyants, M. A., "The Weather Service and Prospects of its Development," PROBLEMY SOVREMENNOY GIDROMETEOROLOGII (Problems in Modern Hydrometeorology), Leningrad, 1977.

85. Petrosyants, M. A., "First Results of the Soviet 'TROPEKS-74' Expedition," METEOROLOGIYA I GIDROLOGIYA, No 3, 1975.

86. Pogosyan, Kh. P., Taborovskiy, N. L., "Advective-Dynamic Principles of Frontological Analysis," TRUDY TsIP, No 7(34), 1948.

87. Popov, Ye. G., VOPROSY TEORII I PRAKTIKI PROGNOZOV RECHNOGO STOKA (Problems in the Theory and Practice of Forecasts of River Runoff), Moscow, Gidrometeoizdat, 1963.

88. Pressman, D. Ya., "Six-Level Model for Short-Range Forecasting Using Full Equations," ANALIZ I PROGNOZ POGODY: TRUDY VSESOYUZNOY KONFERENTSII MOLODYKH UCHENYKH GIDROMETSLUZHBY SSSR (Weather Analysis and Forecast: Transactions of the All-Union Conference of Young Scientists of the USSR Hydrometeorological Service), 1971.

89. PROGNOZY RECHNOGO STOKA GORNYKH I RAVNINNYKH REK. TRUDY GIDROMETTSENTRA SSSR, No 163, 1976.

90. Resnyanskiy, Yu. D., "Parameterization of Integral Dissipation of Turbulent Energy in the Upper Quasihomogeneous Layer of the Ocean," IZV. AN SSSR, FIZIKA ATMOSFERY I OKEANA, Vol 11, No 7, 1975.

91. Sadokov, V. P., Shteynbok, B. D., "Use of Conjugate Functions in the Analysis and Forecasting of Temperature Anomalies," METEOROLOGIYA I GIDROLOGIYA, No 10, 1977.

92. Sadokov, V. P., Vazhnik, A. N., "Theoretical Model of Long-Range Forecasting of Averaged Meteorological Fields," METEOROLOGIYA I GIDROLOGIYA, No 8, 1976.

93. SINOPTICHESKIYE SEZONY: TRUDY GIDROMETTSENTRA (Synoptic Seasons. Transactions of the Hydrometeorological Center), Moscow, No 187, 1977.

94. Sonechkin, D. M., "Statistical Validation in Meteorology," TRUDY GIDROMETTSENTRA SSSR, No 181, 1976.

95. Sonechkin, D. M., "Formulation of the Problem of Dynamic-Stochastic Forecasting by Analogues," TRUDY GIDROMETTSENTRA SSSR, No 181, 1976.

96. Taborovskiy, N. L., "Hydrodynamic Theory of a Baroclinic Atmosphere and Fundamental Problems in Synoptic Meteorology," TRUDY NIU GUGMS, Series II, No 26, 1947.

97. Ter-Mkrtchyan, M. P., Snitkovskiy, A. I., Lukianova, L. Ye., "Use of Discriminant Analysis for Predicting Glaze," TRUDY GIDROMETTSENTRA SSSR, No 90, 1971.

98. Trosnikov, I. V., Yegorova, Ye. N., "Use of Latitude-Longitude Grids for Modeling of General Circulation of the Atmosphere," TRUDY GIDROMETTSENTRA SSSR, No 145, 1974.

99. Trosnikov, I. V., Yegorova, Ye. N., "Use of Empirical Formulas for Computing Radiation Influxes of Energy in the Modeling of General Circulation of the Atmosphere," TRUDY GIDROMETTSENTRA SSSR, No 160, 1975.

100. Ulanova, Ye. S., METODY AGROMETEOROLOGICHESKIKH PROGNOZOV (Methods for Agrometeorological Forecasts), Leningrad, Gidrometeoizdat, 1959.

101. Ulanova, Ye. S., AGROMETEOROLOGICHESKIYE USLOVIYA I UROZHAYNOST' OZIMOY PSHENITSY (Agrometeorological Conditions and the Yield of Winter Wheat), Leningrad, Gidrometeoizdat, 1975.

102. Uspenskiy, B. D., "Prospects for the Development of the Synoptic Method for Short-Range Weather Forecasting," METEOROLOGIYA I GIDROLOGIYA, No 10, 1972.

103. Uspenskiy, B. D., Mertsalov, A. N., Orlova, Ye. M., Petrichenko, I. A., "Peculiarities of the Forecasting of Precipitation in a Numerical Operational Synoptic-Hydrodynamic Model for a Time Up to 36 Hours," TRUDY GIDROMETTSENTRA SSSR, No 176, 1977.

104. Fal'kovich, A. I., DINAMIKA I ENERGETIKA VNUTRITROPICHESKOY ZONY KONVERGENTSII (Dynamics and Energy of the Intertropical Convergence Zone), Leningrad, Gidrometeoizdat, 1979.

105. Khromov, S. P., "A Hundred Years of Our Weather Service," METEOROLOGIYA I GIDROLOGIYA, No 10, 1972.

UDC 551.515.5

TROPOSPHERIC STRUCTURE UNDER TROPICAL CYCLOGENESIS CONDITIONS

Moscow METEOROLOGIYA I GIDROLOGIYA in Russian No 12, Dec 79 pp 22-32

[Article by Doctor of Geographical Sciences L. S. Minina and Ye. N. Arabey, USSR Hydrometeorological Scientific Research Institute, submitted for publication 27 April 1979]

Abstract: In the example of development of typhoon "Carmen" during the period 10-16 August 1978 the authors describe the peculiarities of distribution of temperature and moisture content in the troposphere in an active process of tropical cyclogenesis. The deviations of the values of the meteorological elements from the corresponding values in the standard atmosphere are given as a comparison.

[Text] The second Soviet "Tayfun-78" expedition took place during the period July-November 1978 for studying tropical cyclones in the northwestern part of the Pacific Ocean.

During the period 7-16 August the flagship of the expedition, the scientific research ship "Academik Shirshov," as well as the weather ships "Priliv" and "Priboy," carried out hydrological investigations in the region 22°N, 147°E, forming a small polygon in the form of a triangle with a side of about two degrees.

The weather was relatively dry with few clouds. The ships were on the southern periphery of a subtropical anticyclone where the pressure was 1014-1015 mb. However, already on 8 August an influence began to be felt from the ICZ, moving from the south; there was a decrease in pressure, well-developed cumulus clouds appeared; a shower passed and swell moved from the southeast. On 9 August the swell increased: a new typhoon had developed near the polygon.

The expedition staff decided that beginning at 1200 GMT on 10 August on all three ships there would be soundings four times a day. Using the data from the scientific research ship "Akademik Shirshov," on which the

authors of the article worked, there were computations and averaging of the meteorological parameters of the troposphere during the initial period of tropical cyclogenesis for each of the five defined sounding groups in different parts of the cyclone. The considered parameters included: geopotential, wind, temperature, vertical temperature gradient, moisture content (mixture ratio in g/kg), relative humidity. Using the values of these same parameters for the standard atmosphere in July at 30°N we computed their deviations at an early stage in development of "Carmen" typhoon. In addition, we ascertained the principal differences between the conditions in the troposphere in the considered parts of a tropical cyclone.

Some general information on "Carmen" typhoon. "Carmen" typhoon, in the form of a small depression, developed second in the series of tropical cyclones "Bonnie"-"Carmen"-"Della," generated during the first 10-day period in August.

Initially, during the period 7-8 August, to the northeast of Guam, in the ICZ region, an extensive cloud concentration could be traced. At the beginning of 9 August a tropical depression (1006 mb) was formed in it. Its development occurred very rapidly and already by the end of 10 August it had passed into the stage of tropical storm "Carmen" (996 mb, 20 m/sec). The cyclone remained relatively fixed in position, being situated near 17°N, 145°E. Its development led to descending air movements in its neighborhood. As a result, the polygon was on the northern periphery of the cyclone (Fig. 1a,b), where on 10 and 11 August almost cloudless weather appeared. However, with deepening of the cyclone and its transition on 12 August to a stage of strong tropical storm there was an increase in the central continuous cloud mass. Propagating to the north and simultaneously beginning slow movement toward the northwest, the tropical storm on 12 August affected the region of drift of the vessels (Fig. 1c). The weather deteriorated sharply.

The "Carmen" cloud system had a main mass adjacent to the center of the cyclone, with a diameter 5°latitude x 7°longitude and a tail convective zone with a width from 3 to 5°, extending toward the south and southeast (Fig. 1c). The main cloud mass of the cyclone was situated primarily to the north of its center, that is, to the right of the direction of movement, and with slow movement to the northwest was propagated into the polygon. As can be seen from the photographs, this was at the northeast edge of the polygon. Beginning at 0000 hours on 13 August, with movement of the cyclone in a westerly direction, the polygon was in its tail convective zone (Fig. 1d). Beginning on 14 August the vessels were under the influence of the typhoon periphery and only on 16 August were outside the sphere of its influence.

As a result, there was an average of 4-5 soundings of the central continuous cloud mass (CCCM) at a distance of 300-400 km from the center, the tail convective zone (TCZ) (800 km from the center), its northern

periphery (about 1,000 km from the center), and also the Trades zone, not directly disturbed by the typhoon.

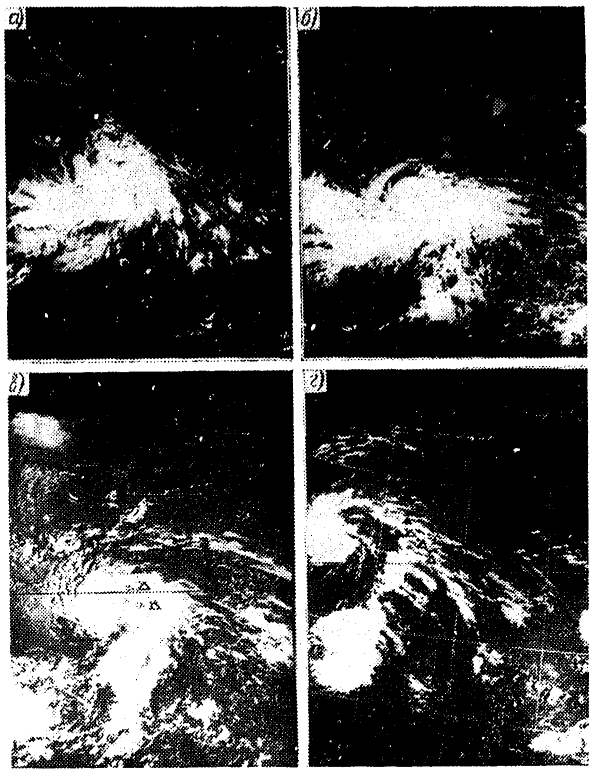

Fig. 1. Development of cloud system of "Carmen" tropical cyclone during the period 10-12 August 1978 according to data from "Meteor-3" meteorological satellite (TV photographs) and position of "Akademik Shirshov" scientific research ship. At time of photograph -- white or black triangle; relative position of scientific research ship 6 and 12 hours after photograph -- contour of triangle. a) tropical depression (17°N, 144° E) at 0555 hours 10 August; b) "Carmen" tropical cyclone (16°N, 144°E) at 0549 hours 11 August; c) strong tropical storm "Carmen" (16°N, 144°E) at 0543 hours 12 August; d) typhoon "Carmen" (21°N, 140°E) at 2320 hours 12 August.

Table 1

Deviation of Temperature Δ T°C, Moisture Content Δ r g/kg and Degree of Saturation of Air Δ U% in Central Continuous Cloud Mass (CCCM) "Carmen" from Conditions in "Mean" Typhoon

Уровень, мб 1	«Средний» тайфун 2			ЦСОМ «Кармен» 3			Разность 4		
	T	r	U	T	r	U	ΔT	Δr	ΔU
100	—75,4			—71,9			3,5		
5 Уровень тропопаузы									
150	—63,3			—64,5			—1,2		
200	—48,6			—50,7			—2,1		
250	—36,3			—37,6			—1,3		
300	—26,3	0,9	60	—27,5	1,1	83	—1,2	0,2	23
400	—12,3	2,5	65	—14,1	2,7	83	—1,8	0,2	18
500	—2,4	5,0	76	—4,7	4,8	86	—2,3	—0,2	10
600	4,8	7,2	81	3,4	6,8	83	—1,4	—0,4	2
700	11,2	10,0	82	10,7	9,7	82	—0,5	—0,3	0
800	16,1	12,8	87	16,3	13,0	87	0,2	+0,2	0
850	18,6	14,5	89	18,6	14,2	92	0	—0,3	3
900	21,0	16,0	89	21,0	16.7	94	0	0,7	5
1000	25,2	18,8	91	27,0	20,5	87	1,8	1,7	—4
P_0	25,2	18,8	91	27,6	20,5	86	2,4	1,7	—5

KEY:

1. Level, mb
2. "Mean" typhoon
3. CCCM "Carmen"
4. Difference
5. Tropopause level

Comparison of "Carmen" typhoon with "mean" typhoon. In order to clarify how typical is the situation of the edge of a cloud mass of a developing cyclone for the conditions of the typhoon itself it was convenient to use the data published by Bell and Kar-Sing [1] on the distribution of meteorological parameters in a "mean" typhoon. The latter were obtained as a result of a careful analysis of sounding data in 101 typhoons for cases when the sounding was in the limits of 100 miles from the center.

The deviation of the mean values for temperature, moisture content and degree of air saturation in typhoon "Carmen" (350 km from the center) from the values for a "mean" typhoon is presented in Table 1. It can be seen that in the lower near-water layer the temperature is 1.8-2.4°C higher and the moisture content is ever greater by 1.7 g/kg than under the conditions of a "mean" typhoon. The higher air temperature in the near-water layer in the region of the "Akademik Shirshov" scientific research ship is attributable to the absence of heavy showers characteristic for the inner parts of a well-developed tropical cyclone on the

northeast margin of the "Carmen" cloud mass. During the daytime and nighttime on 12 August, although rain fell, its quantity did not exceed 0.1 mm. This circumstance was an indirect indication of the onset of descending movements characteristic of the margin of the cloud mass in a tropical cyclone. In actuality, already in the next few hours the CCCM of the cyclone moved out of the polygon of the expeditionary ships (Fig. 1c,d).

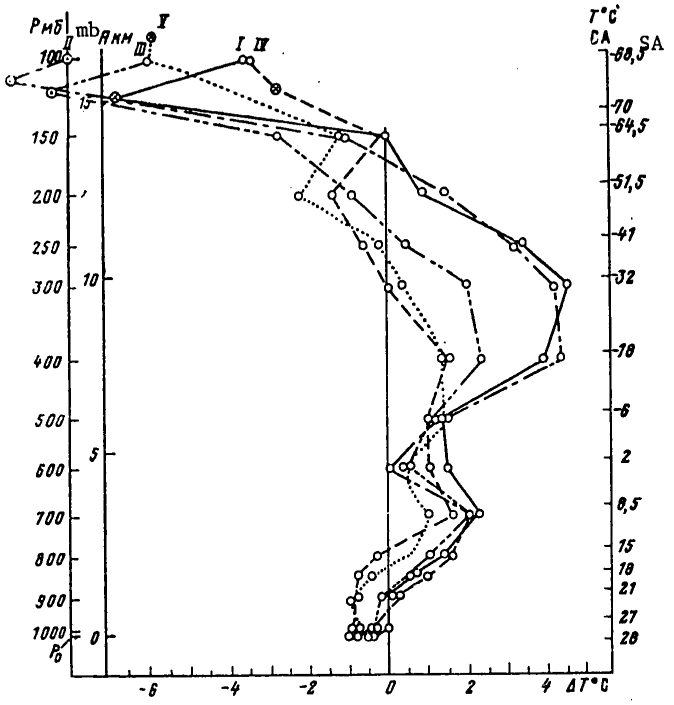

Fig. 2. Profile of vertical distribution of temperature deviation $\Delta T°C$ from standard atmosphere (SA). I) northeastern edge of central continuous cloud mass; II) tail convective zone; III) eastern periphery; IV) northern periphery; V) undisturbed Trades zone.

On this day the temperature of the surface water layer was about 28°C and the air temperature was 27.5°C. As a result, the air moisture content in the near-water layer was increased, whereas saturation was close to the limit, as in a "mean" typhoon. Aloft, to the level 850 mb, the conditions in the developing cyclone "Carmen" were virtually the same as in the "mean" typhoon. From the 600-mb level to the tropopause the temperature at the edge of the main mass of "Carmen" was only 1.2-2.3° lower, but the moisture content was almost the same as in the "mean" typhoon. As a

result of the lower temperature the relative humidity in this layer was even 10-23% greater.

According to Bell and Kar-Sing, in a "mean" typhoon the greatest heating of the troposphere is observed in the layer 600-200 mb. The deviation from standard conditions in a "mean" typhoon, according to their computations [1], attains 3-6°C. Accordingly, the increase in temperature in this same layer on the periphery of "Carmen," being only 1.2-2.3°C less, can be considered to correspond to the conditions of the "mean" typhoon. The fact is that Bell and Kar-Sing made use of sounding data no more than 185 km (100 miles) from the center and sounding of the cloud mass for "Carmen" was at a distance of 300-400 km from the center.

Deviation of meteorological parameters of the troposphere on the periphery of "Carmen" from the standard atmosphere. For a clear representation of the nature of tropospheric disturbance in different parts of a developing tropical cyclone, for each of the five considered groups we computed the deviations of the meteorological elements from the standard atmosphere for July at 30°N. For the isobaric surfaces we examined the deviations of altitude, temperature, vertical gradient and parameters of humidity. Below we will give the deviations of only the three latter parameters as being the most clearly expressed. The temperature deviation ΔT from the standard atmosphere in different parts of the developing cyclone "Carmen" and in the Trades zone is given in Fig. 2. An analysis of the profiles, in particular, reveals a predominance of positive values of the temperature anomaly in almost the entire troposphere for all parts of the cyclone. We note the presence of two maxima: strong in the layer 300-400 mb, that is, the heat nucleus of the cyclone, and poorly expressed near 700 mb. In the boundary layer and below the tropopause ΔT was negative. The value of the temperature anomaly was determined in the investigated part of the cyclone.

The main maximum of the positive anomaly ΔT in the middle troposphere in the region of the cyclone and on its periphery varies in the range from 1.5 to 4.5°.

The secondary maximum of the positive anomaly ΔT, situated in the lower troposphere, is small and in the cyclone region attains 2°C, whereas in the Trades zone it attains 1°C.

A graphic spatial representation of the ΔT anomaly and the vertical gradient $\Delta\gamma$ in different parts of the developing tropical cyclone "Carmen" is given by the vertical section (Fig. 3). The section shows that in the entire region of the tropical storm "Carmen" an extensive and quite intense warm layer was formed in the middle troposphere. The greatest intensity (+4.5°C) and vertical extent (500-175 mb) of the warm region, having the form of a nucleus, is observed in the CCCM and TCZ. In the direction of the cyclone periphery the warm layer drops down and is reduced in altitude (450-300 mb) and intensity (to 1.5-2°C), but it is traced very

clearly. It also exists in the Trades zone (+1.4°C) between 500 and 400 mb. An unexpected finding was that in the TCZ the positive ΔT value in the middle troposphere, as in the CCCM, has a maximum value and attains 3.5-4.5°C. Despite expectations, a considerable ΔT value, up to 2.5°C, was also observed on the eastern periphery of "Carmen," and also up to 1.5°C on the northern periphery and even in the Trades zone, to the east (by 1,700-1900 km) of the developing tropical cyclone. This fact is unqustionably extremely important because it shows that during the period of cyclogenesis in the ICZ region the tropical troposphere, even at a great distance from it, is to some degree already prepared for the formation of the heat nucleus of a future cyclone.

Table 2

Blocking Layers (Numerator -- Number of Blocking Layers, Denominator -- Number of Soundings) in "Carmen" Region and on its Closest Periphery (from A. Tontoko)

Часть циклона * 1		Параметры задерживающих слоев 2			
		нижняя граница, м 3	толщина, м 4	γ ° C/100 м	среднее число задерж. слоев в зондировании 5
I	$\frac{6}{3}$	2400	185	0,18	2,0
II	$\frac{4}{4}$	2165	137	0,30	1,0
III	$\frac{5}{4}$	1870	150	0,25	1,2
IV	$\frac{10}{5}$	2237	227	0,09	2,0
V	$\frac{7}{3}$	2815	217	0,15	2,3

6 * Условные обозначения см. на рис. 2.

KEY:
1. Part of cyclone
2. Parameters of blocking layers
3. Lower boundary, m
4. Thickness, m
5. Average number of blocking layers in sounding
6. For annotations see Fig. 2.

In accordance with the nature of the distribution is the distribution of the anomaly of the vertical gradient $\Delta\gamma$ (Fig. 3). The first thing which we note is that in the entire troposphere there is a predominance of the negative anomaly $\Delta\gamma$. Accordingly, under conditions characteristic for a typhoon in the troposphere there are layers with even a more stable

stratification than in the standard atmosphere. The regions of the two greatest negative deviations (-0.1, -0.2°C/100 m) are concentrated in the layers 850-700 and 600-400 mb. The third region, characteristic only for the periphery of the cyclone, is under the tropopause.

The regions of the positive anomaly $\Delta\gamma$ (to 0.15°C/100 m) were noted in the near-water layer, somewhat above the 700-mb level and near 200 mb. The two latter regions of the increased $\Delta\gamma$ value are observed at the upper boundary of the layer with an increased temperature in the lower troposphere and at the upper boundary of the warm nucleus in the middle troposphere of a developing cyclone.

The investigation of A. Tontoka, a Philippine specialist, working aboard the ship, demonstrated that in the lower half of the troposphere in the "Carmen" region there are several blocking layers with a thickness of 140-230 m (Table 2). More frequently the lower layer was situated near 900 mb; there was a second near 700 mb. Even in the CCCM it was possible to trace blocking layers at an altitude of about 2.5 km with a mean thickness of the layer 185 m and a mean gradient 0.18°C/100 m. It is interesting to note that in the TCZ there is a minimum number of blocking layers (on the average, one per ascent) and a minimum thickness of the layer -- 137 m, with a maximum vertical gradient, whose mean value is 0.30°C/100 m. It is characteristic that the most intense blocking layers (mean gradient 0.09°C/100 m and the greatest mean thickness of the layer 227 m) were observed on the northern periphery of "Carmen"," reflecting the presence of descending air movements here.

Sounding of the developing tropical cyclone "Carmen" with increased frequency was carried out on the northern edge of the CCCM at a distance of 300-400 km from its center. However, as we see, at this great distance the heating of the middle troposphere in the storm stage was felt significantly. It can be postulated that near the very center of "Carmen" it attained a considerably greater value. For example, sounding data in the eye of the typhoons "Alice" (1961) and "Shirley" (1968) revealed a temperature excess relative to the mean (computed for September in the northwestern part of the Pacific Ocean) at 8 and 10°C respectively [1]. In hurricane "Hilda" (1964) over the Gulf of Mexico [2] there was also a temperature excess in the layer 400-250 mb by 8-10°C in comparison with the SA. In addition, the vertical time section of "Hilda" hurricane exhibited the same regularity as we discovered in tropical storm "Carmen" -- specifically, the presence of a sufficiently thick warm layer (ΔT = 2-4°) between 400 and 200 mb at a distance as great as 700-800 km from the hurricane.

Accordingly, it can be concluded that the process of heating of the middle troposphere during tropical cyclogenesis is by no means a local phenomenon and is observed in a great space in the neighborhood of a developing tropical cyclone. A confirmation of this is the computations which we made for

the case of development of typhoon "Tricks" (July 1978) for determining the local pressure change. We discovered that the region of pressure decrease, coinciding at its maximum with the center of a developing cyclone, is propagated over a great territory in the area, exceeding by a factor of 10 the dimensions of the developing cyclone. An intensive pressure decrease is observed in the TCZ region, where, as it could be confirmed, the middle troposphere was also heated, as at the edge of the cyclone CCCM. In the TCZ region independent centers of pressure decrease and small cyclonic centers were formed; the initial impulse for their appearance, presumably, is heating of the troposphere. In this connection the appearance of "offspring" of typhoons in the rear part of tropical cyclones becomes understandable.

Still another layer of increased air temperature, but less clearly expressed, is traced in the lower troposphere over the region of the storm "Carmen," its periphery and the Trades zone remote from it (Fig. 3). In part this warm layer can be related to the presence of blocking layers in the lower troposphere, characteristic for the Trades zone. However, the fact that the maximum of the temperature anomaly is greater in the cyclone region itself, where the blocking layers are thinner and less intensive, and less at the periphery, where they are thicker and more intensive (Table 2), makes it possible to propose another nature of its appearance. In all probability, it is associated with cloud-forming and condensation processes. Moreover, specifically in this same layer in a tropical cyclone there is the maximum moisture content, as will be mentioned again below.

A direct indication of the correctness of such an explanation is the presence of a similar maximum of the ΔT anomaly near the 700-mb level in intensively developed typhoons and hurricanes. Examples of this are the typhoons "Alice" (981 mb, 1961), "Shirley" (969 mb, 1968) and hurricane "Arlene" (978 mb, 1965) [1], as well as hurricane "Hilda" (941 mb, 1964) [2].

A distinguishing characteristic of the investigated region of "Carmen" and the Trades zone during the period of cyclone development is the considerable value of the negative anomaly ΔT above the level 200-150 mb. The greatest value of the anomaly (-6.7°C, -9.4°C) was noted in the TCZ, CCCM and on the eastern periphery of "Carmen" (Fig. 3). This marked temperature decrease was evidently associated with adiabatic cooling of air rising intensively in the cloud system of the tropical cyclone virtually to the level of the tropopause.

Humidity anomaly. The profile of the vertical distribution of deviation of moisture content (Δr g/kg) from the standard atmosphere is shown in Fig. 4. We see that in the cyclone region from the sea surface to the 300-mb level (in the SA there are no data on humidity at greater altitudes) the Δr deviations are positive. The only exception is the layer 750-500 mb in the Trades zone and the layer near 400 mb on the northern

periphery, where the moisture content was less than the norm.

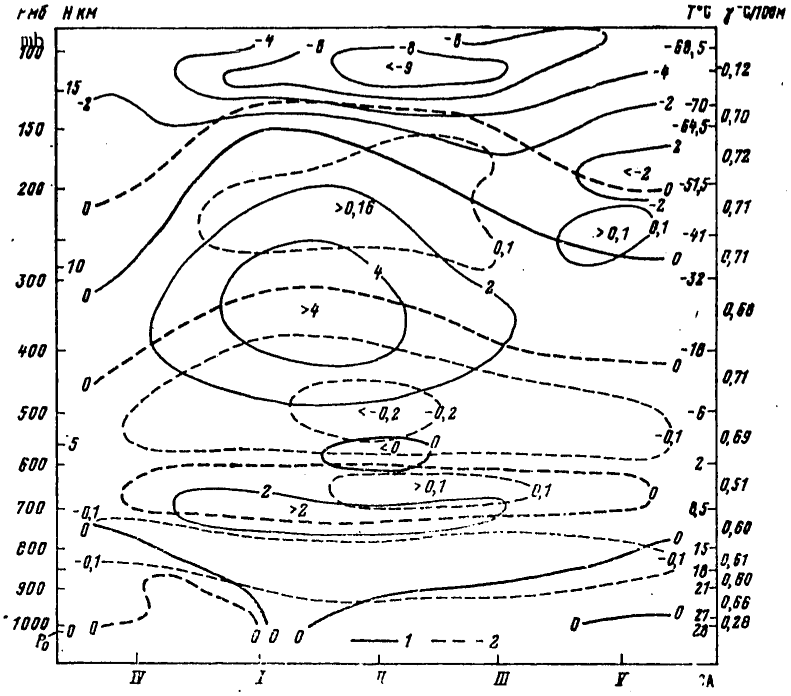

Fig. 3. Deviation of temperature ΔT from standard atmosphere (30°N, July) (1) and its vertical gradient $\Delta\gamma$ (2) in different parts of developing tropical cyclone "Carmen." For annotations see Fig. 2.

We note that the Δr profile is quite consistent vertically in all parts of "Carmen." The maximum value of the deviation is observed in the lower troposphere, in the layer 900-850 mb, from 5.4 in the CCCM to 2.5 g/kg in the Trades zone. The values of the Δr deviation in the CCCM and TCZ are close to one another in the entire troposphere.

The moisture increment (Table 3) is about half the norm at the 900-mb level, near the norm near 600 mb, two times the norm at the 400-mb level and attains almost three times the norm near the 300-mb level. On the eastern periphery of "Carmen" the Δr value is considerably less, but here also to the 400-mb level it is increased by half the norm, whereas near 300 mb -- by a whole norm. On the northern periphery of the cyclone the moisture content to the 500-mb level is insignificantly (by a factor 0.1-0.3) greater than the norm; higher it is less than the norm.

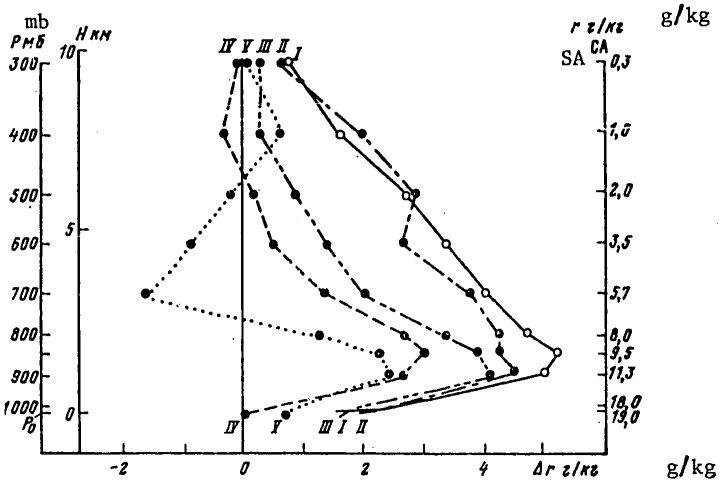

Fig. 4. Profiles of vertical distribution of deviation of moisture content Δr g/kg from standard atmosphere (SA). For annotations see Fig. 2.

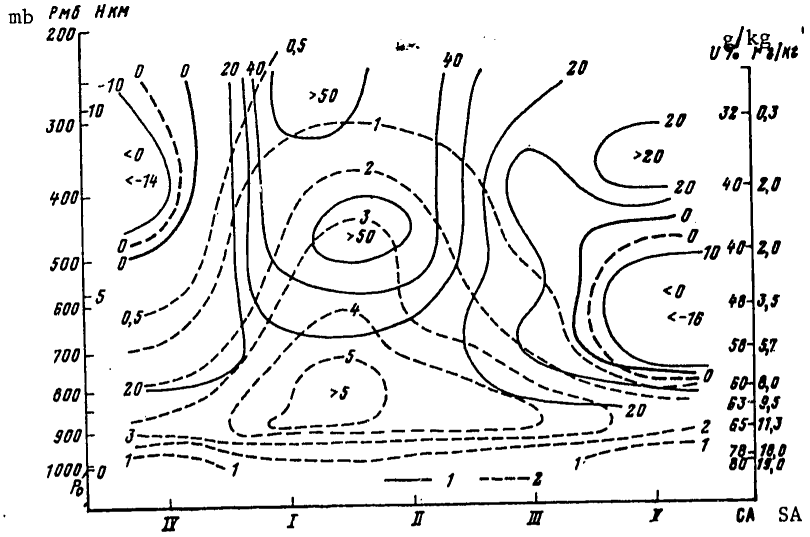

Fig. 5. Deviation of relative humidity ΔU (1) and moisture content Δr (2) from standard atmosphere (30°N, July) in different parts of developing typhoon "Carmen." For annotations see Fig. 2.

The degree of air saturation (Fig. 5) in a tropical cyclone was also considerably above the norm in almost all parts of the cyclone. In the boundary layer below the first blocking layer, near the 900-mb level, on the

cyclone periphery and in the Trades zone ΔU is approximately identical, exceeding the norm by 10-20%; in the cyclone -- by 30%.

Table 3

Ratio of Moisture Content in Developing Tropical Cyclone "Carmen" in g/kg (Numerator) to Norm for Standard Atmosphere in % (Denominator)

Уровень, мб 1	СА 2	IV	I	II	III	V
300	0,3/100	0,3/100	1,1/366	1,0/333	0,6/200	0,4/133
400	1,0/100	0,7/70	2,7/270	3,0/300	1,3/130	1,6/160
500	2,0/100	2,2/110	4,8/240	4,9/245	2,9/145	1,8/90
600	3,5/100	4,0/114	6,8/194	6,2/177	4,9/140	2,6/74
700	5,7/100	7,0/122	9,7/170	9,5/166	7,7/135	4,0/71
800	8,0/100	10,7/134	12,7/160	12,3/155	11,3/141	9,2/115
850	9,5/100	12,5/131	14,8/154	13,8/145	13,4/141	11,7/123
900	11,3/100	13,9/123	16,3/143	15,8/140	15,4/136	13,7/121
1000	18,0/100	18,4/102	20,5/111	20,5/114	20,0/111	18,8/104
P_0	19,0/100	19,0/100	20,5/108	20,5/108	20,4/107	19,7/104

3 Примечание. Условные обозначения см. на рис. 2.

KEY:

1. Level, mb
2. SA (Standard Atmosphere)
3. Note. For annotations see Fig. 2

Above the boundary layer the ΔU value is different. The greatest excess of ΔU (to 40-50%) was noted in the CCCM and TCZ in the layer 600-300 mb. Some increase in ΔU is noted on the closest eastern and northern cyclone peripheries in the layer 600-500 mb, reflecting the general tendency to an increase in ΔU in the cyclone region. Near the 400-mb level on the cyclone periphery it is again possible to trace the ΔU minimum, which from our point of view is attributable to developing compensatory descending movements. With respect to the Trades zone, here, as usual, the air in the layer 800-450 mb is characterized by a great dryness.

The spatial distribution of deviations of total moisture content and relative humidity from the conditions in the standard atmosphere is given in Fig. 5. We see that the tropical storm region is characterized by deep and intensive moistening which can be traced from the near-water layer to the tropopause. On its eastern periphery the moisture content and degree of saturation are also increased, but are incomparably smaller in value. The northern periphery outside the boundary layer is clearly discriminated due to the small moisture content and air dryness.

Summary

1. The value and vertical distribution of temperature, moisture content and degree of saturation on the northern edge of the central cloud mass in tropical cyclone "Carmen" (at a distance 300-400 km from the center) and in its tail convective zone were extremely similar to one another, but are different from the Trades zone of these days and the standard atmosphere. They reflected the typical conditions for a "mean" typhoon.

2. The peculiarities of distribution of meteorological parameters in four parts of the developing tropical cyclone "Carmen" essentially involve the following.

a) In the boundary layer the distribution of meteorological parameters in all parts of the cyclone and on its closest periphery is approximately identical -- temperature within the limits of the standard atmosphere, whereas the moisture content and the degree of saturation are greater.

b) Above the boundary layer they are sharply different from the standard atmosphere and are dependent on the considered part of the cyclone.

In the central cloud mass and in the tail convective zone the distribution of meteorological parameters, against expectations, was identical. A positive temperature anomaly has two maxima: weak in the lower troposphere near the 700-mb level, about which there has been no mention in the literature up to the present time, and intensive -- in the middle troposphere, in the layer 500-200 mb, which reflected the presence of a warm nucleus in the storm "Carmen." The moisture content anomaly and the degree of air saturation exceeded the norm. For example, the moisture content at the 900-mb level increased by 0.5 the norm, near 600 mb -- by the norm, at 400 -- by two times the norm and near 300 mb -- by almost three times the norm.

On the eastern periphery the meteorological parameters with respect to the nature of their distribution are close to the distribution in the central cloud mass and in the tail convective zone, but the magnitude of their deviation from the standard atmosphere is 2-3 times less.

On the northern periphery, in a zone of predominantly clear weather, the magnitude and distribution of meteorological parameters are essentially different from other parts of a developing cyclone. The temperature anomaly here is insignificant. The moisture content and relative humidity are small and decrease sharply above the boundary layer: from the 500-mb level to the tropopause the air is characterized by exceptional dryness (26-30%).

c) The greatest differences in the distribution of meteorological parameters were observed between the central cloud masses of "Carmen" and the region of clear weather adjoining it on the north, where under the influence of a developing cyclone descending movements, suppressing convection, usually occur.

3. A substantial quantity of moisture can enter into a developing cyclone from the entire periphery surrounding it only from the boundary layer region. Outside the boundary layer the principal powerful source feeding a developing cyclone is the tail convective zones carrying water vapor into the cyclone region in almost the entire troposphere. The cloudless periphery (above the boundary layer), where intensive compensating descending movements develop, is the least favorable for supplying moisture to a cyclone.

4. The tail convective zones, with respect to their physical role in tropical cyclogenesis, are accumulators of water vapor, continuously transporting moisture and heat of condensation into the region of the developing cyclone. They can rightfully be called the zones of supply for a tropical cyclone.

The authors express appreciation to A. Tontoka, a Philippine specialist, for assistance rendered in carrying out this investigation.

BIBLIOGRAPHY

1. Bell, G. J., Kar-Sing, T., "Some Typhoon Soundings and Their Comparison With Soundings in Hurricanes," J. APPL. METEOROL., Vol 12, No 2, 1973.

2. Hawkins, H. F., Rubsam, D. T., "Hurricane Hilda, 1964. 3. Degradation of the Hurricane," MON. WEATHER REV., Vol 96, No 10, 1968.

UDC 551.510.528

PECULIARITIES OF DISTRIBUTION OF THE TROPOPAUSE OVER THE EARTH

Moscow METEOROLOGIYA I GIDROLOGIYA in Russian No 12, Dec 79 pp 33-39

[Article by Candidate of Geographical Sciences Z. M. Makhover, Moscow Division of the All-Union Scientific Research Institute of Hydrometeorological Information-World Data Center, submitted for publication 20 April 1979]

Abstract: A study was made of the distribution of the altitude and temperature of the tropopause over the earth in January and July. The author has made a comparison of peculiarities of characteristics of the tropopause in the northern and southern hemispheres and has established the principal patterns of seasonal changes. The mean seasonal and annual values of altitude and temperature of the tropopause are computed for the entire earth, the northern and southern hemispheres.

[Text] Planetary investigations of distribution of the tropopause (especially the characteristics of its altitude and temperature) are acquiring great importance in connection with solution of a number of theoretical problems (in particular, in solution of schemes of general circulation of the atmosphere) and, in addition, are necessary for meeting modern practical requirements (for example, in aviation). However, until now the long-term meteorological regime of the tropopause as a whole for the earth has been studied inadequately. In 1958 an attempt was made to represent the climatography of tropopause pressure and temperature in the zone 80°N-60°S [8], but these maps give an extremely general picture because use was made of a thin network (for example, for the territory of the Soviet Union -- five stations) and nonuniform observations. Two maps of distribution of the mean altitude of the tropopause over the entire earth for December-February and June-August were included in a major multivolume climatological publication [7]. Unfortunately, that publication did not give information either about the network of stations used in preparing the maps or about the observation period. The tropopause is considered here in general, without separation into geographical types (polar and tropical), which is inadequately

sound. From the distribution of isohypses it can be concluded that use was made of a short series of observations for a limited network of stations because the configuration of the isohypses and even the positioning of the centers do not agree with publications based on adequately reliable materials [1, 2, 4, 9].

In further developing earlier studies [1, 3], we compiled maps of the distribution of altitude and temperature of the tropopause over the entire earth on the basis of aerological observations by 350 stations (280 in the northern hemisphere and 70 in the southern hemisphere) for a 10-year period. Over the continents in the temperate zone the stations were distributed uniformly; the coverage in the equatorial regions was poorer; the network over the oceans was very thin. The processing and generalization methods used were the same as for stations in the USSR [3].

The accuracy in computing the mean values of characteristics of the tropopause for the most part is 0.1-0.3 km for altitude and for temperature 0.1-0.5°C.

Now we will analyze the peculiarities of the distribution of mean altitude and temperature of the tropopause using maps for January and July (Fig. 1).

In both hemispheres one can see common patterns corresponding to the distribution of heat and cold in the troposphere: small altitudes in the polar latitudes, an increase toward the low latitudes with maxima in the equatorial region. In the polar and temperate regions in both hemispheres there is only a polar (low and warm) tropopause, whereas in the tropical and equatorial latitudes -- only a tropical (high and cold) tropopause. In the subtropical latitudes it is possible to observe both polar and tropical tropopauses.

We note the different character of distribution of hemispheric isohypses and isotherms -- smooth, without great latitudinal variations in the southern hemisphere and an alternation of ridges and troughs (with formation of closed centers) in the northern hemisphere.

An influence of the underlying surface is apparent. In the southern hemisphere the underlying surface is relatively uniform (water occupies 81% of the entire area); in the northern hemisphere water accounts for 61% of the area and land accounts for 39% of the area. In addition, the distribution of land and water is not the same for different circles of latitude (Table 1). In the southern hemisphere considerable expanses of land fall in the polar regions; the land area is relatively great (20-24%) in the tropical and equatorial latitudes; but in the temperate zone, where the seasonal differences in the thermal regime of the continents and oceans are particularly strong, there is virtually no land (0-4% of the area). In the northern hemisphere the greatest land areas fall in the temperate latitudes (45-61%); in the equatorial regions its areas are approximately the same as in the southern hemisphere; the least land area is found in the polar region.

Table 1

Distribution of Land (%) by Circles of Latitude in Northern and Southern Hemispheres

Полушария 2	Широта, *град* 1																	
	90	80	75	70	65	60	55	50	45	40	35	30	25	20	15	10	5	0
3 Северное	0	20	24	53	76	61	55	58	51	45	42	43	37	32	26	24	22	22
4 Южное	100	100	100	71	1	0	1	2	3	4	9	20	23	24	23	20	24	

KEY:
1. Latitude, degrees
2. Hemispheres
3. Northern
4. Southern

Tropopause in January

In the northern hemisphere extensive continents, Eurasia and North America, are cooled in winter; the surface waters of the Pacific and Atlantic Oceans are relatively warm, which leads to a disruption of the latitudinal variation of isohypses in the polar tropopause with the formation of troughs over the continents and ridges over the oceans (Fig. 1a). A ridge in the Atlantic Ocean is particularly clearly expressed (a reflection of the influence of the Gulf Stream). The formation of a closed region of the low tropopause over East Asia is attributable to the joint influence of monsoonal and circulation factors -- cooling of the continent and predominant cyclonic activity (Aleutian Low). Under the influence of cooling two other close regions of the low tropopause are formed -- in the Central and Canadian-Greenland sectors of the Arctic.

In the southern hemisphere in January there is only one closed region in the low polar tropopause -- over Antarctica; the isohypses of the polar tropopause rather uniformly encircle the globe.

In the low latitudes of the northern hemisphere the polar tropopause is observed near 15°N; in the eastern part of the Atlantic Ocean -- even near 5°N; in the southern hemisphere it does not penetrate into such low latitudes (to 22-24°S). Accordingly, the tropical tropopause in the southern hemisphere is traced in the higher latitudes (to 52-53°S) than in the northern hemisphere (38-42°N).

Thus, in January in the subtropical and partially in the temperate region it is possible to observe both polar and tropical tropopauses. This is the so-called "discontinuity" zone, playing an important role in circulatory

processes: jet streams are associated with it and in this zone there is an intensified air exchange between the stratosphere and troposphere. The width of the "discontinuity" zone is greater in the southern hemisphere (3,000-3,200 km) than in the northern hemisphere (for the most part 2,400-2,700 km); in the southern hemisphere it is displaced into the higher latitudes by 800-1,300 km in comparison with the northern hemisphere.

The temperature field of the tropopause in winter is characterized by a uniform distribution in the southern hemisphere and a complex pattern of isotherms in the northern hemisphere (Fig. 1c). In the southern hemisphere the interrelationship between altitude and temperature of the tropopause is: a low tropopause corresponds to a high temperature and a high tropopause corresponds to a low temperature. In the northern hemisphere there is a low compatability between the fields of altitude and temperature of the polar tropopause. It is possible to note a number of centers of high (or low) temperature of the tropopause, in many cases not coinciding with regions of small (great) altitudes. Examples of this is the region of cold over Greenland, high temperatures over southern Europe and Central Asia, the region of heat in southern Asia displaced southward relative to the closed region of the low tropopause, etc.

The temperature of the tropopause is influenced by the spatial position of the tropopause, its altitude. Also exerting an influence are the peculiarities of circulation (advection of the tropopause), and also the thermal state of the atmosphere, which frequently to great altitudes is dependent on the nature of the underlying surface, its heat capacity and heat conductivity. The alternation of the underlying surface with different thermal properties (for example, land-sea) leads to a curvature of the isotherms, formation of troughs and ridges. The combination of all factors, frequently acting ambiguously, can have the result that a low tropospause will be cold and a high tropopause will be warm. Therefore, the inverse correlation between altitude and temperature of the tropopause (high tropopause - low temperatures, low tropopause - high temperatures) is not always observed and not in all regions [5].

Naturally, in the southern hemisphere, where the surface is more uniform, the tropopause isotherms are smooth. It must also be taken into account that the influence of the underlying surface has a greater effect on the temperatures of the low polar tropopause and a lesser effect on the temperatures of the high tropical tropopause.

In both hemispheres the temperature of the tropical tropopause decreases from the subtropical latitudes to the equator, where there are (primarily in the southern hemisphere) three closed regions with a temperature below -84°C: over the Indian Ocean, in the eastern and western parts of the Pacific Ocean, which correspond to closed regions of great altitudes (more than 17 km).

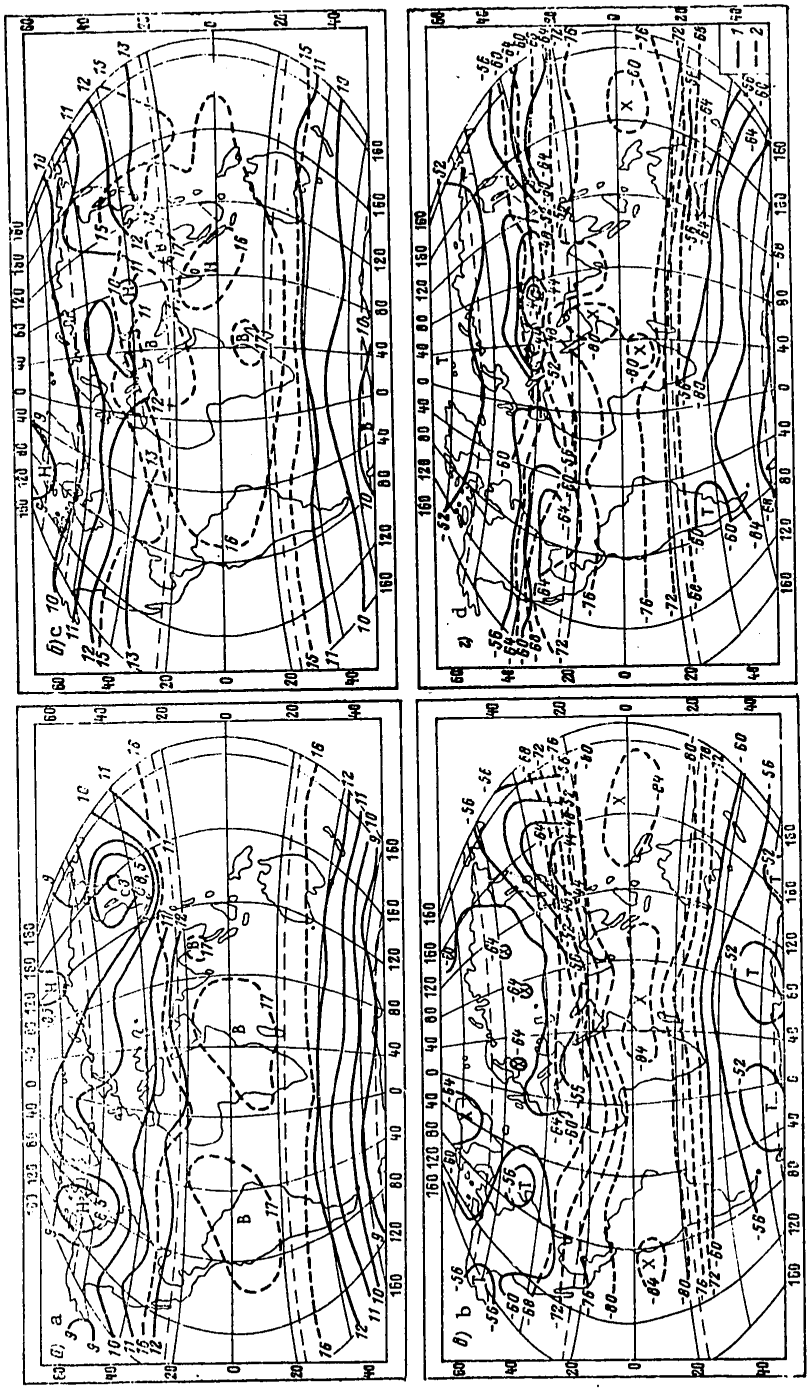

Fig. 1. Distribution of mean altitude (a, b) and mean temperature (c, d) of tropopause in January (a, c) and July (b, d). 1) isolines of polar tropopause, 2) isolines of tropical tropopause

Tropopause in July

In the northern hemisphere (Fig. 1b) the center of the low polar tropopause (altitude less than 9 km) is situated in the Canadian-Greenland sector of the Arctic. An increase in altitude occurs to the south. An exception is the latitudinal region of low tropopause altitudes in regions of the eastern Mediterranean Sea - Northern Caucasus - Central Asia. Existing hypotheses for the time being are unable to explain this phenomenon, but a definite influence is exerted by the great mountain systems situated to the south of this trough in the tropopause.

In the southern hemisphere over Antarctica there is a region of increased altitudes of the polar tropopause (more than 10 km), the reasons for whose formation also for the time being have not found a satisfactory explanation [6]. It can be postulated that in winter, under polar night conditions, a local tropopause is not formed, but there is only advection of the tropopause from the lower latitudes. In winter in the southern hemisphere the advective tropopause is situated higher than the tropopause in the corresponding season in the northern hemisphere where it is formed over the cooled continents. In addition, in the northern hemisphere in the winter there is dominance of a circumpolar vortex, also exerting an influence on the decrease in tropopause altitudes, whereas in Antarctica there is predominance of high-pressure ridges. It is possible that an influence is also exerted by the great elevation of the ice continent.

In July in the northern hemisphere it is summer and therefore everywhere (except in the region of the anomaly eastern Mediterranean Sea - Central Asia) the altitude of the polar tropopause, in comparison with winter, increases, whereas in the southern hemisphere everywhere (except in Antarctica) it decreases. These changes are associated with the annual variation of insolation and are attributable to a change in the mean temperature of the troposphere.

In agreement with the annual variation of mean temperature of the troposphere there is also a decrease in the altitude of the tropical tropopause. In the equatorial zone (from the equator to 12-20°N) in the northern hemisphere in July, in comparison with January, the tropical tropopause lies lower, and in the higher latitudes its altitude increases. As was indicated earlier in [4], the lowering of the tropopause in the equatorial region of the northern hemisphere in July, in comparison with January, occurs due to the increasing distance from the earth to the sun. This factor also is responsible for the equatorial centers of the high tropical tropopause which are less intense and extensive than in January.

The distribution of tropopause temperature is opposite and changes in different seasons (Fig. 1d). In winter (January in the northern and July in the southern hemispheres) the polar tropopause is characterized by a temperature increase from the high to the low latitudes; in summer a decrease in temperature of the polar tropopause from the high to the low latitudes is more indicative.

In winter in the polar region under polar night conditions there is an intensive cooling of the air which is responsible for low tropopause temperatures. In the temperate latitudes the insolation is quite great, and despite the fact that the polar tropopause here lies higher than in the polar region, its temperature is greater. In summer the polar regions under polar day conditions receive a sufficiently great quantity of solar energy, and therefore with a low position of the tropopause its temperature is high. In the temperate latitudes, in comparison with the polar latitudes, the tropopause lies far higher, which leads to an adiabatic decrease in its temperature which is not compensated by the influence of other factors.

In the polar region of the southern hemisphere the temperature of the tropopause is lower than in the corresponding region of the northern hemisphere. The cooling influence of the Antarctic ice continent is expressed here, whereas in the northern hemisphere there are warmer water masses under the ice of the Arctic Ocean.

Table 2

Mean Latitudinal Altitudes and Temperatures of Tropopause and Their Intra-annual Amplitudes

	1 Северная широта, *град*				2 Экватор	Южная широта, *град* 3			
	70	50	30	10		10	30	50	70
	4 Высота, *км*								
6 Январь	9,1	9,7	12,8	16,7	16,9	16,9	15,4	11,1	8,6
7 Апрель	8,6	10,1	13,4	16,7	17,0	16,9	14,5	10,6	8,8
8 Июль	10,1	11,5	15,5	16,0	16,2	16,2	13,3	10,0	9,8
9 Октябрь	9,3	10,8	15,3	16,2	16,4	16,3	14,1	10,3	9,9
10 Год	9,3	10,5	14,2	16,5	16,7	16,6	14,1	10,5	9,3
11 Амплитуда	1,5	1,8	2,7	0,7	0,8	0,7	2,1	1,1	1,3
	5 Температура, °С								
6 Январь	—61,3	—58,6	—62,0	—80,7	—84,0	—83,1	—69,4	—55,8	—52,3
7 Апрель	—54,9	—57,1	—64,6	—80,6	—82,7	—82,0	—66,3	—55,9	—57,2
8 Июль	—51,9	—54,2	—70,0	—75,5	—78,6	—77,6	—62,2	—60,6	—68,5
9 Октябрь	—56,5	—56,8	—68,9	—78,8	—80,2	—79,1	—61,1	—58,2	—66,2
10 Год	—56,1	—55,9	—66,3	—79,1	—81,4	—80,2	—64,6	—57,1	—60,9
11 Амплитуда	9,4	4,4	—8,0	5,2	5,6	5,8	8,3	4,8	16,2

KEY:

1. North latitude, degrees
2. Equator
3. South latitude, degrees
4. Altitude, km
5. Temperature, °C
6. January
7. April
8. July
9. October
10. Year
11. Amplitude

We investigated the general patterns of distribution of altitude and temperature of the tropopause over both hemispheres and also the earth as a whole. From the climatic maps of distribution of the tropopause at the points of intersection of a geographic grid with an interval of 10° in latitude and 10° in longitude we read the altitudes and temperatures of the tropopause (without taking geographic type into account) and computed the mean latitudinal values. Table 2 gives these values for the equator and the circles of latitude 10, 30, 50 and 70° in the northern and southern hemispheres.

The greatest annual amplitudes of altitude of the tropopause are noted in the subtropical regions of both hemispheres where there is an alternation of the two geographic types of tropopause (polar and tropical); the greatest temperature amplitudes are in the polar and subtropical zones.

A direct variation in the altitude of the tropopause (maximum -- in summer of the corresponding hemisphere, minimum -- in winter) is noted in the temperate and subtropical regions. In the subtropics of both hemispheres the temperature variation is inverse the variation in altitude (minimum -- in summer, maximum -- in winter), whereas in the temperate region there are synchronous changes: in summer a high tropopause corresponds to its high temperature; in winter, with low altitudes, the tropopause is cold.

Changes in altitude and temperature of the tropopause in the temperate and subtropical regions are asynchronous by hemispheres -- when there are high values in the northern hemisphere there are low values in the southern hemisphere (and vice versa).

In the polar region of the northern hemisphere the minimum of tropopause altitude is in spring and the maximum is in summer. In the temperature variation the minimum is noted in winter and the maximum in summer. In the high latitudes of the southern hemisphere the annual variation in altitude of the tropopause is singular: the minimum is in summer (January) and the maximum is in spring (October). However, here the temperature of the tropopause has an annual variation similar (with respect to seasons) to changes in the high latitudes of the northern hemisphere: a maximum in summer and a minimum in winter.

In the low latitudes of both hemispheres the annual variation of altitude is synchronous: the maximum falls in January-April, the minimum falls in July. It was noted earlier that the reason for the minimum altitudes of the tropical tropopause in summer in the low latitudes of the northern hemisphere is the increasing (in comparison with winter) distance from the earth to the sun, which leads to a singularity of the annual variation, common with the variation in the southern hemisphere. The tropopause temperature in the low latitudes changes inversely to the altitude variation and therefore in the equatorial zone of both hemispheres the temperature maximum falls in July and the minimum in January.

We carried out computations of the mean seasonal and annual altitudes and temperatures of the tropopause for the entire earth and for hemispheres. In the southern hemisphere the altitude varies little by seasons (from 11.9 to 12.2 km), in the northern hemisphere -- by 1 km (from 11.6 km in winter and spring to 12.6 km in summer). On the whole the mean altitudes for the hemispheres were close (12.0 km in the northern hemisphere and 12.1 km in the southern hemisphere). The tropopause temperature in the northern hemisphere is far greater than in the southern hemisphere (-60.6 and -63.6° C respectively). By seasons in the northern hemisphere it varies from -58.1°C in summer to -62.1°C in winter; in the southern hemisphere -- from -60.3 to -65.5°C respectively. The mean tropopause temperature for the entire earth is -62.1°C (by seasons from -61.0 to -62.9°C).

BIBLIOGRAPHY

1. ATLAS KLIMATICHESKIKH KHARAKTERISTIK TROPOPAUZY NAD SEVERNYM POLUSHARIYEM (Atlas of Climatic Characteristics of the Tropopause Over the Northern Hemisphere), edited by Z. M. Makhover, Moscow, Gidrometeoizdat, 1973.

2. AEROKLIMATICHESKIY ATLAS TROPOPAUZY YUZHNOGO POLUSHARIYA I TEMPERATURNOGO POLYA ZEMLI (Aeroclimatic Atlas of the Tropopause in the Southern Hemisphere and the Earth's Temperature Field), edited by Academician V. V. Shuleykin, Leningrad, Gidrometeoizdat, 1968.

3. Makhover, Z. M., "Altitude and Temperature of the Tropopause Over the Territory of the USSR," METEOROLOGIYA I GIDROLOGIYA (Meteorology and Hydrology), No 3, 1971.

4. Makhover, Z. M., "Altitude and Temperature of the Tropopause Over the Northern Hemisphere," METEOROLOGIYA I GIDROLOGIYA, No 7, 1972.

5. Makhover, Z. M., Nudel'man, L. A., "Correlation Between Altitude and Temperature of the Tropopause," TRUDY NIIAK (Transactions of the Scientific Research Institute of Aeroclimatology), No 66, 1970.

6. Chuprina, V. I., "Characteristics of the Tropopause Over the Southern Hemisphere," TRUDY NIIAK, No 59, 1969.

7. Crutcher, H. L., "Temperature and Humidity in the Troposphere," WORLD SURVEY OF CLIMATOLOGY, VOL 4. CLIMATE OF THE FREE ATMOSPHERE, Amsterdam-London-New York, Elsevier Publishing Company, 1969.

8. Goldie, N., Moore, J. G., Austin, E. E., "Upper Air Temperature Over the World," GEOPHYSICAL MEMOIRS, No 101, 1958.

9. Ramandham, R., Subbaramayja, I., Rao, N., Jaganmohana, Patnik, I. L., "The Tropopause Over India," Vol 75, No 4, 1969.

UDC 551.510.41;551.521.32

POSSIBILITIES OF DETERMINING CO AND N_2O PROFILES FROM MEASUREMENTS ON SLANT PATHS IN THE MICROWAVE SPECTRAL RANGE

Moscow METEOROLOGIYA I GIDROLOGIYA in Russian No 12, Dec 79 pp 40-48

[Article by Candidates of Physical and Mathematical Sciences Yu. M. Timofeyev and V. V. Rozanov, Leningrad State University, submitted for publication 20 April 1979]

Abstract: On the basis of numerical modeling the authors examine the possibilities of using the results of measurement of transparency and outgoing thermal radiation of the atmosphere on slant paths in the microwave spectral range for the purpose of reconstructing the vertical profiles of CO and N_2O content. A method is proposed and investigated. It makes it possible to obtain the atmospheric transmission function for the entire path of radiation formation on the basis of data from measurements of outgoing radiation in slant directions. The accuracy of the method (with $h_0 \geqslant 10$ km and in the absence of measurement errors) is 10^{-3}-10^{-2} of the transmission value. The limiting accuracy in reconstructing the CO and N_2O content profiles is quite high and is approximately 0.7% and 4% respectively in the altitude range 5-45 km. The "real" accuracy in determining the CO and N_2O profiles (with errors in measuring transparency of 1%, which is equivalent to the errors in measuring outgoing radiation of 2°C) is 15-20% and 10-30% in the altitude range 5-35 km.

[Text] Introduction. Radiophysical methods are being used more and more extensively in order to obtain various kinds of information on the parameters of the physical state of the atmosphere [1, 6]. Indirect methods have been developed and are being successfully developed for determining

the vertical profiles of temperature and humidity when registering radioemission both by ground facilities and by apparatus carried aboard artificial earth satellites [3, 4, 20]. During recent years there has been intensive development of satellite methods for indirect measurements of the vertical profiles of the content of small gas components in the atmosphere for the purpose of creating a global system for observations of the state of the ozonosphere. For example, in a number of studies [8, 9, 11, 12] there was an investigation of the potential accuracy of indirect methods based on an interpretation of measurements of transparency and thermal radiation in the infrared (IR) range on slant paths. It should be noted that there are possibilities for the solution of similar inverse problems in the microwave spectral range as well. The physical basis for this is the presence of rotational absorption spectra of small gas components. This spectral range has already been successfully used for surface measurements of the total content of O_3, N_2O and CO [2, 18].

In a study by the authors of [19] there was an analysis of the results of computations of atmospheric transparency and outgoing radiation (brightness temperature) in different CO and N_2O absorption rotational lines on slant paths. These computations made it possible to carry out a preliminary selection of the optimum absorption lines and spectral resolution, to study the influence of absorption in the wings of the H_2O and O_3 lines and also to estimate the variations of transparency and brightness temperature with different variations of atmospheric parameters. The results of solution of the direct problem indicated the considerable possibilities (in contrast to the considerations expressed in [12]) of use of the microwave range and the considered geometry of measurements from an artificial earth satellite in the case of an indirect determination of the composition not only of the stratosphere, but also the upper troposphere even when there are crystalline clouds present on the path of the ray. All this makes more timely a more careful analysis of the accuracy of the indirect method on the basis of numerical modeling of solution of the inverse problem.

Method for Solution of Inverse Problem and Details of Computations

The mathematical basis for solution of inverse problems in the thermal range is the well-known integral form of the transfer equation, which for the considered geometry can be written in the following way:

$$I_{\Delta\nu}(h_0) = \int_{s_1}^{s_2} B_{\bar{\nu}}[T(s)] \frac{\partial P_{\Delta\nu}(s_2, s; h_0)}{\partial s}\, ds. \qquad (1)$$

Here $I_{\Delta\nu}(h_0)$ is the intensity of atmospheric emission (erg/(cm^2·sec·sr·cm^{-1} cm^{-1})); s is a coordinate read along the sighting ray; s_1 and s_2 are the coordinates of the points of entry of the ray into the atmosphere and its emergence; $B_{\bar{\nu}}[T(s)]$ is the Planck function at the temperature T(s) and with the frequency $\bar{\nu}$; $P_{\Delta\nu}(s_2, s; h0)$ is the atmospheric transmission function from the point s_2 to the point with the coordinate s; h_0 is the minimum

distance of the ray from the planetary surface.

In order to determine the vertical profiles of the content of absorbing components in numerical experiments use was made of a method proposed and investigations reported (for the IR range) in [11]. In this method the solution of the inverse problem is broken down into two stages:

1) Determination of the transmission function for the sought-for i-th absorbing component for the entire path of radiation formation -- $P^i_{\nabla\nu}(h_0)$ (henceforth the superscript i will be assigned to the absorption lines for CO or N_2O and the superscript "O" will be assigned to the O_2 line, the subscript is omitted) is possible using simultaneous measurements of the outgoing radiation (brightness temperatures) in the oxygen lines, the content of oxygen in the atmosphere being known, and the sought-for i-th absorbing component.

2) Solution of the nonlinear operator equation $\vec{P}^i = \hat{C}^i[\hat{A}\vec{q}_i]$ relative to the sought-for $q_i(s)$ profile.

In the modeling of solution of the inverse problem it was assumed that measurements of outgoing radiation are made in different CO and N_2O absorption lines and also in the oxygen line at λ = 2.54 mm with a spectral resolution of the measurements $\Delta\nu$ = 20 MHz. Then, in accordance with the method proposed in [11], the transmission function $P^i(h_0)$ is determined by the following expression:

$$P^i(h_0) = 1 - \frac{I^i(h_0)}{B^i[T^0_э(h_0)]}, \qquad (2)$$

[э = ef(fective)] where the effective brightness temperature in the oxygen line T^0_{ef} is equal to

$$T^0_э(h_0) = \frac{C_2\nu_0}{\ln\left[1 + \frac{C_1\nu_0^3(1 - P^0(h_0))}{I^0(h_0)}\right]}, \qquad (3)$$

where C_1 and C_2 are known constants in the formula for the Planck function.

As is well known, the transmission function $P^i(h_0)$, obtained on the basis of expression (2), is related to the sought-for profile of the absorbing gas by the following expression [5]:

$$P^i(h_0) = \int_{(\Delta\nu)} \varphi(\nu - \nu') \exp\left[-\int_{s_1}^{s_2} q_i(s)\,\rho(s)\,S(s)\,f(\nu, \nu_0; s)\,ds\right] d\nu, \qquad (4)$$

where $\rho(s)$ is air density; S(s) is the intensity of the absorption line; $f(\nu, \nu_0; s)$ is the form of the line contour; $q_i(s)$ is the mixing ratio of the sought-for gas; $\varphi(\nu - \nu')$ is the instrument function for the spectral instrument; ν_0 is the position of the center of the spectral line.

In order to determine the $q_i(s)$ profile we used an iteration method for solving the linearized equation (3), which has the following form:

$$\delta P^i(h_0) = \int_{S_1}^{S_2} \left\{ \int_{(\Delta\nu)} \overline{P^i}(h_0)\, \rho(s)\, S(s)\, f(\nu, \nu_0; s)\, \varphi(\nu - \nu')\, d\nu \right\} \delta q_i(s)\, ds, \quad (5)$$

where $\delta P^i(h_0) = P^i(h_0) - \overline{P^i}(h_0)$ is the deviation of the measured atmospheric transmission from the mean for the target altitude h_0; $\delta q_i(s) = q_i(s) - \overline{q_i}(s)$ is the deviation of the true profile of the absorbing gas from the mean.

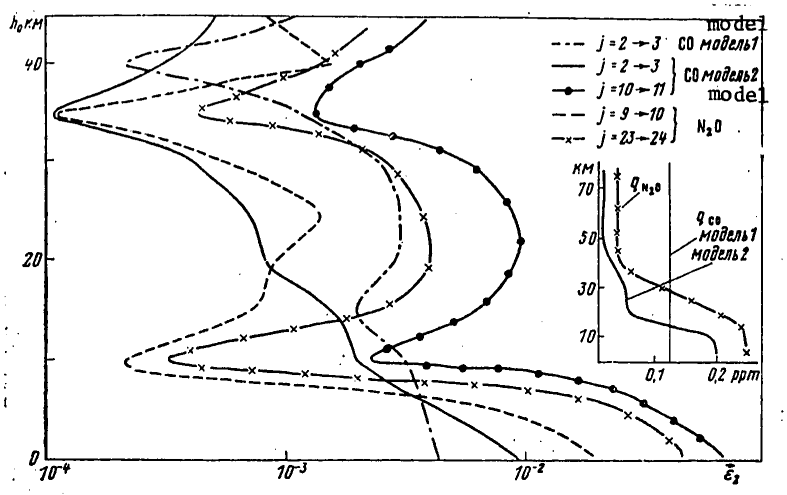

Fig. 1. Dependence of errors in excluding the influence of temperature $\vec{\varepsilon}_2$ from the target altitude h_0 for different CO and N_2O absorption lines ($f_{2\to3}$ = 11.53; $f_{10\to11}$ = 42.23; $f_{9\to10}$ = 8.36; $f_{23\to24}$ = 20.05 cm^{-1}).

Equation (5) is the initial equation for constructing a linear mathematical model which after use of quadrature formulas assumes the form

$$\delta\vec{P} = A\,\delta\vec{q}, \quad (6)$$

where $\delta\vec{P}$ is a vector the number of whose components is equal to the number of the target altitudes $h_0(m)$, $\delta\vec{q}$ is the sought-for vector of the dimensionality n, A is a matrix of the dimensionality m x n.

In numerical experiments whose results are analyzed below we used the following initial information:

1) The parameters of individual spectral lines of CO and N_2O were computed using the known method [10]. Similar data for the O_2 line with λ = 2.54 mm were taken from [16]. The form of the line contour was selected in accordance with [7].

2. Data on the vertical profiles of temperature, air density and the content of water vapor and ozone were taken from a model of the standard atmosphere [17]. The vertical profiles of the distribution of the content of CO (model 2) and N_2O were constructed on the basis of an analysis of studies [13-15, 21] and are cited in the insert in Figure 1; they were used from methodological considerations for study of the influence of the type of profile of reducible gas on the accuracy of solution of the inverse problem.

Analysis of Accuracy of Indirect Method

The accuracy in determining the vertical profiles of the content of gas components of the atmosphere is dependent on many factors: errors in measuring thermal radiation or atmospheric transparency, accuracy of the method for excluding the influence of temperature (when making measurements of thermal radiation), errors in linearization and errors in solving the linear system (6), accuracy in stipulating the radiation model, etc. Taking into account that expression (2) has an approximate character, and also the presence of errors of a different nature, the linear model (6) must be written in the following form:

$$\delta \vec{F} = A \delta \vec{q} + \vec{\varepsilon}_1 + \vec{\varepsilon}_2 + \vec{\varepsilon}_3. \qquad (7)$$

The use of the two stages in solving the inverse problem makes it possible on the basis of one expression (7) to analyze the accuracy in the reconstruction of the vertical profiles of content in both transparency measurements and in measurements of atmospheric outgoing radiation on slant paths.

Depending on the type of considered satellite experiment the errors $\vec{\varepsilon}_k$ (k= 1, 2, 3) on the right-hand side of equation (7) have the following sense. In the case of measurements of thermal radiation $\vec{\varepsilon}_1$ is the error in determining atmospheric transparency (using formula (2)), caused by random errors in measuring radiation $\vec{\varepsilon}_I$ (frequently expressed in terms of the brightness temperature of radiation -- $\vec{\varepsilon}_T$, $\vec{\varepsilon}_2$ are the systematic errors arising with conversion from the values $I^i(h_0)$ to the values $P^i(h_0)$ (errors in "excluding the influence of temperature"). In the case of measurements of atmospheric transparency $\vec{\varepsilon}_1$ are the errors in measuring transparency and $\vec{\varepsilon}_2 = 0$. Finally, $\vec{\varepsilon}_3$ in both types of experiments are linearization errors which are minimized in the process of iteration solution of system (6).

Relationship between random errors in measuring radiation $\vec{\varepsilon}_1$ (or $\vec{\varepsilon}_T$) and errors in determining $P^i(h_0)$ ($\vec{\varepsilon}_1$). Taking into account the relationship between the I^i and I^0 values (formula (2, 3)), it is easy to obtain the following relationship between the values of the absolute error in measuring brightness temperature σ_T and the errors in determining atmospheric transparency:

$$\sigma_P = \frac{\sigma_T}{B^i[T_э^0]}\left[\left(\frac{\partial I^i}{\partial T^i}\right)^2 + \left(\frac{\partial B^i[T_э^0]}{\partial T_э^0}\frac{I^i}{B^i[T_э^0]}\frac{\partial T_э^0}{\partial I^0}\frac{\partial I^0}{\partial T^0}\right)^2\right]^{1/2}, \quad (8)\ *$$

where T^i and T^0 are the brightness temperatures in the absorption lines CO (N_2O) and O_2 respectively.

Numerical computations of the parameters entering into (8) indicated that in the region of target altitudes h_0 = 10-45 km the error in measuring radiation for the spectral range which we considered, expressed in terms of brightness temperature and equal to 2 K, corresponds on the average to an error in transmission values $\sigma_P = 9 \cdot 10^{-3}$.

Accuracy in excluding influence of temperature. The value of the systematic errors $\vec{\varepsilon}_2$, as follows from formula (2), is determined by the difference in the effective temperatures of radiation in the absorption lines of the sought-for gas (CO or N_2O) and oxygen. It can be shown that in a general case the $\vec{\varepsilon}_2$ value is determined by the following relationship:

$$\varepsilon_2^i(h_0) = I^i(h_0)\left\{\frac{B^i[T_э^i(h_0)] - B^i[T_э^0(h_0)]}{B^i[T_э^i(h_0)]\,B^i[T_э^0(h_0)]}\right\}, \quad (9)$$

[э = ef(fective)]

where the superscript i denotes the components of the composition (CO or N_2O), T_{ef} is determined using formulas similar to formula (3). It follows from expression (9) that ε_2 is the smaller the lesser the quantity of outgoing radiation and the weaker is the dependence of the Planck function on temperature.

Figure 1 shows the dependences $\vec{\varepsilon}_2(h_0)$ for the centers of different CO and N_2O absorption lines. It follows from the figure that in most cases $\vec{\varepsilon}_2 < 10^{-2}$ and only with $h_0 < 10$ km for some lines there is a marked increase in $\vec{\varepsilon}_2$ caused by the different nature of formation of outgoing radiation in the lines of CO or N_2O and oxygen at these altitudes. It should be emphasized that in the range of altitudes 10-40 km of interest to us for a number of spectral lines the $\vec{\varepsilon}_2$ values are approximately 10^{-3}, which indicates a high accuracy of the proposed method for conversion from the $I^i(h_0)$ values to the $P^i(h_0)$ values. The cited data pertain to the case of exclusion of the influence of temperature for the intensity of radiation. However, it can be shown that in the case of measurements with a finite angular resolution the accuracy of the method changes little since there is retention of an identical nature of the formation of outgoing radiation in the lines O_2 and CO (N_2O), although in a somewhat lesser altitude range h_0 (15-40 km).

---

* It is assumed that the measurements in the lines of oxygen and the small gas component have an identical accuracy.

Limiting accuracy of solution of inverse problem. Now we will give the results of solution of the inverse problem of reconstructing the vertical profiles $q_i(s)$ for the case of an isothermic atmosphere ($\vec{\varepsilon}_2 = 0$), absence of random measurement errors ($\vec{\varepsilon}_1 = 0$) and precise allowance for the influence of water vapor and ozone. This makes it possible to evaluate the limiting accuracy in reconstructing the vertical profiles of CO and N_2O content.

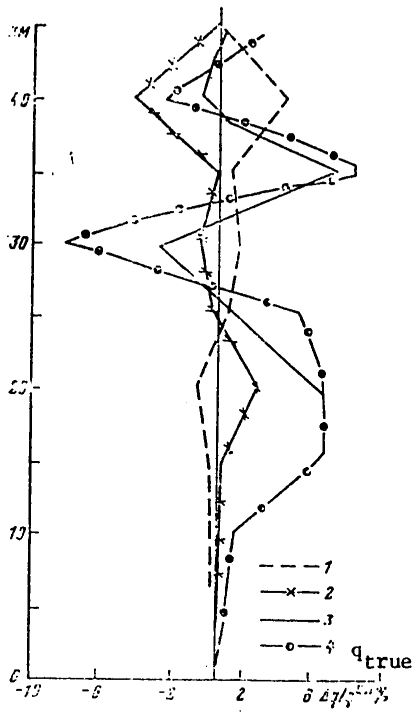

Fig. 2. Limiting accuracy in solution of inverse problem. 1) relative error in reconstructing profile of CO content, j = 2→3, model 1, $\bar{q}$ = 0.06 ppm; 2) same, only for initial approximation $\bar{q}$ = 0.18 ppm; 3) relative error in reconstructing profile of N_2O content, j = 23→24, $\bar{q}$ = 0.25 ppm; 4) same, only for initial approximation $\bar{q}$ = 0.25 ppm; 4) same, only for initial approximation $\bar{q}$ = 0.025 ppm.

Figure 2 presents the relative errors (relative to the true $q_i(s)$ profiles) in reconstructing $q_{N_2O}(s)$ and $q_{CO}(s)$ (model 1) when using measurements in the absorption lines j = 23→24 and j = 2→3 respectively and two different initial approximations $\bar{q}_i(s)$. The figure shows that the maximum errors in reconstruction can attain approximately 8% for N_2O (h_0 = 30-35 km) and 4%

for CO (h_0 = 40 km). The mean reconstruction errors for all h_0 are about 4.1 and 0.7% respectively. The result indicates a quite good conditionality of the linear system (6). The figure shows also that the change in the initial approximation to a 100% solution exerts little influence on the limiting accuracy of the method.

"Real" accuracy of the indirect method. For a quantitative characterization of the accuracy in reconstructing the profiles of small gas components we then use a sample mean square relative error $\delta(z)$ computed using the formula

$$\delta(z) = \sqrt{\frac{\frac{1}{10}\sum_{l=1}^{10}[q^{\text{ИСТ}}(z) - q_l^{\text{В}}(z)]^2}{(q^{\text{ИСТ}}(z))^2}}, \qquad (10)$$

[ИСТ = true]

where $q^{true}(z)$ and $q^{rec}(z)$ are the true and reconstructed values of the mixing ratio of the sought-for gas at the altitude z (l is the number of the random error record). The reconstruction accuracy characteristics cited below were obtained when using measurements of transparency for the level of random measurement errors σ_p = 0.01, and when using measurements of thermal radiation for the level of random measurement errors $\sigma_T \approx 2$ K and systematic errors in excluding the influence of temperature of about $2 \cdot 10^{-3}$ of transparency.

Figure 3 shows the dependences $\delta(z)$ with the above-mentioned measurement error for different conditions of numerical experiments. A common peculiarity in the behavior of all the $\delta(z)$ curves is an appreciable increase in the error in reconstruction when $z \geqslant 30$ km. Whereas in the altitude range 5-30 km the relative errors for the most part are 10-30%, when $z > 30$ km they can attain 50 or more percent. This phenomenon is caused by a rapid increase in atmospheric transparency with an increase in h_0 and thereby a decrease in the relative accuracy of measurements. An increase in the accuracy of reconstruction can be attained by an increase in spectral resolution or the use of stronger absorption lines. For example, transition from the CO line j = 2→3 to the stronger line j = 10→11 makes it possible to increase the accuracy appreciably (compare curves 2 and 4) and reconstruct the CO content when $z > 15$ km.

Comparison of curves 1 and 4 makes it possible to analyze the accuracy of the method in dependence on the type of sought-for profile. It follows from a comparison of the data in Fig. 3 (curves 1 and 4) that the relative errors in reconstructing the altitude-variable CO profile (model 2) can be several times greater than for the constant profile (model 1). This phenomenon was caused, in particular, by the considerably lesser absorption values in model 2 (compare models 1 and 2) and an increase in the relative measurement error.

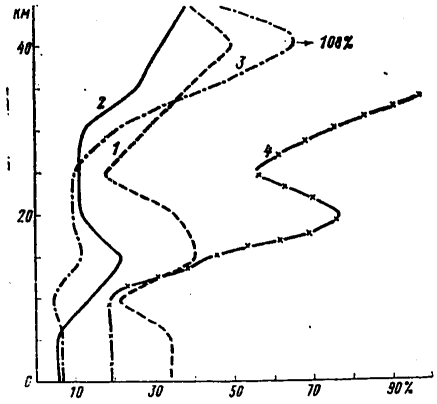

Fig. 3. Mean square errors in reconstructing (%) vertical profiles of CO and N_2O content.

Influence on method accuracy due to temperature dependence A(T) and absorption by wings of the H_2O and O_3 lines. The temperature dependence of the kernels of the linearized equation (6) was governed by the dependence of the intensity and half-widths of the lines on temperature. Evaluations of the influence of the dependence A(T) on accuracy of solution of the inverse problem show that even in a case when the kernels are computed using temperature profiles corresponding to another season, the mean characteristics of accuracy in reconstruction change by only several percent. It is easy to avoid this worsening of accuracy by using information on T(z) present, for example, in measurements of radiation in the oxygen line.

On the basis of the results of solution of the direct problem [19] it can also be shown that when $h_0 \geqslant 20$ km the absorption of radiation by the wings of the water vapor and ozone lines can be taken into account with sufficient accuracy on the basis of mean climatic data. With lesser ray perigee altitudes there must be more complete information on the H_2O and O_3 content, which can be obtained with simultaneous measurements of transparency or thermal radiation in the corresponding absorption lines.

Summary. 1. In this paper we have proposed and investigated a method for obtaining the atmospheric transmission values for the entire path of formation of radiation from measurements of outgoing radiation in slant directions. It is shown that in the majority of cases with $h_0 \geqslant 10$ km the accuracy of this method is 10^{-3}–10^{-2} of the transmission values.

2. The limiting accuracy in reconstructing the profiles of content of N_2O and CO in the case of a spectral resolution $\Delta\nu = 20$ MHz is quite high in the considered experiments. The mean errors in reconstruction for the CO line $j = 2 \rightarrow 3$ are 0.7% and for the N_2O line $j = 23 \rightarrow 24$ -- 4.1% in the altitude range 5-45 km.

3. With errors in measuring atmospheric transparency of 1%, which is equivalent to the errors in measuring outgoing radiation of 2 K, the accuracy in determining the content of CO and N_2O is: CO -- 15-20% in the region of altitudes 5-35 km (j = 10→11, model 2), N_2O -- 10-30% in this same altitude range (j = 23→24). When using the transition j = 2→3 for reconstructing CO the reconstruction errors in the case $h_0 \geqslant 15$ km exceed 50%.

4. Allowance for the temperature dependence of the kernels of the corresponding integral equation, and also absorption in the wings of the H_2O and O_3 lines is possible with $h_0 \geqslant 20$ km without a loss in accuracy on the basis of climatological data. In the case of lesser altitudes h_0 it is necessary to have more precise information which can be obtained on the basis of additional measurements of transparency or thermal radiation in the corresponding absorption lines.

The cited results indicate a need for further study of the possibilities of using the microwave range for determining the characteristics of atmospheric composition and in particular, an examination of the instrumental possibilities of satellite measurements of transparency and thermal radiation for the considered measurement scheme.

*****

BIBLIOGRAPHY

1. Basharinov, A. Ye., Gurvich, A. S., Yegorov, S. T., RADIOIZLUCHENIYE ZEMLI KAK PLANETY (The Earth's Radioemission as a Planet), Moscow, Nauka, 1974.

2. Voronov, V. M., Kislyakov, A. G., Kukina, E. P., "Content of CO and N_2O in the Earth's Atmosphere from Observations of Their Rotational Spectral Lines," IZV. AN SSSR, FIZIKA ATMOSFERY I OKEANA (News of the USSR Academy of Sciences, Physics of the Atmosphere and Ocean), Vol 8, No 1, 1972.

3. Gurvich, A. S., Demin, V. V., "Determination of the Total Moisture Content in the Atmosphere According to Measurements on the Artificial Earth Satellite 'Cosmos-243'," IZV. AN SSSR, FIZIKA ATMOSFERY I OKEANA (News of the USSR Academy of Sciences)(Physics of the Atmosphere and Ocean), Vol 6, No 8, 1970.

4. Yershov, A. T., Lebskiy, Yu. V., Naumov, A. P., Plechkov, V. M., "Determination of the Vertical Temperature Profile from Ground Measurements of Terrestrial Radiation in the Region $\lambda = 5$ mm," IZV. AN SSSR, FIZIKA ATMOSFERY I OKEANA, Vol 11, No 12, 1975.

5. Kondrat'yev, K. Ya., Timofeyev, Yu. M., TERMICHESKOYE ZONDIROVANIYE ATMOSFERY SO SPUTNIKOV (Thermal Sounding of the Atmosphere from Satellites), Leningrad, Gidrometeoizdat, 1970.

6. Kondrat'yev, K. Ya., Rabinovich, Yu. I., Timofeyev, Yu. M., Shul'gina, Ye. M., MIKROVOLNOVOYE DISTANTSIONNOYE ZONDIROVANIYE OKRUZHAYUSHCHEY SREDY (Microwave Remote Sounding of the Environment), Obninsk, 1975.

7. Naumov, A. P., "Absorption of Radio Waves in the Earth's Atmosphere by Admixture Gases," IZV. VUZOV, RADIOFIZIKA (News of Colleges, Radiophysics), Vol 25, No 5, 1972.

8. Rozanov, V. V., Timofeyev, Yu. M., "Possibilities of Determining the Content of Small Gas Components in the Atmosphere from Satellites," METEOROLOGIYA I GIDROLOGIYA (Meteorology and Hydrology), No 11, 1974.

9. Rozanov, V. V., Timofeyev, Yu. M., "Possibilities of Determining the Content of N_2O and CH_4 in the Atmosphere on the Basis of Interpretations of Measurements of the Spectral-Angular Structure of Thermal Radiation," IZV AN SSSR, FIZIKA ATMOSFERY I OKEANA, Vol 11, No 10, 1975.

10. Townes, Ch., Shavlov, L., RADIOSPEKTROSKOPIYA (Radiospectroscopy), Moscow, IL, 1959.

11. Timofeyev, Yu. M., Rozanov, V. V., "Use of Measurements of Outgoing Thermal Radiation for Determining the Vertical Profiles of Small Gas Components in the Atmosphere," IZV. AN SSSR, FIZIKA ATMOSFERY I OKEANA, Vol 12, No 9, 1976.

12. Ludwig, C. B., Griggs, M., Malkus, W., Bartle, E. R., "Measurement of Air Pollutants from Satellites. I. Feasibility Considerations," APPL. OPTICS, Vol 13, No 6, 1974.

13. Goldman, A., Murcray, D. G., Murcray, F. H., Williams, W. J., "Balloon-Borne Infrared Measurements of the Distribution of N_2O in the Atmosphere," J. OPT. SOC. AMER., Vol 63, No 7, 1973.

14. Isakson, I. A., "The Production and Distribution of Nitrogen Oxides in the Lower Stratosphere," PURE AND APPL. GEOPHYS., Vol 106-108, 1973.

15. Junge, C. E., "The Cycle of Atmospheric Gases -- Natural and Man-Made," QUART. J. ROY. METEOROL. SOC., Vol 96, No 413, 1972.

16. McClatchey, R. A., Benedict, W. S., Glough, S. A., "Atmospheric Absorption Line Parameters Compilation," AFCRL-TR-75-0096, 26 June 1973, ENV. RES. PAPER, No 434.

17. McClatchey, R. A., Fenn, R. W., Salby, V. E., "Optical Properties of the Atmosphere (Third Edition)," AFCRL-72-0497, 24 Aug 1972, ENV. RES. PAPER No 411.

18. Simubakuro, F. I., Smith, P. L., Wilson, W. J., "Estimation of the Ozone Distribution from Measurement of Millimeter Wavelength Absorption," JGR, Vol 80, No 21, 1975.

19. Timofeyev, Yu. M., Rozanov, V. V., USE OF THE INFRARED MICROWAVE RADIATION FOR DETERMINING THE CONTENT OF MINOR GASEOUS CONSTITUENTS OF THE ATMOSPHERE. RADIATION OF THE ATMOSPHERE, Leningrad University Press, Leningrad, 1976.

20. Waters, J. W., Kunzi, K. F., Pettyjohn, R. L., Poon, K. L., Staelin, D. H., "Remote Sensing of Atmospheric Temperature Profiles With the Nimbus-5 Microwave Spectrometer," J. ATMOS. SCI., Vol 32, No 10, 1975.

21. Whitten, R. C., Sims, J. S., Turco, R. P., "A Model of Carbon Compounds in the Stratosphere and Mesosphere," JGR, Vol 78, No 24, 1973.

UDC 551.551.8

CHARACTERISTICS OF EXCEEDING OF A STIPULATED CONCENTRATION LEVEL IN A STATIONARY JET

Moscow METEOROLOGIYA I GIDROLOGIYA in Russian No 12, Dec 79 pp 49-56

[Article by O. I. Vozzhennikov, Institute of Experimental Meteorology, submitted for publication 20 April 1979]

Abstract: On the basis of a statistical model of a Laykhtman-Gifford jet the author has derived expressions for computing the frequency and mean duration of discharges of a concentration above a stipulated level at a fixed point in space. Methods for computing the parameters entering into these expressions are given.

[Text] At the present time one can hardly dispute the fact that the decisive influence of harmful substances on the organisms of living creatures and plants is exerted not so much by the mean background of the concentration of an impurity as by the presence of high (exceeding the maximum admissible concentration by several times) concentrations whose lifetime may be short in comparison with the observation time. In this connection the study of the spatial and temporal scales of fluctuations of the impurity is an important and timely problem. Unfortunately, in modern models of atmospheric contamination by industrial sources rather little attention is being devoted to allowance for fluctuations. The latter can be attributed both to the small number of theoretical studies devoted to this problem and the absence of reliable experimental data obtained under natural conditions.

In this article we propose a method for computing the number of exceedings of a stipulated level and the mean duration of the excess on the basis of the Gifford statistical model of a jet [2].

Formulation of Problem

We will examine a stationary jet from a point source in the surface layer of the atmosphere. We will assume that fluctuations of the concentration of impurity in the jet are caused by transverse (relative to the directions

of the mean wind) random oscillations of the jet axis. (Such random oscillations of the jet are frequently called meandering.) These random oscillations of the jet axis arise under the influence of turbulent eddies whose scales are comparable in magnitude with the characteristic width of the jet or are much greater than it. Due to the continuity of the turbulence spectrum in the atmosphere the meandering phenomenon will occur until the width of the jet exceeds the turbulence scale. In the latter case turbulence can be characterized by a single length scale -- the turbulence scale, that is, a so-called diffusion regime sets in which is usually described by the semiempirical theory of turbulent diffusion.

As noted above, here we will examine only the transverse fluctuations of the jet axis in the horizontal plane. In actuality, if the source is a surface source or diffusion times $t \gg H/u_*$ are considered (u_* is dynamic velocity, H is source altitude), as a result of the fact that the vertical dimensions of the eddies are limited by the distance to the earth's surface, the vertical meandering of the jet can be neglected. The problem of making an allowance for transverse fluctuations of the jet axis also arises for the integral of the concentration along the vertical axis, since under natural conditions the study of the propagation of an impurity in a transverse direction is accomplished by photographing the jet from above with the use of flightcraft. We will also assume that the diffusion of the impurity along the vertical coordinate z and the transverse coordinate y occurs independently; we will neglect diffusion along the wind direction in comparison with advective transfer. With these assumptions, in accordance with the Laykhtman [3] and Gifford jet models, the distribution of instantaneous concentration assumes the form

$$\chi = \chi_z (2\pi\Sigma_R V_c^2) \exp\left[-\frac{(y-D_y)^2}{2\Sigma_R^2}\right], \qquad (1)$$

where $\chi_z(x, z)$ is the distribution of the mean concentration from a stationary linear source, Σ_R^2 is the dispersion of coordinates of particles relative to the center of gravity of the jet, V_{mean} (V_c) is the mean velocity of transfer of matter, D_y is the distance from the center of gravity of the jet to the x axis.

On the assumption that χ is a stationary random process, the formula for the mean frequency of exceedings of some fixed level c_χ has the form [5]

$$N(c_\chi) = \int_0^\infty \dot{\chi} w_{2\chi}(c_\chi, \dot{\chi})\, d\dot{\chi}, \qquad (2)$$

where $w_{2\chi}(\chi, \dot{\chi})$ is the two-dimensional probability of the χ process and its time derivative $\dot{\chi}$ at the coinciding moments in time.

Thus, computations of the frequency of exceeding of the level of the χ processes can be carried out if the function $w_{2\chi}(\chi, \dot{\chi})$ is known.

Derivation of Fundamental Formulas

The two-dimensional probability density $w_{2\chi}$ is obtained most simply if we stipulate the normal distribution of the random function $D_y(t)$ which, as a result of (1), will also be stationary. It is easy to show [5] that the joint probability density of the processes D_y and $\dot{D}_y$ constitutes a two-dimensional normal density:

$$w_{2D}(D_y, \dot{D}_y) = (2\pi\Sigma_D\dot{\Sigma}_D)^{-1} \exp\left(-\frac{D_y^2}{2\Sigma_D^2} - \frac{\dot{D}_y^2}{2\dot{\Sigma}_D^2}\right), \tag{3}$$

where Σ_D^2, $\dot{\Sigma}_D^2$ is the dispersion of coordinates of the jet axis and their time derivative respectively.

Using the formula for the transformation of probabilities for functionally related values, the density $w_{2\chi}(\chi, \dot{\chi})$ is easily expressed through the joint probability density $w_{2D}(D_y, \dot{D}_y)$:

$$w_{2\chi}(\chi, \dot{\chi}) = w_{2D}\left(\varphi(\chi), \frac{d\varphi}{d\chi}\dot{\chi}\right)\left(\frac{d\varphi}{d\chi}\right)^2, \tag{4}$$

where the φ function is determined by the expression

$$\varphi = y \mp \Sigma_R\sqrt{-2\ln\frac{\chi}{\chi_0}}, \tag{5}$$

and

$$\chi_0 = \frac{\chi_s}{\sqrt{2\pi}\,\Sigma_R V_c}.$$

[c = mean]

$$+ w_{2D}\left(y + \Sigma_R\sqrt{-2\ln\frac{\chi}{\chi_0}},\ \Sigma_R\frac{\dot{\chi}}{\chi\sqrt{-2\ln\frac{\chi}{\chi_0}}}\right)\left(\frac{d\varphi}{d\chi}\right)^2.$$

The inverse (1) transform (5) is two-valued and therefore the joint distribution χ, $\dot{\chi}$ at the coinciding moments in time is the sum of the densities

$$w_{2\chi}(\chi, \dot{\chi}) = \left[w_{2D}\left(y - \Sigma_R\sqrt{-2\ln\frac{\chi}{\chi_0}} - \Sigma_R\frac{\dot{\chi}}{\chi\sqrt{-2\ln\frac{\chi}{\chi_0}}}\right) + \right. \tag{6}$$

Substituting (6) into (2), after simple but unwieldy computations with the use of (3) we finally obtain:

$$N = \frac{\sqrt{-R_D''(0)}}{\pi} e^{-\frac{y^2}{2\Sigma_D^2}}\left(\frac{c_\chi}{\chi_0}\right)^\lambda \operatorname{ch}\left(2m\lambda\sqrt{-\ln\frac{c_\chi}{\chi_0}}\right),\ c_\chi < \chi_0, \tag{7}$$

$$N = 0 \qquad c_\chi \geq \chi_0,$$

where

$$m = \frac{y}{\sqrt{2}\,\Sigma_R},\quad \lambda = \frac{\Sigma_R^2}{\Sigma_D^2},\quad -R_D''(0) = \frac{\dot{\Sigma}_D^2}{\Sigma_D^2}$$

is the second derivative at zero of the normalized correlation function $< D_y(t)\, D_y(t+\tau) > / \sigma_D^2$ (the symbols denote stochastic averaging), τ is the time shift.

Knowing the frequency of exceedings of a stipulated level by concentration fluctuations, it is possible to compute the mean duration of presence of the χ process above the c_χ level in accordance with the formula

$$<\tau> = \frac{1}{N}(1 - W_1), \tag{8}$$

where $W_1(c_\chi)$ is the one-dimensional probability density function of the concentration.

We will compute $1 - W_1(\chi)$ on the assumption that the probability density $w_{1\,D}(D_y)$ is Gaussian. Using the known rules for the transformation of probabilities, we obtain

$$w_{1\chi}(\chi) = \left[w_{1D}\left(y - \Sigma_R \sqrt{-2 \ln \frac{\chi}{\chi_0}}\right) + \right. \tag{9}$$

$$\left. + w_{1D}\left(y + \Sigma_R \sqrt{-2 \ln \frac{\chi}{\chi_0}}\right)\right]\left(\frac{d\varphi}{d\chi}\right)$$

or

$$w_{1\chi}(\chi) = \frac{1}{\chi_0}\sqrt{\frac{-\lambda}{\pi \ln \frac{\chi}{\chi_0}}}\, e^{-\frac{y^2}{2\Sigma_D^2}} \left(\frac{\chi}{\chi_0}\right)^{\lambda-1} \operatorname{ch}\left(2\, m\lambda \sqrt{-\ln \frac{\chi}{\chi_0}}\right). \tag{10}$$

From (10) it is easy to obtain the integral distribution function

$$1 - W_1(c_\chi) = \int_{c_\chi}^{\chi_0} w_{1\chi}(\chi')\, d\chi'. \tag{11}$$

In the Gifford model the random value of the concentration has a maximum value χ_0 which is the upper limit in the integral (11).

Substituting (10) and (11) into (8), after simple transformations we obtain

$$<\tau> = \frac{1}{2N}\left[\operatorname{erf}(\zeta_1) + \operatorname{erf}(\zeta_2)\right], \tag{12}$$

where

$$\operatorname{erf}(\zeta) = \frac{2}{\sqrt{\pi}} \int_0^{\zeta} e^{-\zeta'^2}\, d\zeta', \quad \zeta_{1,2} = \pm m\sqrt{\lambda} + \sqrt{-\lambda \ln \frac{c_\chi}{\chi_0}}.$$

Now we will investigate expression (7). First of all we see from it that the frequency of exceedings of the level is maximum on the axis of the mean jet (y = 0) and decreases toward the periphery of the jet. It is easy to understand this result. In the proposed model the frequency of exceedings of the level is determined by the number of "passages" of the jet through a fixed point in space in a unit time. And since most of the probability of positions of the jet is concentrated in the neighborhood of the point y = 0, the jet intersects this point most frequently.

Next, it is easy to demonstrate that the dependence of the frequency of exceedings of the level has a maximum. We introduce the variable

$$\eta = \sqrt{-\ln \frac{c_\chi}{\chi_0}}.$$

Then expression (7) can be rewritten in the form

$$N = N_0 e^{-\lambda\eta^2} \operatorname{ch}(2m\lambda\eta), \tag{13}$$

where

$$N_0 = \frac{\sqrt{-R_D''(0)}}{\pi} e^{-\frac{v^2}{2\Sigma_D^2}}.$$

The point of the extremum is found from the transcendental equation

$$m \operatorname{th}(2m\lambda\eta) = \eta. \tag{14}$$

Equation (14) has two solutions. The first solution is trivial $\eta_1 = 0$. The second solution exists if $m > 1/\sqrt{2\lambda}$ or $y > \Sigma_D$. Using an asymptotic expansion of the function th ζ with $\zeta \ll 1$, we obtain an evaluation of the second solution $\eta_2 \approx m$. It is easy to show that the point η_2 is the point of the maximum. When $y < \Sigma_D$, $N(\eta)$ decreases monotonically with an increase in η. As a comparison we note that the $N(\eta)$ function for a nonmeandering jet, obtained in [1], has a maximum point only when $\eta = 0$. Qualitatively the presence of a maximum of the $N(\eta)$ function for a particular model when $\eta \neq 0$ can be explained in the following way. Assume that at some point y_0 there is a counter of the number of exceedings of some fixed concentration level. The counter is triggered when $\chi > c_\chi$ and the duration of the excess τ_{ex} is a finite value. In this case the total number of excesses N_T can be estimated using the formula

$$N_T \approx \frac{T}{\tau_B} P, \tag{15}$$

[B = ex(cess)] where P is the probability that at the point y_0 $\chi > c_\chi$, T is observation time.

If the level is very small, the measurement point y_0 will virtually all the time be in the jet, that is, P in order of magnitude will be close to unity and τ_{ex} will have the order of T. In this case $N_T \approx 1$ and N $1/T \to 0$ when $T \sim \infty$. With an increase in level τ_{ex} will decrease and N will accordingly increase. If a high level c_χ is stipulated, then τ_{ex}

will be small, but finite, and the probability P that $\chi > c_x$ will tend to zero. Thus, $N_T \sim T/\tau_{ex\ min} \to 0$. With $y < \Sigma_D$ this effect does not appear (within the framework of this model). Since it can be demonstrated that P is not less than 1/2 and accordingly $N \approx \text{const}/\tau_{ex}$, that is, there is a monotonic increase in N with an increase in level.

Evaluation of Parameters

The mean frequency of exceedings of a stipulated concentration level and the mean duration of the excess are determined by the three parameters $\sqrt{-R_D''(0)}$, Σ_R and Σ_D, which must be expressed through the measured turbulent and diffusion values.

First we will compute the second derivative together with the correlation function $B_D = \langle D_y(t_1) D_y(t_2) \rangle$. And in particular, we note that in the Gifford model the fluctuations of the jet axis are completely determined by pulsations of the transverse component of Euler velocity v. In this case the equation for the trajectory of the center of gravity can be written in the form

$$\frac{dD_y(t)}{dt} = v(D_y, t). \tag{16}$$

We form the correlation

$$\left\langle \frac{dD_y(t_1)}{dt_1} \frac{dD_y(t_2)}{dt_2} \right\rangle = \frac{\partial^2 B_D}{\partial t_1 \partial t_2} = \langle v(D_y(t_1), t_1)\, v(D_y(t_2), t_2) \rangle \tag{17}$$

or, using the property of stationary random processes [5]:

$$\frac{\partial^2 B_D}{\partial t_1 \partial t_2} = -\frac{d^2 B_D}{d\tau^2} = \langle v(0)\ v(\Delta D_y, \tau) \rangle, \tag{18}$$

where

$$v(0) = v(0, 0),\ \Delta D_y = D_y(t_1) - D_y(t_2),\ \tau = t_2 - t_1.$$

With $\tau = 0$ ($t_2 = t_1$) we obtain

$$\left.\frac{d^2 B_D}{d\tau^2}\right|_{\tau=0} = -\langle v^2(0) \rangle = -\sigma_v^2. \tag{19}$$

Hence

$$\sqrt{-R_D''(0)} = \frac{\sigma_v}{\Sigma_D}. \tag{20}$$

In order to evaluate the parameters Σ_D and Σ_R we use the results of the theory of similarity of Lagrangian turbulence in the atmospheric surface layer. In accordance with [7], the following expressions are correct for the dispersions Σ_R^2, Σ_D^2 and Σ_y^2 (Σ_y^2 is the dispersion of coordinates of particles from a fixed source:

$$\Sigma_R^2 = \beta_R u_*^2 t^2,\ \Sigma_D^2 = \beta_D u_*^2 t^2,\ \Sigma_y^2 = \alpha_y u_*^2 t^2, \tag{21}$$

where u_* is dynamic velocity, β_R, β_D, α_y are universal constants between which there is the correlation [2]:

$$\alpha_y = \beta_R + \beta_D. \tag{22}$$

At the present time there are extremely few data on these universal constants. Below we give estimates of these constants on the basis of diffusion experiments in project "Prarie Grass." The results of these experiments are given in [6]. Data on Σ_y for a neutral atmospheric stratification of the atmosphere are approximated well by a power-law dependence

$$\Sigma_y = 0{,}22\ x^{0{,}87}, \tag{23}$$

where x is the distance from the source to the measurement point. Data on relative diffusion are approximated by the dependence

$$\Sigma_R = 0{,}06\ x^{0{,}92}. \tag{24}$$

Proceeding on the basis of the theory of similarity of Lagrangian turbulence it is possible to evaluate the universal constants accurately. This requires that the diffusion time in expressions (21) be expressed through the distance traveled by a particle. The mean distance covered by the particle, in accordance with [5], is determined from the expression

$$\langle x \rangle = \frac{u_* t}{k} \ln \frac{k u_* t}{e z_0}, \tag{25}$$

where k is the Karman constant, e is the base of natural logarithms, z_0 is the roughness parameter.

If we neglect the longitudinal diffusion of particles in comparison with transfer of a particle by the wind, we can make the replacement $x \sim \langle x \rangle$ [7].

The solution of the transcendental equation is

$$\zeta \ln \zeta = \xi, \tag{26}$$

where $\zeta = \frac{k u_* t}{e z_0}$, $\xi = \frac{k^2 x}{e z_0}$,

is formally represented in the form $\zeta = a \xi^{\alpha}$, where a and α are dependent on ζ, $\alpha = 1 - 1/\ln \zeta$. In the range $10 < \zeta < 10^3$ the exponent α is equal to approximately 0.87. In this case the factor $a \approx 0.43$.

Comparing formula (23) with the expression $\zeta = 0.47 \xi^{0.87}$ with $z_0 = 1$ cm (in accordance with data from "Prarie Grass") we obtain $\alpha_y \approx 2.15$. In the range $10^3 < \zeta < 10^4$ the exponent $\alpha \approx 0.92$ and $a \approx 0.27$. Comparing formula (24) with the expression $\zeta = 0.27 \xi^{0.92}$, we obtain the evaluation

$\beta_R \approx 0.5$, hence $\beta_D \approx 1.85$.

Numerical Example

As an example we will make a numerical evaluation of N and $\langle\tau\rangle$ for conditions of neutral stratification with $c_\chi = \langle\chi\rangle$, y = 0. The Laykhtman-Gifford model gives the following distribution of the mean concentration when y = 0.

$$\langle\chi\rangle = \frac{\Sigma_R}{\Sigma_y}\chi_0. \tag{27}$$

With these assumptions formulas (7) and (12) are considerably simplified:

$$N(\langle\chi\rangle) = \frac{\sigma_v}{\pi\Sigma_D}\left(\frac{\Sigma_R}{\Sigma_y}\right)^{\lambda}, \tag{28}$$

$$\langle\tau\rangle = \frac{1}{N}\operatorname{erf}\left(\sqrt{-\lambda\ln\frac{\Sigma_R}{\Sigma_y}}\right). \tag{29}$$

In the case of a neutral atmospheric stratification, according to the data cited in [4], $\sigma_v \approx 2.0\ u_*$; thus we finally obtain

$$N(\langle\chi\rangle) \approx \frac{2u_*}{z_0}\left(\frac{x}{z_0}\right)^{-0.87}, \tag{30}$$

$$\langle\tau\rangle \approx \frac{0{,}4\,z_0}{u_*}\left(\frac{x}{z_0}\right)^{0{,}87}. \tag{31}$$

With $z_0 = 0.01$ m, $u_* = 0.5$ m/sec, x = 100 m, we obtain $N \approx 0.033$ sec^{-1}, $\langle\tau\rangle \approx 24.2$ sec.

It can be seen from expressions (30) and (31) that the frequency of the excesses decreases with distance from the source and the mean duration of the excesses increases. The latter formulas are cited for values $\zeta < 10^3$. With high ζ values the dependence of N and $\langle\tau\rangle$ on the roughness parameter disappears and the expressions assume the following form:

$$N(\langle\chi\rangle) \approx \frac{5u_*}{x}, \tag{30'}$$

$$\langle\tau\rangle \approx \frac{0{,}16\,x}{u_*}. \tag{31'}$$

Summary

The Laykhtman-Gifford jet model at the present time is the only one making it possible to take into account the influence of meandering on the statistical characteristics of concentration fluctuations.

The numerical evaluations of the frequency and mean duration of the excesses were entirely reasonable and corresponded to "common sense." Accordingly, the results of this article can be recommended for engineering computations and evaluations. An experimental checking of the formulas derived in this article would be of great interest.

BIBLIOGRAPHY

1. Vozzhennikov, O. I., "On the Number of Exceedings of a Stipulated Level by Concentration Fluctuations," TRUDY IEM (Transactions of the Institute of Experimental Meteorology), No 21(80), 1978.

2. Gifford, --, "Statistical Model of a Smoke Jet," ATMOSFERNAYA DIFFUZIYA I ZAGRYAZNENIYE VOZDUKHA (Atmospheric Diffusion and Air Contamination), Moscow, IL, 1962.

3. Laykhtman, D. L., FIZIKA POGRANICHNOGO SLOYA (Boundary Layer Physics), Leningrad, Gidrometeoizdat, 1961.

4. Lamli, Dzh., Panovskiy, G., STRUKTURA ATMOSFERNOY TURBULENTNOSTI (Structure of Atmospheric Turbulence), Moscow, Mir, 1966.

5. Levin, V. R., TEORETICHESKIYE OSNOVY STATISTICHESKOY RADIOTEKHNIKI (Theoretical Principles of Statistical Radioengineering), Moscow, Sovetskoye Radio, 1974.

6. METEOROLOGIYA I ATOMNAYA ENERGIYA (Meteorology and Atomic Energy), translated from English, edited by N. L. Byzova and K. P. Makhon'ko, Leningrad, Gidrometeoizdat, 1971.

7. Monin, A. S., Yaglom, A. M., STATICHESKAYA GIDROMEKHANIKA (Statistical Hydromechanics), Part I, Moscow, Nauka, 1965.

UDC 551.576.11

VERTICAL PROFILE OF PARAMETERS OF MICROSTRUCTURE OF STRATUS CLOUDS

Moscow METEOROLOGIYA I GIDROLOGIYA in Russian No 12, Dec 79 pp 57-61

[Article by Candidate of Chemical Sciences E. L. Aleksandrov and K. B. Yudin, Institute of Experimental Meteorology, submitted for publication 20 April 1979]

Abstract: This paper presents the results of measurements of the vertical profile of parameters of the spectrum of cloud particle- and droplet-sizes in marine and continental stratus clouds. The form of the measured spectra and the relative dispersion of the distribution of cloud droplet sizes correspond to data from the regular condensation theory.

[Text] Data on the microstructure of stratiform clouds and its changes with altitude are necessary for solving many problems related to the propagation of radiation and also for study of the conditions for forming of the spectrum of cloud droplets. Particularly important are detailed data on the fine-droplet, poorly studied part of the spectrum. A detailed investigation of the microstructure of clouds became possible only in recent years due to the introduction of modern photoelectronic apparatus for continuous automatic measurements of the size spectra of cloud droplets. Over the course of many years the sampling of droplets has been by the methods of precipitation on object glasses covered with a viscous mixture. Due to the small volumes of the sample it is frequently necessary to have recourse to the combining of samples from different parts of a cloud or even different clouds for the purpose of accumulating the greatest possible number of trapped droplets for a representative evaluation of their distribution [4, 5, 8]. In addition, inertial methods for the sampling of cloud droplets with subsequent microphotographing do not provide reliable data on the concentration of droplets with a radius less than 1.5-2μm.

In this paper the size distribution of droplets was measured using a photoelectric counter [1] in the range of radii from 0.5 to 40μm. The entire range was divided into 31 channels with a channel width varying proportionally to the logarithm of radius. The error in measuring droplet size is

constant in the entire range and is 18% and their concentrations do not exceed 20%. The spatial resolution of the measurements is about 30 m with a flight speed of 220 km/hour. In each sample in which we computed the parameters of an individual spectrum we took for the analysis a total of 7.5 cm^3 of cloud medium in which there were from 500 to 6,000 droplets, depending on their concentration. The data cited below were averaged for 50-100 individual spectra and thus are statistically reliably ensured.

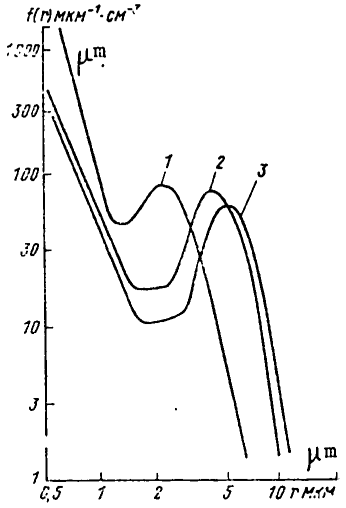

Fig. 1. Distribution of droplets and water-enveloped nuclei by sizes in continental stratus cloud. 1) near lower boundary, 2) in middle part of cloud, 3) in upper third of cloud.

The characteristic spectra of cloud droplets shown in Fig. 1 correspond with respect to the form of the spectra obtained in a theoretical analysis of the cloud-formation process [10]. In the spectra two parts are quite clearly discriminated: droplet and water-enveloped condensation nuclei. The separation of the spectrum into two parts is caused by supersaturation in the cloud. In that part of the cloud where supersaturation increases, there is formation of droplets on water-enveloped nuclei. The forming droplets absorb the vapor excess and supersaturation begins to fall. At this moment the separation of the spectrum begins; its droplet part continues to increase, despite a decrease in supersaturation.

The part of the spectrum containing water-enveloped nuclei was described by an inverse power-law distribution in the form

$$f(r) = A\,(r/r_0)^{-\nu},$$

Table 1

Параметр 1	2 Уровень (Z/H)					
	0,0—0,1	0,1—0,3	0,3—0,5	0,5—0,7	0,7—0,9	0,9—1,0
A мкм$^{-1}\cdot$см$^{-3}$ 3	90±40	65±23	55±16	50±7	50±5	40±30
ν	4,3±1,0	3,2±0,6	2,9±0,4	3,0±0,3	3,2±0,5	3,9±1,7
n см$^{-3}$	270±190	135±75	110±50	100±25	105±25	105±75
$\delta_м$% 4	0,083±0,036	0,064±0,015	0,055±0,009	0,055±0,009	0,052±0,012	—
W г$\cdot$м$^{-3}$ 5	0,08±0,04	0,13±0,03	0,15±0,03	0,18±0,02	0,20±0,02	0,06±0,04
N см$^{-3}$	160±75	260±30	260±25	260±25	240±12	200±55
$\bar{r}$ мкм	2,6±0,5	4,6±0,4	4,6±0,4	5,1±0,3	5,2±0,3	3,1±1,1
$\sigma/\bar{r}$	0,40±0,20	0,30±0,05	0,28±0,03	0,28±0,3	0,31±0,03	0,36±0,06
A мкм$^{-1}\cdot$см$^{-3}$	3±2	8±2	16±4	40±4	72±9	10±4
ν	6,6±1,6	4,5±0,7	4,0±0,4	3,7±0,3	3,5±0,3	4,0±0,8
n см$^{-3}$	25±19	25±11	45±15	90±15	165±35	30±18
$\delta_м$%	0,098±0,100	0,057±0,039	0,048±0,025	0,043±0,015	0,040±0,009	—
W г$\cdot$м$^{-3}$	0,03±0,01	0,10±0,02	0,18±0,02	0,27±0,03	0,35±0,06	0,22±0,05
N см$^{-3}$	55±20	70±8	70±7	70±6	67±5	35±8
$\bar{r}$ мкм	4,0±0,8	8,8±1,0	9,5±1,0	11,0±0,9	12,0±0,9	10,5±1,9
$\sigma/\bar{r}$	0,38±0,16	0,26±0,05	0,20±0,02	0,20±0,01	0,21±0,02	0,22±0,04

KEY:

1. Parameter
2. Level (Z/H)
3. μm
4. max, %
5. g·m^{-3}

where A is a normalizing factor numerically equal to the value of an inverse power function with $r = r_0 = 1\mu m$. The A and ν parameters were computed by the least squares method. The parameters of the distribution function describing the droplet part of the spectrum were computed using the modal radius values and the modal distribution function values, as well as the liquid-water content, computed on the basis of the measured distribution. The errors in determining the mean radius $\bar{r}$ and the relative dispersion σ/r, caused by computation of liquid water content using the measured value, cut off in the direction of large droplets, as a result of the inadequacy in statistics, as indicated by the estimates, do not exceed 15%.

The maximum supersaturation in the cloud was computed using the position of the minimum in the measured distribution using the empirical expression $\delta_{max}\% = 0.1/r_{min}$ [2], where δ_{max} is the maximum supersaturation in the cloud formation process (%), and r_{min} is the radius (μm) corresponding to the minimum of the distribution function. The employed estimation method is quite rigorous [3, 10]. However, it must be remembered that the position of the minimum in the spectrum of particle sizes is dependent not only on the maximum supersaturation value attained in the cloud but also on its current value. The analysis indicated that this circumstance leads to an error in determining δ_{max} not exceeding 50%.

Table 1 gives the vertical profiles of the principal parameters of the microstructure of two stratus clouds with a thickness of 200-300 m. In the first case (upper part of the table) the measurements were made during the autumn in the central region of the European USSR, and in the second case (lower part of the table) in the summer period over the sea in the Arctic region. With respect to the nature of the synoptic situation both cases can be classified as air-mass cloud cover in a pressure field with a small gradient. Their close temperatures are combined in the range from 0 to 3°C; the temperature gradients are close -- about 0.67°C per 100 m; a blocking layer is present. Isothermy was observed over the continental cloud and an inversion was observed over the marine cloud.

The measurements were made from an IL-14 aircraft while gaining altitude in circles with a vertical speed of 0.5 m/sec. With a cloud thickness 200-300 m the ascent continued for 7-10 minutes during which there were no appreciable changes in cloud cover. A total of 400-600 samples were analyzed during the time of the sounding. Table 1 gives the parameters of the microstructure, averaged by layers whose levels were expressed by the ratio of altitude of the layer from the cloud base to its thickness Z/H. The variability of the parameters within the layer is also indicated in the table. In particular, it must be emphasized that it does not give the parameters of spectra averaged by layers but the averaged parameters of 50-100 individual spectra in each layer.

Both cases are characterized by an identical distribution of liquid-water content vertically -- with a maximum in the upper third of the cloud. A concentration of cloud droplets which is virtually constant with altitude

is characteristic for both clouds. The increase in liquid-water content with altitude is caused only by an increase in the mean radius $\bar{r}$ of the droplets. The variations in liquid-water content, concentrations and mean radius of droplets in the cloud, except for narrow layers with a thickness of 20-30 m at the upper and lower boundaries, fall in the range 10-12%. However, the droplet concentration in a continental cloud is almost four times greater than in a marine cloud and accordingly there is a difference in their mean radius.

The greatest differences are in the vertical variation of the concentration of water-enveloped condensation nuclei n with a radius greater than 0.5μm. In a continental cloud it decreases with altitude almost by a factor of three, and in a marine cloud increases by a factor of more than four. This can be attributed to the properties of the underlying surface: the land is a source of aerosols -- condensation nuclei, and they are lost over the sea, which causes a different sign of the vertical gradient of a definite concentration of nuclei. The absence of an intensive source of nuclei over the sea also explains the lesser absolute concentration of droplets and nuclei in marine clouds. The marked decrease in the concentration of water-enveloped nuclei in the upper part of a marine cloud can evidently be attributed to the influence of drier air above the cloud from an inversion layer evaporating water from the water-enveloped nuclei, which leads to a decrease in their size below the the instrument response threshold -- 0.5 μm.

The maximum supersaturation in both clouds is 0.04-0.06%, but its variations are very great, which is attributable, in particular, to the great random errors in determining the minimum of the distribution function, which has a considerable extent, whereas the values of the distribution function themselves in this region fluctuate greatly as a result of the inadequacy of statistics. We note the increased value (0.08-0.1%) of the maximum supersaturation at the lower boundary of the cloud cover, that is, where there is formation of the cloud spectrum. It is possible that in the highest-lying layers of the cloud the position of the minimum of the distribution function, from which the maximum supersaturation was determined, was displaced under the influence of current supersaturation. However, it is also impossible to exclude the possibility of a change in maximum supersaturation in the process of formation of different layers in the cloud.

The narrow spectra of cloud droplets are the most remarkable in the collected material. In a continental cloud the relative dispersion $\sigma/\bar{r}$ is equal to 0.28-0.30, which corresponds to the α parameter of the gamma-distribution 10-12. In the middle part of a sea cloud the spectra of cloud droplets are still narrower: the relative dispersion decreases to 0.20, that is, α = 24. In the overwhelming majority of measurements made earlier in stratiform clouds relatively broad spectra with $\sigma/r > 0.4$ ($\alpha < 5$) [7, 8, 9] were obtained. Two possible mechanisms are usually advanced for an explanation of the experimental results: spatial nonuniformity of condensation nuclei [6] and stochastic nature of condensation processes [10, 11].

The principal hypotheses used in stochastic condensation theory are that the growth of droplets occurs in variable temperature, pressure and humidity fields changing in space and in time in conformity to random laws governed by atmospheric turbulence.

The relative dispersion of the spectrum of cloud droplets obtained in this investigation corresponds satisfactorily to predictions of regular condensation theory [11] and does not require the invoking of any additional mechanisms for explaining the experimental data.

We feel that the high $\sigma/\bar{r}$ values obtained in experiments carried out earlier were caused by shortcomings in the sampling and processing methods. The most important of these are the great spatial averagings, the nonlinearity of the precipitation coefficient on a background of droplets of different sizes and broad differential windows in the region of small droplets where the distribution function has a deep minimum.

The measurement method did not make it possible to investigate the distribution of cloud droplets with a radius greater than 20 μm, whose concentration is low.

Accordingly, the data obtained in this study do not give information on the possible mechanisms of formation of precipitation in warm clouds, but they make possible an experimental checking of the results of theoretical investigations of formation of the spectrum of cloud droplets and confirm the presence of a fine-droplet fraction detected earlier by indirect optical methods.

BIBLIOGRAPHY

1. Aleksandrov, E. L., et al., "Airborne Photoelectric Instrument for Measuring Cloud Droplets," TRUDY IEM (Transactions of the Institute of Experimental Meteorology), No 19(72), 1978.

2. Aleksandrov, E. L., Klepikova, N. V., Yudin, K. B., "Experimental Evaluation of Maximum Supersaturation in the Cloud Formation Process," TRUDY IEM, No 7(45), 1974.

3. Aleksandrov, E. L., Sedunov, Yu. S., "Method for Estimating the Supersaturation Arising in the Formation of the Liquid-Drop Phase in Clouds," DOKLADY AN SSSR (Reports of the USSR Academy of Sciences), Vol 188, No 5, 1969.

4. Borovikov, A. M., et al., FIZIKA OBLAKOV (Cloud Physics), Leningrad, Gidrom eoizdat, 1961.

5. Zaytsev, V. A., Ledokhovich, A. A., PRIBORY DLYA ISSLEDOVANIYA OBLAKOV I TUMANOV I IZMERENIYA VLAZHNOSTI (Instruments for Investigating Clouds and Fogs and Measuring Humidity), Leningrad, Gidrometeoizdat, 1970.

6. Kabanov, A. S., Mazin, I. P., Smirnov, V. I., "Influence of the Spatial Inhomogeneity of the Concentration of Nucleating Droplets on the Spectrum of Their Sizes in a Cloud," IZV. AN SSSR, FIZIKA ATMOSFERY I OKEANA (News of the USSR Academy of Sciences, Physics of the Atmosphere and Ocean), Vol 6, No 3, 1970.

7. Levin, L. M., ISSLEDOVANIYA PO FIZIKE GRUBODISPERSNYKH AEROZOLEY (Investigations of Coarsely Dispersed Aerosols), Moscow, USSR Academy of Sciences, 1961.

8. Mazin, I. P., MIKROFIZIKA KAPEL'NYKH OBLAKOV (Microphysics of Droplet Clouds), TsAO, 1969.

9. Nevzorov, A. N., Shugayev, V. F., "Characteristics and Measurements of the Local Microstructure of Clouds," TRUDY TsAO (Transactions of the Central Aerological Observatory), No 106, 1974.

10. Sedunov, Yu. S., FIZIKA OBRAZOVANIYA ZHIDKOKAPEL'NOY FAZY V ATMOSFERE (Physics of Formation of the Liquid-Drop Phase in the Atmosphere), Leningrad, Gidrometeoizdat, 1972.

11. Stepanov, A. S., "Condensation Growth of Cloud Droplets in a Turbulent Medium With Allowance for the Nonadiabaticity of Pulsations and in the Low Liquid-Water Content Approximation," IZV AN SSSR, FIZIKA ATMOSFERY I OKEANA, 11, No 3, 1975.

UDC 551.577.7: 546.11.03(47+57)

SOME PECULIARITIES OF THE SPATIAL AND TEMPORAL DISTRIBUTION OF TRITIUM IN PRECIPITATION OVER THE TERRITORY OF THE USSR

Moscow METEOROLOGIYA I GIDROLOGIYA in Russian No 12, Dec 79 pp 62-66

[Article by Candidate of Technical Sciences S. M. Vakulovskiy, A. I. Vorontsov, I. Yu. Katrich and Ye. I. Koslyy, Institute of Experimental Meteorology and Institute of Applied Geophysics, submitted for publication 6 April 1979]

Abstract: It is demonstrated that in precipitation, with a change in the geographical longitude of the collection place in the range 35-135°E, there is a linear change in the mean annual concentrations of tritium. The change in mean annual tritium concentrations with latitude in the range 35-70°N is not monotonic and has a maximum in the latitude zone 52-56°N. Analytical expressions are derived for determining the mean annual concentrations of tritium in precipitation at points where observations are not made. An analytical expression is proposed for describing the temporal change in mean annual tritium concentrations in precipitation.[1]

[Text] During the period 1973-1977 the scientific research institutes of the USSR State Committee on Hydrometeorology and Environmental Monitoring continued observations of the tritium content in precipitation at 18 stations in the USSR, initiated in 1969. The results of these observations made it possible to obtain experimental data on the mean monthly tritium concentrations in precipitation during this period of time and ascertain a number of peculiarities in the spatial distribution of tritium.

Table 1 gives the ratios of the mean annual tritium concentrations in precipitation k_i at the mentioned stations during the observation period 1973-

[1] This is the basic content of an article reported at the scientific-coordination conference at Bratislava in March 1979.

1977 to the mean annual tritium concentrations in precipitation, collected in Moscow during this same period of time.

Table 1

Values of Ratios of Tritium Concentration in Precipitation at Observation Stations to Tritium Concentrations in Precipitation at Moscow -- k_i

	Пункт 1	1973	1974	1975	1976	1977	2 Среднее значение
3	Ташкент	1,0	0,6	0,8	0,6	0,8	0,76±0,18
4	Тбилиси	0,9	0,6	0,6	0,7	0,8	0,72±0,14
5	Одесса	0,7	0,6	0,8	0,7	0,7	0,70±0,07
6	Ростов	0,9	0,7	0,7	0,7	0,7	0,74±0,09
7	Хабаровск	1,7	0,9	1,0	1,1	0,9	1,12±0,34
8	Иркутск	1,4	1,3	1,4	1,5	1,2	1,36±0,12
9	Сковородино	1,5	1,3	1,4	1,4	1,4	1,40±0,07
10	Омск	1,5	1,2	1,1	1,0	1,1	1,18±0,19
11	Новосибирск	1,5	1,2	1,2	1,1	1,2	1,24±0,15
12	Москва	1	1	1	1	1	1
13	Пермь	1,2	0,9	0,9	1,3	0,9	1,04±0,19
14	Енисейск	1,0	1,1	1,2	1,2	1,0	1,10±0,09
15	Якутск	1,7	1,2	1,2	1,1	1,4	1,32±0,24
16	Архангельск	0,9	1,0	0,6	0,7	0,7	0,78±0,17
17	Салехард	1,0	1,0	1,2	0,9	1,0	1,02±0,12
18	Дудинка	1,2	1,2	1,4	0,9	1,0	1,14±0,19
19	Холмск	0,9	0,4	0,5	0,6	0,6	0,60±0,17
20	Петропавловск-на-Камчатке	0,9	0,4	0,4	0,4	0,6	0,54±0,22

KEY:

1. Station
2. Mean value
3. Tashkent
4. Tbilisi
5. Odessa
6. Rostov
7. Khabarovsk
8. Irkutsk
9. Skovorodino
10. Omsk
11. Novosibirsk
12. Moscow
13. Perm'
14. Yeniseysk
15. Yakutsk
16. Arkhangel'sk
17. Salekhard
18. Dudinka
19. Kholmsk
20. Petropavlovsk-na-Kamchatke

The data in Table 1 show that there is a stable spatial distribution of the mean annual tritium concentrations in precipitation in the territory of the USSR despite the almost annual injections of tritium in the northern hemisphere during the considered period.

It should be noted that the stability of the ratios of the mean annual tritium concentrations at any two stations is observed not only for the territory of the USSR, but also for the entire northern hemisphere. For example, the ratio of the mean annual tritium concentrations in

precipitation (Huddinge, Goteborg, Sweden); Vienna, Austria; Tokio, Japan; Bethel, Alaska; Moscow) to the tritium concentrations in precipitation (Ottawa, Canada), computed on the basis of the data cited in [2, 11, 14], equal -- 0.72±0.13 (1958-1969), 0.98±0.12 (1961-1971), 0.33±0.07 (1961-1971), 0.73±0.19 (1962-1969), 0.95±0.25 (1962-1967) respectively.

The stability of the ratios of the mean annual tritium concentrations makes it possible to determine the tritium concentration C at points where no observations are made of the tritium content on the basis of the results of measurements of its concentrations at other points, for example, at Moscow (C_M), using the expression

$$C_{i\,(\varphi,\,\psi)} = k_{i\,(\varphi,\,\psi)}\, C_M, \qquad (1)$$

where $k_{i(\varphi,\psi)}$ is the ratio of the mean annual tritium concentration at a point with the coordinates φ — latitude in degrees, ψ longitude in degrees to the concentration in Moscow.

The dependence of the k_i value on longitude is determined from the ki values obtained from experimental data (Table 1) by constructing a graph $k_i = f_{(\psi,\ \varphi = \text{const})}$ for narrow latitude zones (46-49°), (54-56°), (62-69°) in the longitude range 35-135°E (Fig. 1).

Figure 1 shows that in a narrow latitude zone the value of the ratio of tritium concentrations in dependence on the longitude of the place of sampling of precipitation with movement from west to east increases monotonically ("continental effect") [10] and can be approximated by a straight line:

$$k_{i\,(\psi_i,\ \varphi_H = \text{const})} = k_{(\psi_H,\ \varphi_H)} + 0{,}005\ (\psi_i - \psi_H). \qquad (2)$$

[H = obs] Here φ_{obs} is the latitude of the observation point, ψ_{obs} is the longitude of the observation point, ψ_i is current longitude (all three values in degrees).

Assuming the dependence $k_{(\psi)}$ to be linear with one and the same slope within the limits of the USSR in the latitude zone 35-70°, we will examine the latitude dependence of the ratios of tritium concentrations in precipitation at any fixed longitude (for example, at the longitude of Moscow). The distribution of the ratios of the tritium concentrations, obtained on the basis of experimental data (Table 1), scaled using expression (2) to the longitude of Moscow, is given in Fig. 2.

Figure 2 shows that in the latitude zone 35-70° the ratio of the tritium concentrations in precipitation with a change in the latitude of the place of sampling of precipitation does not change monotonically, as occurs for the longitude variation, and attains maximum values in the region 52-56°N.

This maximum is evidently attributable to the fact that in the latitude zone (50-60°) over the territory of the USSR there is an increased frequency of occurrence of jet streams [7], which leads to an intensive entry of radioactive substances into the troposphere from the stratospheric reservoir [9]. In addition, in the latitude zone 50-60° in the territory of the USSR there is maximum evaporation of moisture [6], which causes a secondary entry of tritium into the atmosphere [13, 16].

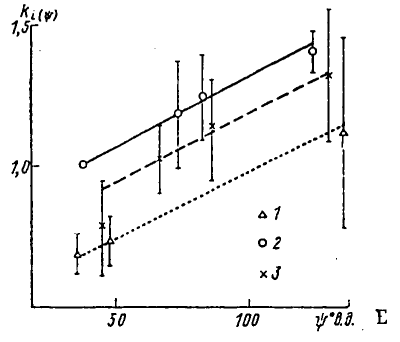

Fig. 1. Dependence of k_i on longitude. 1) 46-49°N (Odessa, Rostov, Khabarovsk), 2) 54-56°N (Moscow, Omsk, Novosibirsk, Skovorodino), 3) 62-69°N (Arkhangel'sk, Salekhard, Dudinka, Yakutsk).

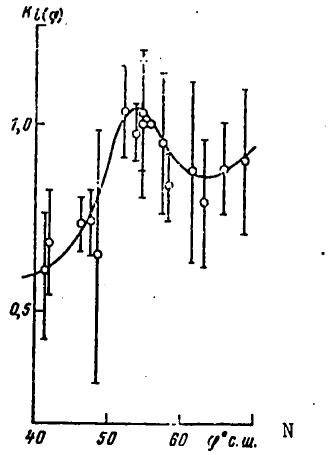

Fig. 2. Dependence of k_i on latitude at longitude of Moscow.

The dependence of the k_i value on latitude can be approximated by the following expression:

$$k_{i\,(\varphi,\ \psi\,=\,\mathrm{const})} = 0{,}57\ e^{0{,}014\,(\varphi-35)} + 0{,}3\ e^{-[0{,}18\,(\varphi-53{,}5)]^2}. \qquad (3)$$

For prediction purposes it also seems interesting to find an analytical expression describing the temporal change in the mean annual tritium concentration in precipitation. The results of observation of the tritium content in precipitation during the period 1963-1967 [3] indicated that in the absence of tritium injections into the atmosphere the expression for the mean annual tritium concentration in precipitation at any point can be represented in the form

$$C_{(t_0+\Delta t)} = C_{\text{косм}} + C_{t_0} e^{-\frac{0,693}{T_{0,5}}\Delta t}, \quad (4)$$

[KOCM = cosmic radiation] where $C_{(t_0 + \Delta t)}$ is the tritium concentration in the sought-for year in tritium units, C_{t_0} is the tritium concentration in the year selected for the beginning of reckoning in tritium units, t_0 is the year of beginning of reckoning, $\Delta t = 1, 2, 3, \ldots$ is the number of years elapsing from t_0, C_{cosm} is the tritium concentration in precipitation (tritium units) caused by cosmic radiation, $T_{0.5}$ is the half-life of tritium concentrations in precipitation (years).

In the case of carrying out of tests of thermonuclear weapons in predicting the mean annual tritium concentration in precipitation it is necessary to take into account the additional entry of tritium ΔQ into the atmosphere and computations of the predicted tritium concentration can be made using the formula

$$C_{(t_0+\Delta t)} = C_{\text{косм}} + C_{t_0} e^{-\frac{0,693}{T_{0,5}}\Delta t} + \alpha \Delta Q, \quad (5)$$

where ΔQ is the quantity of injected tritium in Mki, α is the tritium concentration (tritium units) in precipitation caused by its reserve in the northern hemisphere atmosphere, equal to 1 Mki.

Since the literature contains no data on the tritium concentration in precipitation during the period preceding the onset of tests of thermonuclear weapons, the C_{cosm} value can be estimated on the basis of the results of analysis of samples of river and lake water taken prior to 1951 and also old wines. The legitimacy of such an estimate is indirectly confirmed by investigations carried out in 1975-1976 [1] in which it was demonstrated that the tritium concentration in precipitation and river water (within the limits of the territory of the river basins) is virtually the same. According to the results of analysis of five samples of surface waters and six samples of old wines [13] the mean C_{cosm} value is 2.5±0.5 tritium units.

It is obvious that the $T_{0.5}$ and α values must be dependent on the altitude of the atmospheric layer in which the tritium injection occurred. According to estimates cited in [3] for different latitude zones in the northern hemisphere (excluding the territory of the USSR), during the period 1963-1967 the $T_{0.5}$ value varied in the range 1.1-1.3 years. The $T_{0.5}$ value for Moscow, which we computed using data on the tritium concentrations in precipitation during the period 1963-1967 [2, 11], was 1.7±0.2 years. The $T_{0.5}$ value, as an average for the USSR, computed from the results of observations of the tritium content in precipitation during the periods 1971-1972 and 1975-1976 (during these periods there were no powerful thermonuclear shots in the atmosphere), was 2.4 and 2.1 years respectively.

An evaluation of the α parameter was made for two observation intervals. For a series of tests of thermonuclear weapons in 1961-1962 the α value, computed from the relationship of the measured mean annual concentration

of tritium in precipitation in Moscow in 1963 [11] to the total tritium supply in the northern hemisphere atmosphere, obtained using data on the total intensity of the shots due to the synthesis reaction during this same period of time [4, 15], taking into account a tritium yield of 0.7 kg per megaton of shot intensity [8], was 0.94 tritium unit/l Mki.

In 1967 and successive years an additional quantity of tritium was injected into the atmosphere as a result of thermonuclear shots in the atmosphere carried out in the Chinese People's Republic. For this series of shots the α value, computed using data on the tritium reserve in the northern hemisphere atmosphere in 1970 [5] and our data on the mean annual tritium concentration in precipitation in Moscow, was 1.3 tritium unit/Mki.

We could not make a similar estimate of the α value for the period 1973-1977 due to the lack of data on the tritium reserve in the northern hemisphere atmosphere during this same period of time and it is proposed that this be done in the future when the lacking data are acquired.

BIBLIOGRAPHY

1. Vakulovskiy, S. M., Vorontsov, A. I., Katrich, I. Yu., Koloskov, I. A., Rovinskiy, A. Ya., Roslyy, Ye. I., "Tritium in Precipitation, Rivers and Seas Washing the Territory of the Soviet Union," ATOMNAYA ENERGIYA (Atomic Energy), Vol 44, No 5, 1978.

2. Vinogradov, A. P., Devirts, A. L., Dobkina, E. I., "Present-Day Content of Tritium in Natural Waters," GEOKHIMIYA (Geochemistry), No 10, 1968.

3. Zhigalovskaya, T. N., Katrich, I. Yu., Roslyy, Ye. I., Malakhov, S. G., "Some Characteristics of the Distribution of Tritium in Natural Waters," METEOROLOGICHESKIYE ASPEKTY RADIOAKTIVNOGO ZAGRYAZNENIYA ATMOSFERY. TRUDY MEZHDUNARODNOGO SIMPOZIUMA, TBILISI, 15-20 OKTYABRYA 1973 (Meteorological Peculiarities of Radioactive Contamination of the Atmosphere) (Transactions of the International Symposium, Tbilisi, 15-20 October 1973), Leningrad, Gidrometeoizdat, 1975.

4. Izrael', Yu. A., Stukin, Ye. D., GAMMA-IZLUCHENIYE RADIOAKTIVNYKH VYPADENIY (Gamma Radiation of Radioactive Fallout), Moscow, Atomizdat, 1967.

5. "Sources and Effect of Ionizing Radiation," NAUCHNYY KOMITET OON PO DEYSTVIYU ATOMNOY RADIATSII. DOKLAD ZA 1977. GENERAL'NOY ASSAMBLEYE (UN Scientific Committee on the Effect of Atomic Radiation. Report for 1977, General Assembly), Vol I, UN, New York, 1978.

6. MIROVOY VODNYY BALANS I VODNYYE RESURSY ZEMLI, MGD (World Water Balance and the Earth's Water Resources, International Hydrological Decade), Leningrad, Gidrometeoizdat, 1974.

7. Kulirova, Yu. V., "Some Peculiarities of Jet Streams Over the Territory of the USSR," TRUDY TsAO (Transactions of the Central Aerological Observatory), No 33, 1960.

8. Leypunskiy, O. I., "Radioactive Danger of Explosions of a Clean Hydrogen Bomb," ATOMNAYA ENERGIYA (Atomic Energy), Vol 3, No 12, 1957.

9. Nazarov, L. Ye., Malakhov, S. G., Gaziyev, Ya. I., Vasil'yev, A. S., "Latitudinal and Meridional Distributions of Concentrations of Beta-Active Products of Nuclear Shots in the Troposphere," TRUDY IEM (Transactions of the Institute of Experimental Meteorology), No 5, 1970.

10. Soyfer, V. N., Romanov, V. V., Gasilina, N. K., Roslyy, Ye. I., "On the Screening Effect of the Continents Determining the Isotopic Composition of Atmospheric Moisture (According to Data on the Spatial-Temporal Distribution of Tritium in Atmospheric Precipitation in the Temperate Latitudes of the Northern Hemisphere)," DOKLADY AN SSSR (Reports of the USSR Academy of Sciences), Vol 201, No 1, 1971.

11. Yakimenko, L. M., Kuznets, E. D., Tsionskiy, V. M., "Tritium Content in Atmospheric Precipitation Falling in Moscow in 1962-1963," ATOMNAYA ENERGIYA, Vol 20, No 1, 1966.

12. Buttlar, H., Libby, W. E., "Natural Distribution of Cosmic Ray Produced Tritium," 11, 2, INORGANIC AND NUCLEAR CHEMISTRY, Vol 1, 1955.

13. Ehhalt, D. H., "Vertical Profiles and Transport of HTO in the Troposphere," JGR, Vol 76, No 30, 1971.

14. ENVIRONMENTAL ISOTOPIC DATA: WORLD SURVEY OF ISOTOPE CONCENTRATIONS IN PRECIPITATION, No 1 (1953-1963), No 2 (1964-1965), No 3 (1960-1967), No 4 (1968-1969), IAEA, Vienna, 1969, 1970, 1971, 1973.

15. Leventhal, J. S., Libby, W. F., "Tritium Geophysics from 1961-1962 Nuclear Tests," JGR, Vol 13, No 8, 1968.

16. TRITIUM AND OTHER ENVIRONMENTAL ISOTOPES IN THE HYDROLOGICAL CYCLE, IAEA, Vienna, STI/DOC/10/73, 1967.

UDC 551.(46.01:5)

PARAMETERIZATION OF THE ACTIVE LAYER IN A MODEL OF LARGE-SCALE INTERACTION BETWEEN THE OCEAN AND THE ATMOSPHERE

Moscow METEOROLOGIYA I GIDROLOGIYA in Russian No 12, Dec 79 pp 67-75

[Article by Professor B. A. Kogan and Candidates of Physical and Mathematical Sciences V. A. Ryabchenko and D. V. Chalikov, Institute of Oceanology, submitted for publication 20 April 1979]

Abstract: The article describes a local variant of an integral model of the active layer intended for use in computing joint circulation of the ocean and atmosphere. Two assumptions lie at the basis of the model: 1) a proportionality between integral dissipation and the production of turbulent energy of mechanical and convective origin and 2) on total dissipation of mechanical turbulent energy within the limits of the Ekman boundary layer. As demonstrated by the results of a numerical experiment carried out applicable to the conditions at weather station N, the proposed model ensures a cyclicity of the solution (with stipulation of the external parameters by periodic functions of time) and a fair correspondence between the computed and observed annual variation of temperature and the thickness of the upper quasihomogeneous layer in the ocean.

[Text] The parameterization of processes in the active layer of the ocean, like any other processes on a "submesh" scale, must satisfy at least three principal requirements:

1) be as complete as possible, that is, take into account all the principal physical factors controlling the temporal evolution of surface temperature;

2) be sufficiently simple that the expenditures of computer time on its realization be much less than the expenditures on solution of the equations for a large-scale model;
3) in all respects be reliable, that is, must ensure obtaining at least a qualitatively correct result with the most diversified set of external parameters.

It is difficult to satisfy all these requirements, which in many respects are mutually exclusive, and therefore it is necessary to seek a compromise, leaving some of them unsatisfied. As an example we will make use of the parameterization model for the active layer proposed in [1]. With its use within the framework of a model of global interaction between the ocean and the atmosphere [3] it was found that this model, in addition to the fact that it requires relatively great expenditures of computer time, is exceedingly complex in the sense of establishing in advance the admissible region of values of the input parameters and formulation of a procedure making it possible to avoid fictitious solutions. In this connection, in the block for the upper layer of the ocean in the IOAN (Institute of Oceanology) model it was necessary to introduce a number of simplifications equivalent to the introduction of some limitations on the solution.

The scheme for parameterization of the active layer of the ocean considered in this article, to a greater degree than in [1], satisfies the requirements enumerated above. It is intended for inclusion in the IOAN-3 large-scale interaction model which has now been developed. The latter is an improved version of the employed models IOAN-1 and IOAN-2. A detailed description of the structure of both these models can be found in [2]. Each consists of four main blocks: atmospheric block, individual blocks for the boundary layers of the atmosphere and ocean and a block for the deep ocean. In constructing the oceanic part of the model it was assumed that all the short-period (with a period less than a year) changes in the ocean, caused by the stated atmospheric effect, are concentrated only in the active layer. At its lower boundary the water temperature and the components of current velocity were considered stipulated and were determined in the deep ocean block. The introduction of such an assumption was dictated by the striving to reduce computation time. However, it has the shortcoming that it excludes the possibility of taking into account the feedback between the deep and surface layers of the ocean, and this means, between the deep layer of the ocean and the atmosphere. In the developed model (IOAN-3) this restriction is removed by the inclusion of a quasigeostrophic multilevel model of a baroclinic ocean. Below we describe a local variant of a scheme for parameterization of the active layer of the ocean used in it.

Adhering to [18], within the limits of the active layer of the ocean we discriminate an upper quasihomogeneous layer (QHL) with the thickness h and the seasonal thermocline underlying it in which turbulence is assumed to be absent. Assume that at the base of the QHL there is a temperature jump equal to $T_s - T_h$, where T_s is the water temperature in the QHL (it is

assumed to be nondependent on depth), T_h is the water temperature at the upper boundary of the seasonal thermocline. We will assume further that the absorption of short-wave radiation occurs at the ocean surface. Then integration within the limits of the QHL of the heat budget equation, serving for determining T_s, is written in the form

$$h\frac{dT_s}{dt} = q_0 - q_h, \tag{1}$$

where q_0 and q_h are the specific (normalized for the volumetric heat capacity of sea water) heat fluxes at the free surface and at the lower boundary of the QHL respectively.

In order to determine T_h we make use of the circumstance that the temperature in the seasonal thermocline changes more slowly than in the QHL, so that the dependence of T_h on time can be taken into account parametrically, assuming

$$\frac{dT_h}{dt} = \gamma\left(\frac{dh}{dt} - w_h\right), \tag{2}$$

where w_h is the vertical velocity component at the level z = h (in the local variant of the parameterization scheme it is considered known), γ is the temperature gradient at the upper boundary of the seasonal thermocline, the determination of which will be discussed below.

We will supplement (1), (2) by a turbulent energy budget equation integrated within the limits of the QHL, Neglecting the diffusion flux of turbulent energy at the boundary with the seasonal thermocline and invoking the hypothesis of quasistationarity of the turbulent regime in the QHL (the validation of these assumptions can be found, for example, in [4, 21]), we have the equation

$$G + M_0 - D + \frac{1}{2}\, g\alpha_T h\,(q_0 + q_h) = 0, \tag{3}$$

where G and D are the integral shear generation and dissipation of turbulent energy within the limits of the QHL; M_0 is the flux of turbulent energy at the ocean surface, generated by the collapse of wind waves, $\alpha_T = -2.6\cdot10^{-4}$ K^{-1} is the coefficient of thermal expansion of sea water, g is the acceleration of free falling.

Now we will make specific the expressions for the first three terms in (3). If we limit ourselves to periods of time much greater than the inertial period and assume that the current velocity at the free surface is proportional to dynamic wind velocity u_* with a proportionality factor $c_0 C_D^{-1/2}$ (here c_0 is the wind coefficient, C_D is the coefficient of resistance of the sea surface), on the basis of the equations of motion written for the QHL in an Ekman approximation,

$$G = \left(\frac{\tau_x^h}{\rho_0}\, u_h + \frac{\tau_y^h}{\rho_0}\, v_h\right) + \frac{c_0}{C_D^{1/2}}\frac{\rho_a}{\rho_0}\, u_*^3, \tag{4}$$

where τ_x^h, τ_y^h and u_h, v_h are the components of shearing stress and current velocity at the lower boundary of the QHL, ρ_0 and ρ_a are the mean densities of water and air respectively.

In order to evaluate the flux of turbulent energy M_0 we will use the results in [19], according to which the energy lost by the waves during their collapse and then changing into turbulent energy is equal to

$$M_0 = \alpha E_B / T, \tag{5}$$

[B = wave] where $\alpha = \exp(-1/16\beta)$ is a numerical factor unambiguously determined by the constant β of the equilibrium interval in the Phillips wind waves spectrum [22], $E_{wave} = g\sigma_\eta^2$ is the total energy of surface gravitational waves, normalized to water density, per unit surface area, σ_η is the dispersion of wave amplitudes, related to the frequency spectrum $S(\omega)$ by the expression

$$\sigma_\eta^2 = 2\int_0^\infty S(\omega)\, d\omega;$$

$$T = 2\pi\left(\frac{\int_0^\infty S(\omega)\, d\omega}{\int_0^\infty \omega^2 S(\omega)\, d\omega}\right)^{1/2}$$

-- the characteristic period of the waves, ω is their frequency.

Then, in accordance with [6],

$$S(\omega) = \begin{cases} 0 & \text{when} \quad \omega \leqslant \omega_1, \\ \beta g^2 \omega^{-5} & \text{when} \quad \omega > \omega_1, \end{cases}$$

where $\omega_1 \sim g/u_*$.

The substitution of the cited expressions into (5) gives

$$M_0 = c_1 u_*^3. \tag{5'}$$

It goes without saying that the latter expression remains valid only with u_* equal to or greater than some definite value u_{*c} with which wave collapse begins. With lesser u_* values there is no wave collapse, which can be taken into account by assuming the constant c_1 in (5') to be equal to zero.

Now we will briefly discuss the expression for integral dissipation D. One of the simplest and in general natural assumptions concerning D (a detailed analysis of the numerous now existing hypotheses of this kind is given in the review articles [4, 7, 21]) is the assumption of a proportionality between the integral dissipation and the production of turbulent energy

$$D = (c_1 + c_2)\, c_3 u_*^3 + c_4 g \alpha_T \frac{h}{4} (q_0 - |q_0|). \tag{6}$$

Here the first term on the right-hand side characterizes the dissipation of turbulent energy of mechanical origin; the second characterizes the dissipation of turbulent energy of convective origin, $c_2 = c_0 C_D^{-1.2} (\rho_a / \rho_0)$, c_3 and c_4 are new numerical constants.

However, as was demonstrated in [15, 21], this assumption has one serious shortcoming: with the stipulation of q_0 as a harmonic function of time it does not ensure that the solution will enter a periodic regime. It is easy to understand the reason for this if it is recalled that the work performed by the wind does not change sign in the course of the entire cycle. Accordingly, with a fixed c_3 value the difference between mechanical production and the dissipation of turbulent energy remains positive and different from zero, which in turn (with a fixed c_4 value) leads to a deepening of the QHL from cycle to cycle. We now know of several methods for overcoming this difficulty. In essence, they are all reduced to the assumption of an intensification of dissipation with an increase in the thickness of the QHL.

For example, in [21] the constants $(1 - c_3)$ and $(1 - c_4)$ were recommended to be assumed equal to zero with sufficiently high h values, which is actually equivalent to the assumption of a total dissipation of the entire produced turbulent energy within the limits of a layer. In [10, 13, 17, 20] the authors introduced some background dissipation value which was assumed to be proportional to h and independent of local conditions at the ocean surface.

Evidently, the most likely explanation of the existence of a relationship between integral dissipation and the thickness of the QHL was given in [8, 14]. According to [14], the rate of dissipation of turbulent energy, determined by the rate of energy transfer from large to small eddies, is inversely proportional to the typical time scale of large eddies. The latter, in the case of a small thickness of the QHL and $q_0 = 0$ will be equal to hu_*^{-1}, in the case of a great thickness -- $|l|^{-1}$ (here l is the Coriolis parameter). Accordingly, the integral dissipation in the first case will be proportional to u_*^3, in the second case -- $h|l|u_*^2$. The interpolation formula, combining these special cases, will have the form $D \sim u_*^3 (1 + c_5 h|l|/u_*)$.

We will make use of these considerations and rewrite (6) in the form

$$D = (c_1 + c_2)\, c_3 u_*^3 (1 + c_5 h|l|/u_*) + c_4 g \alpha_T \frac{h}{4} (q_0 - |q_0|), \tag{6'}$$

ensuring, as we will see below, the proper asymptotic behavior for an increase in the thickness of the QHL, and most importantly, its entry into a periodic regime.

After the substitution of (4), (5'), (6') into (3) we obtain

$$q_h + \frac{2}{g\alpha_T h}\left(\frac{\tau_x^h}{\rho_0} u_h + \frac{\tau_y^h}{\rho_0} v_h\right) = \\ = -C_1 q_0 - C_2 \frac{u_*^3}{g\alpha_T h}\left(1 - C_3 \frac{h|l|}{u_*}\right), \tag{7}$$

where

$$C_1 = \begin{cases} (1 - c_4) & \text{with } q_0 < 0, \\ 1 & \text{with } q_0 > 0, \end{cases}$$

$$C_2 = 2(c_1 + c_2)(1 - c_3), \quad C_3 = c_3 c_6/(1 - c_3),$$

and since the dissipation of turbulent energy of mechanical origin cannot exceed the production, the factor $(1 - C_3 h|l|/u_*)$ in the last term at the right must be either less than unity with $h < u_*/C_3|l|$, or equal to zero with $h \geqslant u_*/C_3|l|$, as is clear from the above formulas. The latter condition it is easy to understand, is equivalent to the assumption that the entire produced turbulent energy of mechanical origin dissipates within the limits of the Ekman boundary layer.

Now we will determine the turbulent fluxes of heat and momentum at the base of the QHL. For this purpose we will discriminate two regimes in the process of temporal evolution of the QHL: sinking ($dh/dt - w_h > 0$) and rising ($dh/dt - w_h < 0$) of the lower boundary of the QHL. In the first case, as usual (for example, see [18]), we will assume that the turbulent fluxes of heat and momentum at the level $z = h$ were caused by the entrainment of fluid from the seasonal thermocline; in the second case they are equal to zero. In other words,

$$q_h = \begin{cases} (T_s - T_h)\left(\frac{dh}{dt} - w_h\right), & \text{with } \left(\frac{dh}{dt} - w_h\right) > 0, \\ 0 & \text{with } \left(\frac{dh}{dt} - w_h\right) \leqslant 0, \end{cases} \tag{8}$$

$$\left(\frac{\tau_x^h}{\rho_0}, \frac{\tau_y^h}{\rho_0}\right) = \begin{cases} -(u_h, v_h)\left(\frac{dh}{dt} - w_h\right) & \text{with } \left(\frac{dh}{dt} - w_h\right) > 0, \\ 0 & \text{with } \left(\frac{dh}{dt} - w_h\right) \leqslant 0. \end{cases} \tag{9}$$

In writing the expressions for

$$\left(\frac{\tau_x^h}{\rho_0}, \frac{\tau_y^h}{\rho_0}\right)$$

we assumed that the fluid in the seasonal thermocline is at rest and therefore $u_h = (u_h, v_h)$ is the velocity drop at the lower boundary of the QHL. According to [23], $|u_h| \approx 10 (\rho_a/\rho_0)^{1/2} u_*$. Substituting this evaluation and expressions (8), (9) into the equation for the turbulent energy

budget (7), we find

$$-C_1 q_0 - C_2 \frac{u_*^3}{g \alpha_T h}\left(1 - C_3 \frac{h|l|}{u_*}\right) = \begin{cases} (1 + 0{,}26\ \mathrm{Ri}^{-1})\ q_h & \text{with } \left(\frac{dh}{dt} - w_h\right) > 0, \\ 0 & \text{with } \left(\frac{dh}{dt} - w_h\right) \leqslant 0, \end{cases} \tag{10}$$

where $\mathrm{Ri} = -g \alpha_T h\ (T_s - T_h)/u_*^2$ is the global Reynolds number.

Thus, the determination of the four unknowns -- T_s, T_h, q_h and h was reduced to solution of the system of equations (1), (2), (8), (10), satisfying the appropriate initial conditions or the condition of periodicity of the sought-for characteristics in the problem of seasonal evolution of the active layer in the ocean.

In order to evaluate the numerical constants figuring in (1), (2), (8), (10) we will use data from laboratory experiments and field measurements. First we will examine a free convection regime when $u_* = 0$, $q_0 < 0$. In this case equation (10) is written in the form

$$-q_h/q_0 = C_1, \tag{11}$$

characterizing the proportionality between the turbulent heat fluxes at the free surface and at the lower boundary of the QHL. A summary of the experimental constants C_1 obtained by different authors is given in [24]. Accordingly, the overwhelming majority of C_1 evaluations is concentrated in the interval from 0.1 to 0.3. Henceforth we will assume that $C_1 \simeq 0.2$.

In another limiting regime of purely mechanical mixing, when $q_0 = 0$, $u_* \neq 0$, the equation for the budget of turbulent energy (10) is transformed to the form

$$(1 + 0{,}26\ \mathrm{Ri}^{-1}) \frac{1}{u_*}\left(\frac{dh}{dt} - w_h\right) = C_2 \mathrm{Ri}^{-1}\left(1 - C_3 \frac{h|l|}{u_*}\right). \tag{12}$$

Hence, with $\mathrm{Ri} \geqslant 10$ and $l = 0$ we have the expression

$$\frac{1}{u_*}\left(\frac{dh}{dt} - w_h\right) = C_2 \mathrm{Ri}^{-1},$$

indicating a proportionality between the rate of entrainment normalized to u_* (in this case -- $(dh/dt - w_h)$) and Ri^{-1}. The very same result was obtained in an analysis of data from laboratory experiments in a stratified fluid in which the velocity shear was created by the effect of constant frictional stress applied to the surface. Assuming $c_1 = 0$, which corresponds to the experimental conditions, in accordance with [16] we find $C_2 = 2c_2(1 - c_3) \approx 0.24 \cdot 10^{-3}$. However, by definition $c_2 = c_0 C_D^{-1/2}\ (\rho_a/\rho)$. Assuming $c_0 \approx 2 \cdot 10^{-2}$ and $C_D \approx 1.2 \cdot 10^{-3}$ (the reliability of the selected c_0 and C_D values can be judged on the basis of the summaries presented in [5, 6]),

we have $(1 - c_3) = 0.13$. Then, in accordance with [6], the values of the constant β of the equilibrium interval and the proportionality factor in the expression for ω_l are equal to $5.85 \cdot 10^{-3}$ and 0.032 respectively. Accordingly, $c_1 \approx 0.45 \cdot 10^{-3}$ and then in the presence of collapsing of waves ($u_* \geqslant u_{* c}$) in place of $C_2 \simeq 0.24 \cdot 10^{-3}$ we will have $C_2 = 2(c_1 + c_2)(1 - c_3) \approx 0.38 \cdot 10^{-3}$.

Now we will turn again to an analysis of a situation encountered in a regime of rising of the lower boundary layer of the QHL. It can be seen from (10) that the equality of the left-hand side of the equation to zero can be satisfied only when $q_0 > 0$, that is, during a period of heating of the ocean surface. Such a situation corresponds to the expression

$$h = -C_2 \frac{u_*^3}{g \alpha_T q_0} \left(1 - C_1 C_3 \frac{u_*^2 |l|}{g \alpha_T q_0}\right)^{-1}. \tag{13}$$

In the special case of zero q_0 values it leads to an expression for the thickness of the Ekman boundary layer in a quasistationary drift current

$$h = C_3^{-1} \frac{u_*}{|l|}, \tag{14}$$

where the C_3 constant has the order of 100 (see [14]). Henceforth we will assume that $C_3 = 60$.

The system of equations (1), (2), (8), (10), with the above-mentioned values of the numerical constants C_1, C_2, C_3 and with the neglecting of the second term in parentheses at the right in (10) is used in computing the seasonal evolution of the active layer in the ocean. Before proceeding to a discussion of its results, in the seasonal evolution process we will discriminate two time intervals requiring special examination. Reference is to the end of the cooling period when the temperature jump at the lower boundary of the QHL can be close to zero and the onset of the heating period with typical for it small values of the heat flux at the ocean surface. In the first case the principal reason for the sinking of the QHL is nonpenetrating convection, for whose description it is sufficient to make use of the first three equations of the system and the condition $T_h = T_s$. Thus, in this case in place of (1), (2), (8), (10) we will have

$$\frac{dT_s}{dt} = \frac{q_0}{h}, \quad \frac{dh}{dt} - w_h = \frac{q_0}{\gamma h}, \quad T_h = T_s, \tag{15}$$

and the conversion from (1), (2), (8), (10) to (15) must be accomplished with $(T_s - T_h)$ attaining some prestipulated δT_* value.

In the second case, as indicated by observational data (in particular, see [9]), the change in h occurs approximately as follows: against the background of the old QHL with a thickness of about 100-200 m a new upper quasihomogeneous layer begins to form. Its thickness at the moment of change in the sign on q_0 must be dependent only on u_* and l. In order to

take this peculiarity into account we will assume that with a change of the sign on q_0 the thickness of the QHL changes in a jump from its maximum value at the end of the cooling period to a new value determined by formula (14). The temperature T_s of the new QHL remains unchanged and is equal to the temperature T_s^0 of the old QHL.

Finally, from the reasonings cited above it follows that at the beginning of the period of heating $q_h = 0$. The same equality exists during the remaining period of heating (with rising of the QHL) and therefore in the layer between the old and new bases of the QHL (that is, in the main part of the seasonal thermocline) the temperature must not experience any changes relative to its value at the end of the cooling period. However, in actuality this is not the case. Evidently, under the influence of the sporadic turbulence generated with the overturning of internal waves the temperature in the seasonal thermocline varies with time and in it some temperature distribution extremely far from homogeneous is established there. In order to take this circumstance into account we will replace the stepped temperature profile in the considered layer (during the heating period the model reproduces precisely such a profile with finite values of the time interval) by a linear function of depth whose parameters will be determined from the conditions of continuity of temperature at the lower boundary of the old QHL and maintenance of the heat content within the limits of the entire active layer. Such a replacement is accomplished only when $(dh/dt - w_h) < 0$. After cessation of rising of the QHL the temperature profile near the upper boundary of the seasonal thermocline remains unchanged up to the new annual cycle.

A solution of the system of equations (1), (2), (8), (10) was obtained by the Runge-Kutta method applicable to the problem of seasonal evolution of the active layer in the neighborhood of weather station N in the Pacific Ocean (φ = 30°N, λ = 140°W). All the necessary initial information was taken from [11]. It was also demonstrated in that source that the selected region is characterized by slight advection and it can be assumed that

$$w_h = 0,\ \gamma = -0{,}05\ \text{K/m},\ q_0 = \hat{q}_0 \sin(\omega t - \pi/2),\ \bar{u}_* = \hat{u}_* \sin(\omega t + \pi/2) + \bar{u}_*,$$

[K = coulomb] where $\hat{q}_0 = 1.79 \cdot 10^{-5}$ K m/sec is the amplitude of the seasonal fluctuations of the heat flux at the surface, $\hat{u}_* = 0.052$ m/sec and $\bar{u}_* = 0.232$ is the amplitude of the oscillations and the mean annual dynamic wind velocity, ω is the frequency of the oscillations, t is time.

The computations began from the moment of transition from negative to positive q_0 values (moment of ending of the cooling period) and continued for a period of 15 years. The initial values of thickness of the QHL and temperature were assumed equal to h = 120 m, $T_s = T_h$ = 18°C; the limiting value of the temperature jump δT at the base of the QHL and the critical value u_* c of dynamic wind velocity were 0.1°C and 0.25 m/sec. The periodic regime was considered steady when the thicknesses h at any two moments in time separated

from one another by a period differ by more than 0.01%. It was found that such a condition is already satisfied after three annual cycles.

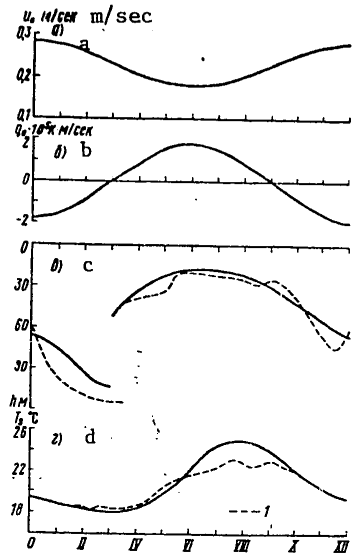

Fig. 1. Annual variation of dynamic wind velocity (a), heat flux at surface (b), thickness (c) and temperature (d) of upper quasihomogeneous layer at weather station N in Pacific Ocean. 1) observed annual variation of thickness and temperature of upper quasihomogeneous layer using data from [12].

The results of the computations presented in Fig. 1 reproduce well the observed peculiarities in the seasonal evolution of temperature of the QHL. An example of this is the phase shift between the moments of the maximum values q_0 (end of June) and T_s (end of August). The absence of a second maximum in the seasonal variation of surface temperature observed early in October probably can be attributed to exclusion of the salinity effect and failure to take into account the feedback between q_0 and T_s. In quantitative respects the results of the computations and the observational data on surface temperature agree fairly well with one another. Unfortunately, the same cannot be said about the thickness of the QHL, but, in addition to the limitations on the model itself, here it must be remembered that there are certain difficulties in determining h on the basis of experimental data. In any case the model ensures a qualitative similarity of the computed and observed changes in the thickness of the QHL (see Fig. 1), and this is not insignificant.

What has been said, as well as the fact that the model described above is quite economical (computations of evolution of the active layer of the ocean for a year requires not much more than 8 sec of computer time on a BESM-6 electronic computer), indicates the possibility of using it within the framework of a model of joint circulation of the ocean and the atmosphere.

*****

BIBLIOGRAPHY

1. Belevich, M. Yu., Chalikov, D. V., "Parameterization of the Upper Quasihomogeneous Layer and the Seasonal Thermocline in the Ocean," METEOROLOGIYA I GIDROLOGIYA (Meteorology and Hydrology), No 3, 1978.

2. Zilitinkevich, S. S., Monin, A. S., Chalikov, D. V., "Interaction Between the Ocean and the Atmosphere," FIZIKA OKEANA. T I. GIDROFIZIKA OKEANA (Physics of the Ocean), Vol I, Hydrophysics of the Ocean, Moscow, Nauka, 1978.

3. Zilitinkevich, S. S., Monin, A. S., Turikov, V. G., Chalikov, D. V., "Numerical Modeling of the Joint Circulation of the Ocean and Atmosphere," DOKLADY AN SSSR (Reports of the USSR Academy of Sciences), Vol 230, No 3, 1976.

4. Zilitinkevich, S. S., Resnyanskiy, Yu. D., Chalikov, D. V., "Theoretical Modeling of the Upper Layer of the Ocean," ITOGI NAUKI I TEKHNIKI. MEKHANIKA ZHIDKOSTI I GAZA (Results of Science and Engineering. Fluid and Gas Mechanics), Vol 12, 1978.

5. Kagan, B. A., "Interaction Between the Ocean and the Atmosphere (Theoretical Models of the System of Boundary Layers of the Atmosphere and Ocean)," ITOGI NAUKI I TEKHNIKI. OKEANOLOGIYA (Results of Science and Engineering. Oceanology), Vol 1, 1971.

6. Kitaygorodskiy, S. A., FIZIKA VZAIMODEYSTVIYA ATMOSFERY I OKEANA (Physics of Interaction Between the Atmosphere and Ocean), Leningrad, Gidrometeoizdat, 1970.

7. Kitaygorodskiy, S. A., "Dynamics of the Upper Thermocline in the Ocean," ITOGI NAUKI I TEKHNIKI. OKEANOLOGIYA, Vol 4, 1977.

8. Resnyanskiy, Yu. D., "Parameterization of Integral Dissipation of Turbulent Energy in the Upper Quasihomogeneous Layer of the Ocean," IZV. AN SSSR, FIZIKA ATMOSFERY I OKEANA, Vol 11, No 7, 1975.

9. Turner, G., EFFEKTY PLAVUCHESTI V ZHIDKOSTYAKH (Buoyancy Effects in Fluids), Moscow, Mir, 1977.

10. Alexander, R. C., Kim, J. W., "Diagnostic Model Study of Mixed-Layer Depths in the Summer North Atlantic," J. PHYS. OCEANOGR., Vol 6, No 3, 1976.

11. Davies, R. W., Haney, R., "The Role of Surface Mixing in the Seasonal Variations of the Ocean Thermal Structure," J. PHYS. OCEANOGR., Vol 6, No 4, 1976.

12. Dorman, C. E., Paulson, C. A., Quinn, W. H., "An Analysis of 20 Years of Meteorological and Oceanographic Data from Ocean Station N," J. PHYS. OCEANOGR., Vol 4, No 4, 1974.

13. Elsberry, R. L., Fraim, T. S., Trapnell, R. N., "A Mixed Layer Model of the Oceanic Thermal Response to Hurricanes," JGR, Vol 81, No 6, 1976.

14. Garwood, R. W., "An Oceanic Mixed Layer Model Capable of Simulating Cyclic States," J. PHYS. OCEANOGR., Vol 7, No 3, 1977.

15. Gill, A. E., Turner, J. S., "A Comparison of Seasonal Thermocline Models With Observations," DEEP SEA RES., Vol 23, No 5, 1976.

16. Kantha, L. H., Phillips, O. M., Azad, R. S., "On Turbulent Entrainment at a Stable Density Interface," J. FLUID. MECH., Vol 79, Part 4, 1977.

17. Kim, J. W., "A Generalized Bulk Model of the Oceanic Mixed Layer," J. PHYS. OCEANOGR., Vol 6, No 5, 1976.

18. Kraus, E. B., Turner, J. S., "A One-Dimensional Model of the Seasonal Thermocline, II. The General Theory and its Consequences," TELLUS, Vol 19, No 1, 1967.

19. Longuet-Higgins, M. S., "On Wave Breaking and the Equilibrium Spectrum of Wind-Generated Waves," PROC. ROY. SOC., London, A310, No 1501, 1969.

20. Niiler, P. P., "Deepening of the Wind-Mixed Layer," J. MARINE RES., Vol 33, No 3, 1975.

21. Niiler, P. P., Kraus, E. B., "One-Dimensional Models of the Upper Ocean," MODELLING AND PREDICTION OF THE UPPER LAYERS OF THE OCEAN (ADV. STUDY INST., URBINO, ITALY), Oxford, e. a. Pergamon Press, 1977.

22. Phillips, O. M., "On Equilibrium Range in the Spectrum of Wind-Generated Waves," J. FLUID. MECH., Vol 4, Part 3, 1958.

23. Phillips, O. M., "Entrainment," MODELLING AND PREDICTION OF THE UPPER LAYERS OF THE OCEAN (ADV. STUDY INST., URBINO, ITALY, 1975), Oxford, et al., Pergamon Press, 1977.

24. Stull, R. B., "The Energetics of Entrainment Across a Density Interface," J. ATMOS. SCI., Vol 33, No 7, 1976.

UDC 556.166

COMPUTATIONS OF RUNOFF RATES AND TRAVEL TIME OF WATER FROM SLOPES IN DETERMINING MAXIMUM RAIN-INDUCED DISCHARGES FOR SMALL DRAINAGE BASINS

Moscow METEOROLOGIYA I GIDROLOGIYA in Russian No 12, Dec 79 pp 76-82

[Article by Candidate of Technical Sciences I. K. Sribnyy, Ukrainian Scientific Research Institute of Hydroengineering and Melioration, submitted for publication 23 March 1979]

Abstract: On the basis of the author's investigations recommendations are given on determination of runoff rates and travel time of water from slopes when determining maximum rain-induced discharges for small drainage basins with nonuniform runoff taken into account. The roughness coefficients for the slope surfaces and other coefficients entering into the computation formulas are determined more precisely.

[Text] The absolute value of the maximum shower-induced discharges in small drainage basins is dependent to a considerable degree on the rates of runoff and the travel time of water from slopes. The greater the runoff rate and the lesser the travel time of the water from the slopes, the more rapid is the formation of the maximum discharges from showers and their absolute value will be greater since with an increase in the duration of the shower its intensity decreases and vice versa [2-4, 8, 9, 11, 13].

In the norms for computations of the maximum shower-induced discharges [9, 13], as well as in [7], and elsewhere, the mean rates of runoff of water from the slopes are determined using the improved formula derived by M. M. Protod'yakonov and G. A. Alekseyev

$$v = ml^{1/4} A^{1/2}, \quad (1)$$

where m is the roughness coefficient for slopes; I is the slope in %; A = qL is the quantity of water flowing along the slope in a width of 1 km; q is the runoff modulus in m^3/sec from 1 km^2; L is the length of the area of simultaneous runoff above the considered section in km.

The basis for equation (1) is the empirical Protod'yakonov formula which he derived on the basis of experiments in small runoff areas for determining the rates of runoff of water from slopes under the condition of uniform runoff

$$v = k_2 A^{1/2} I^{3/16}, \quad (2)$$

where k_2 is a coefficient dependent on the roughness of the surface of the slopes.

However, in nature there are virtually no ideally even slopes and the runoff from the slopes occurs nonuniformly with its concentration in individual small channels, as a result of which the hydraulic radius and the velocity of the slope flows accordingly increase [8]. As a result, the mean rates of runoff of water from the slopes, determined using formula (1), will differ considerably from those measured in nature.

In addition, in the norms [9, 13], and also in studies [1, 7] the roughness coefficients for the slope surfaces do not adequately take into account the vegetation and the types of soil working. For example, only a grassy cover -- thin, intermediate and dense -- is taken into account. At the same time, on most of the worked slopes grain crops are also cultivated, there are plowed lands of different types, the plants may be sown in furrows or sown without furrows and therefore the roughness coefficients for these types of vegetation cover can differ very greatly from those recommended for a grassy surface.

For cultivated lands the roughness coefficients are recommended for well-worked and roughly worked surfaces. However, in agricultural production such a breakdown of cultivated lands is inadequate. Cultivated lands can be worked both along and across the slope, with or without actual cultivation, and when growing field crops furrows are run in different directions along the slope. Among the anti-erosion measures which can be taken are the construction of ridges, embankments, slitting, etc.

It is therefore unclear to what type of field working -- good or bad -- different surfaces should be assigned in accordance with these recommendations.

I. A. Kuznik as early as 1962 pointed out that in the hydrological literature no use is made of the generally accepted terminology and classification of agricultural fields and that cultivated fields in many cases are not differentiated with respect to the types of working [5]. Unfortunately, these correct comments were not taken into account in the drawing up of SN 435-72 and as before an outdated terminology and classification of agricultural fields, 50 years old, is employed.

In formulas (1) and (2) the rate of runoff of water from slopes is also dependent on the runoff coefficients, which determine the value of the parameter A entering into the formulas.

The coefficients of runoff from slopes are dependent on vegetation, the system for working the soil and the surface slope and can vary up to 400% [4, 11].

However, the norms [9, 13] recommend identical runoff coefficients and the slope is not taken into account for workable and for unworkable surfaces.

As a result it is extremely difficult to determine the rate of runoff and the travel time of water from slopes using the formulas cited in [7-9, 13] for the specifically investigated conditions of slopes, depending on the types of working of the soil, vegetation and slopes and the maximum discharges induced by showers can be determined with considerable errors.

In addition, a number of authors have proposed and investigated other formulas for determining current velocities on slopes and in small watercourses [6, 14], which have differences and frequently are justified on the basis of formulas (1), (2). Therefore, it cannot be said that the recommended formulas (1), (2) are most correct.

In studies [11, 12], on the basis of our investigations, we derived and validated a formula for determining current velocities of water in the primary network of small channels for extremely small watercourses when the water runs off the slopes, with nonuniform runoff taken into account. This formula has the following form:

$$v = 0.0254\, a_3 \sqrt[3]{i\, \alpha_{max} k_{\alpha}\, b_{chan} L_{slope} I_{slope}}, \qquad (3)$$

where a_3 is the coefficient dependent on the roughness coefficient of the surface of slopes in the Bazen formula; i is the mean intensity of the shower during the travel time from the slope, mm/min; α_{max} is the maximum runoff coefficient during the period of formation of maximum discharges with a slope of 9° in dependence on the soils and the methods for working them and vegetation, k_{α} is the coefficient of the influence of slopes on runoff in comparison with data on the runoff coefficients obtained with a slope of the areas of 9°; it is determined using the formula

$$k_{\alpha} = 1 \pm 0{,}01\, P_{\text{укл}} (I^{\circ} - 9), \qquad (4)$$

[УКЛ = slope] P_{slope} is the percentage change in runoff with a change in slope by 1° in dependence on the methods for working the soil and vegetation, %; I° is slope in degrees; b_{chan} is the width of the primary channel network along the slope, m; L_{slope} is the length of the slope, m; I_{slope} is the slope.

Using formula (3) it is possible to determine the current velocity in any considered section of the slope. The velocity at all times increases with an increase in the length of the slope since the discharges in the channels continue to increase.

The mean rate of water runoff from the slope from the water divide to the mouth will be less than the maximum in the lower part of the slope. In order to determine the mean rate of water runoff from the slope it is necessary to divide the slopes into several sectors; the greater the number of sectors into which the slope is broken in length, the more precise will be the determination of the rate of water runoff. For each of the sectors we calculated the mean velocities, which are then summed for determining the mean rate of runoff from the entire slope. This mean runoff rate can be determined as the mean weighted rate using the equation

$$v_{mean} = \frac{v_1 l_1 + (v_1 + v_2) l_2 + \ldots + (v_{n-1} + v_n) l_n}{2L},$$

where v_1, $v_2 \ldots v_{n-1}$, v_n is the current velocity in the lower part of each sector of the slope, m/sec, l_1, $l_2, \ldots, l_{n-1}$, l_n are the lengths of the sectors of the slope between the computation points, m; L is the total length of the slope, m.

If the slope is identical or changes little along its length and the slope is covered with uniform vegetation or is worked in a single direction, the mean rate of water runoff from the slopes can be determined using the formula

$$v_{mean} = k v_{max}, \quad (6)$$

where v_{mean} [$v_{cp} = v_{mean}$] is the mean rate of water runoff from the slopes, m/sec; k is the factor for conversion from the maximum rate in the lower part of the slope to the mean runoff rate of water from the slope; v_{max} is the maximum rate of water flow in the lower part of the slope and is determined using formula (3), m/sec.

The coefficient of the ratio of the mean rate of water runoff from the slope to the maximum at the bottom of the slope is determined using the formula

$$k = \frac{\sqrt[3]{l_1}\, l_1 + \left(\sqrt[3]{l_1} + \sqrt[3]{l_2}\right) l_2 + \ldots + \left(\sqrt[3]{l_{n-1}} + \sqrt[3]{l_n}\right) l_n}{2L \sqrt[3]{L}}. \quad (7)$$

Computations show that this coefficient is from 0.65 to 0.73 in dependence on slope length. Taking into account the sinuosity of the flows, this coefficient on the average can be assumed equal to k = 0.65.[[M. M. Protod'yakonov recommends that it be assumed that K = 0.60 [8].]

Taking into account what has been said above, the mean rate of water runoff from any slope with an identical surface and slope is determined using the formula

$$v_{mean} = 0.016\, a_3 \sqrt[3]{i_{\alpha max}\, k_{\alpha}\, b_{chan} L_{slope} I_{slope}}.$$

The travel time of the water from the slope is determined as the quotient

Table 1

Roughness Coefficients (n_B) for Slopes in Bazen Formula and Corresponding Coefficients (a_3) in Formulas (3), (8)

Characteristics of Slope Surface	Coefficients	
	n_B	a_3
Irrigation furrows with straight, clean and smooth bottom	1.25	8.5
Same furrows, inadequately planed; relatively straight and even channels of watercourses with constant water flow	1.50	7.5
Furrows in inter-row cultivated crops along slope; unsodded even slopes; relatively even and straight rills on slopes and along bottom of gullies	1.75	6.4
Plowed fields with cultivation; rills on slopes and along bottom of gullies with uneven bottom, sinuous, encumbered with rock and overgrown with vegetation; channels of ravines overgrown with vegetation, without rills	2.75	4.9
Overgrown furrows in inter-row cultivated crops along slope; natural pasture with thin grass	3.75	4.1
Natural pasture with mown gass of intermediate density; grains	5.5	3.2
Natural pasture with unmown grass of intermediate density	7.0	2.7
Natural pasture with dense grass; biennial dense grass	9.0	2.3
Lumpy overgrown surface; very dense grass	12.0	1.9

FOR OFFICIAL USE ONLY

APPROVED FOR RELEASE: 2007/02/08: CIA-RDP82-00850R000200050012-1

$$t = \frac{L_{скл}}{v_{ср}}. \qquad (9)$$

Table 2

Maximum Coefficients of Runoff from Showers (α_{max}) in Dependence on Layer of Precipitation, Vegetation, Soils and Their Working Systems With Surface Slope of 9°

1 Почвы	Суточный слой осадков, мм 2	Необрабатываемые склоны 3: редкая трава, кустарник на площади до 50% 5	Необрабатываемые склоны 3: средняя трава, кустарник на площади более 50%	Обрабатываемые склоны 4: пахота вдоль склона 6 7	Обрабатываемые склоны 4: пахота поперек склона 8
9 Супесчаные	12 до 80	0,50	0,40	0,25	0,20
	80—100	0,55	0,44	0,28	0,23
	100—120	0,60	0,48	0,31	0,26
	120—150	0,65	0,52	0,34	0,29
	>150	0,70	0,55	0,35	0,30
10 Суглинистые	12 до 80	0,60	0,50	0,35	0,30
	80—100	0,65	0,54	0,39	0,33
	100—120	0,70	0,58	0,43	0,36
	120—150	0,75	0,62	0,47	0,39
	>150	0,80	0,65	0,50	0,40
11 Глинистые	до 80	0,70	0,60	0,45	0,40
	80—100	0,75	0,64	0,48	0,43
	100—120	0,80	0,68	0,51	0,46
	120—150	0,85	0,72	0,54	0,49
	>150	0,90	0,75	0,55	0,50

KEY:

1. Soils
2. Daily precipitation layer, mm
3. Unworkable slopes
4. Workable slopes
5. Thin grass, scrub over area up to 50%
6. Intermediate grass, scrub over area up to 50%
7. Plowing along slope
8. Plowing across slope
9. Sandy loam
10. Clayey loam
11. Clayey
12. up to

For the purpose of more precise determination of the runoff coefficients, the roughness coefficients and rates of water runoff for different surfaces and slopes the specialists of the Ukrainian Scientific Research Institute of Hydroengineering and Melioration during 1969-1975 carried out special experiments in extensive runoff areas (up to 2,000 m^2) with different soil fertility with different slopes with the assistance of artificial sprinkling. The great extents of the areas made it possible to bring the artificial conditions for the formation of runoff closer to natural conditions to a far greater degree than was the case up to this time in the USSR and made it possible to use these data for more precise determination of the runoff coefficients, roughness coefficients for the surfaces

of slopes and the rates of water runoff in dependence on slopes, methods for working the soil and the vegetation on slopes for small areas of drainage basins and make a more precise determination of the values of the other parameters entering into the computation formulas (3), (4), (8), (9).

These experiments once again demonstrated that the runoff of water from the slopes does not occur in a thin uniform layer but with a concentration of the runoff into individual small channels along the primary network of small channels forming in microrelief depressions on the slopes.

The a_3 coefficient, dependent on the surface roughness of the slopes, must be adopted in accordance with Table 1, prepared for the most part on the basis of the above-mentioned experiments, and also refined for individual types of slope surface in accordance with studies [6, 10, 14].

The coefficient of maximum runoff α_{max} for a slope of 9° must be adopted in accordance with Table 2, prepared on the basis of the above-mentioned experiments for clayey loam soils.

For other types of soils the values of the maximum runoff coefficient in the table were corrected in accordance with [9, 13].

The width of the primary network of small channels along the slope b_{chan} varies in dependence on the methods for working the soil, vegetation on the slopes and the length of the slopes. The steeper the slopes, the lesser is this width because the runoff rates will be greater and the runoff coefficients will also be greater and a lesser drainage basin area will be required for forming the primary network of small channels, and vice versa. The longer the slopes, the greater will be the increase in the width of the drainage basins of the primary network of small channels along the slope since the larger rills, as a result of natural irregularities toward the bottom of the slope gradually intercept increasingly smaller rills.

In the case of longitudinal plowing with furrows along the slope runoff will not be formed in every furrow because due to the irregularity of microrelief and inexact plowing some furrows will intercept runoff from adjacent ones.

On a surface well worked by plowing the width of the drainage basins of the primary network of small channels will be greater than on an inadequately evened surface. Therefore, the width of the drainage basins of the primary network of small channels along the slope is established on the spot in each specific case when carrying out field investigations.

In the absence of these data, with a length of the slopes up to 300 m and a steepness from 2 to 10° this width (b_{chan}) as an average in the computation can be taken in accordance with the data in Table 3, prepared on the basis

of the experiments which have been carried out and field investigations of the slopes.

The percentage change in runoff in dependence on the methods for working the soil and vegetation on the surface of the slopes can be taken in accordance with the data in Table 4, prepared on the basis of the above-mentioned experiments.

Table 3

Mean Computed Width of Drainage Basins of Primary Channel Network Along Slope With Length of Slopes Up to 300 m

State of slope surface	b_{chan} m
Plowing with furrows along slope	2
Plowing with cultivation along slope	4
Plowing with cultivation across slope	6
Plowing with furrows across slope	12
Pasture	16

Table 4

Coefficient of Influence of Slope on Runoff in Dependence on Vegetation and System for Working the Slopes

Characteristics of vegetation and system for working slopes	R_{slope} % %
Pasture with thin grass	2
Pasture with intermediate grass	3
Plowing along slope	4
Plowing across slope	6

Our experiments indicated a good agreement between experimental data on measurements of water current velocities on slopes with computed data, determined using formulas (3), (8), whereas the computed velocities of the water flow, determined using formulas (1), (2) had a discrepancy with experimental data up to 100%.

Our investigations made it possible to derive and validate formulas for determining the rates of water flow on slopes taking into account the non-uniform runoff in dependence on the methods for working the soil, vegetation and slopes and refine the values of the parameters entering into the computation formulas, which will find use in determining the maximum shower-induced discharge for small drainage basins.

A determination of the rate of water flow on a slope in any considered section must be carried out using formula (3), whereas a determination of the mean rate of water runoff from slopes is made using formulas (5), (8).

BIBLIOGRAPHY

1. Artem'yev, S. S., Boldakov, Ye. V., Zhuravlev, M. M., RASCHET LIVNEVOGO STOKA S MALYKH VODOSBOROV (Computation of Shower-Induced Runoff from Small Drainage Basins), Moscow, Transport, 1965.

2. Biryukov, I. N., "Computation Curves of Maximum Intensities of Showers With a Different Frequency of Recurrence," MAKSIMAL'NYY STOK S MALYKH BASSEYNOV (Maximum Runoff from Small Basins), Moscow, Transzheldorizdat, 1940.

3. Vishnevskiy, P. F., ZLIVI I SLIVOVIY STIK NA UKRAINI (Showers and Shower-Induced Runoff in the Ukraine), Kiev, Vid-vo AN URSR, 1964.

4. Gudzon, N., OKHRANA POCHVY I BOR'BA S EROZIYEY (Soil Conservation and Contending With Erosion), Moscow, Kolos, 1974.

5. Kuznik, I. A., AGROLESOMELIORATIVNYYE MEROPRIYATIYA, VESENNIY STOK I EROZIYA POCHV (Agricultural-Silvicultural Melioration Measures, Spring Runoff and Soil Erosion), Leningrad, Gidrometeoizdat, 1962.

6. Lalykin, N. V., Mol'chan, Ya. O., "Determination of Travel Time of High Water in the Channels of Small Watercourses," GIDROMELIORATSIYA TA GIDROTEKHNICHNE BUDIVNITSTVO (Hydromelioration and Hydroengineering in the Future), No 1, L'viv, Vishcha Shkola, 1974.

7. Moklyak, V. I., Zuzanskiy, N. B., "Determination of the Maximum Shower-Induced Runoff," GIDROTEKHNIKA I MELIORATSIYA (Hydroengineering and Melioration), No 6, 1978.

8. Protod'yakonov, M. M., "Principal Points in the Modern Theory of Runoff of Surface Waters," MAKSIMAL'NYY STOK S MALYKH BASSEYNOV (Maximum Runoff from Small Basins), Moscow, Transzheldorizdat, 1940.

9. RUKOVODSTVO PO OPREDELENIYU RASCHETNYKH GIDROLOGICHESKIKH KHARAKTERISTIK (Manual on Determination of Computed Hydrological Characteristics), Leningrad, Gidrometeoizdat, 1973.

10. Slastikhin, V. V., VOPROSY MELIORATSIY SKLONOV MOLDAVII (Problems in Melioration of Slopes in Moldavia), Kishinev, Gosizdat, 1954.

11. Sribnyy, I. K., "Protective Anti-erosion Structures," VODOKHOZYAYSTVENNOYE STROITEL'STVO NA MALYKH REKAKH (Water Management Construction on Small Rivers), Kiev, Budivel'nik, 1977.

12. Sribnyy, I. K., "Computations of Rates of Water Flow on Slopes Subjected to Erosion," GIDROTEKHNIKA I MELIORATSIYA (Hydroengineering and Melioration), No 12, 1977.

13. UKAZANIYA PO OPREDELENIYU RASCHETNYKH GIDROLOGICHESKIKH KHARAKTERISTIK (SN 435-72) (Instructions on Determination of Computed Hydrological Characteristics (SN 435-72)), Leningrad, Gidrometeoizdat, 1973.

14. Cherkasov, A. A., MELIORATSIYA I SEL'SKOKHOZYAYSTVENNOYE VODOSNABZHENIYE (Melioration and Agricultural Water Supply), Moscow, Sel'khozgiz, 1959.

UDC 556.142

THEORETICAL ANALYSIS OF DEPENDENCE OF THE SOIL WATER YIELD COEFFICIENT ON THE RATE OF CHANGE IN GROUND WATER LEVEL

Moscow METEOROLOGIYA I GIDROLOGIYA in Russian No 12, Dec 79 pp 83-90

[Article by Candidates of Technical Sciences I. L. Kalyuzhnyy and K. K. Pavlova, State Hydrological Institute, submitted for publication 28 February 1979]

Abstract: The authors give a theoretical analysis of the change in ground water level in an elementary soil column. It is shown that the soil water yield coefficient is dependent not only on the method of its determination, but also on the rate of decrease (increase) of the ground water level.

[Text] The characteristics of water yield and saturation deficit coefficients can be determined by different methods [2, 4, 5]. It must be recalled that neither of these parameters is a constant value for a particular type of soil or ground. As noted in a number of studies [2-4], the water yield coefficient and saturation deficit are determined among various other factors by initial soil-ground moisture content and the rate of change of ground water level. However, the role of the latter factors has not been ascertained with sufficient accuracy in quantitative respects.

In this paper we give a theoretical analysis of the dependence of the water yield and saturation deficit coefficients on the rate of change in ground water level.

As demonstrated in [1, 5], the rate of water movement in completely filled pores can be computed using the Poiseuille equation, transformed by Kozeny

$$V_i = \frac{\gamma g}{\Delta \delta} Ie \left(\frac{w_i}{z_i}\right)^2, \quad (1)$$

where V_i is the rate of water movement in the i-th pore with the head gradient I, γ is fluid density, Δ is fluid viscosity, w_i/z_i is the ratio of pore area to its wetted perimeter, e is a constant dependent on pore

configuration, g is the acceleration of free falling, δ is the coefficient of lengthening of the filtration path.

Since the ground particles in large part have the most different configuration, up to and including horizontally arranged platelets, on the basis of experimental studies we consider it more correct to assume this coefficient on the average to be equal to 2.0. Then, substituting into formula (1) the w_i and z_i values for a cylindrical pore and constant e for circular pores equal to 0.5, we obtain

$$V_i = \frac{\gamma g I r^2}{16 \Delta}, \tag{2}$$

where r is the radius of a cylindrical pore, which can be determined from the height position of the water held in a particular pore (H_k).

Now we will examine a limiting case -- the conditions which are observed in an experimental determination of the water yield coefficient when a pressure equal to atmospheric pressure is initially observed at the surface of a column of ground of the height H and virtually instantaneously falls toward its base. Then in the i-th pore the water at each moment in time will move under the influence of a variable piezometric gradient equal to

$$I = \frac{H - H_k - h}{H - h}, \tag{3}$$

where H_k is the height of the capillary rising of water in a pore with the length H, h is the position of the level from the surface of the column at the time τ.

However, the time-variable rate in the i-th pore V_i is equal to

$$V_i = \frac{dh}{d\tau} = V_i' \frac{H - H_k - h}{H - h}. \tag{4}$$

The solution of this equation with the boundary conditions $\tau = 0$ and h = 0 gives

$$\tau = \frac{1}{V_i}\left[h - H_k \ln\left(1 - \frac{h}{H - H_k}\right)\right], \tag{5}$$

where τ is the time from onset of the experiment, V_i is the rate of water movement in the i-th pore with I equal to 1 (is determined from equation (2)).

It is impossible to solve this equation for h. Therefore, it is desirable to compute the τ value with a series of h values and construct a nomogram for finding h with any τ value.

Both equation (2) and equation (4) give the upper limit for the rate of water movement in a pore. Accordingly, equation (5) gives the lower limit of the τ value.

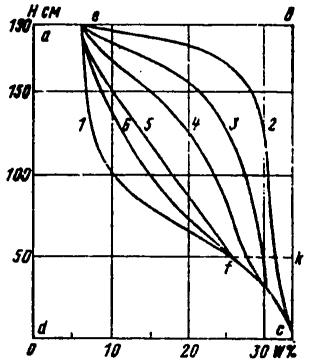

Fig. 1. Computed curves of change in moisture at different time intervals from onset of water yield. 1) equilibrium curve of moisture distribution; 2) curve of moisture distribution after 10 min; 3) after 30 min; 4) after 60 min; 5) after 120 min; 6) after 360 min

Table 1

Change in Water Yield With Time (Column Section — 100 cm^2, Height — 190 cm, Moisture Equilibrium Distribution Curve is Shown in Figure 1)

Время 1	Водоотдача, $см^3$ 2	Коэффициент водоотдачи μ 3	Время 1	Водоотдача, $см^3$ 2	Коэффициент водоотдачи μ 3
0 10 мин 4	830	0,044	6 00	3237	0,170
0 30	1431	0,075	12 00	3323	0,175
1 00	1897	0,0998	24 00	3334	0,176
2 00	2833	0,149	48 00	3337,9	0,176
3 00	2994	0,158	72 00	3338,0	0,176

KEY:
1. Time
2. Water yield, cm^3
3. Water yield coefficient
4. min

A series of extremely important conclusions can be drawn from equation (5).

1. The time for water decrease in the pore (to a stipulated "stop" h) is inversely proportional to the filtration rate in this pore when I = 1.

2. Upon attaining equilibrium, when h becomes equal to $H - H_k$, the time τ is equal to infinity. It therefore follows that we can never attain equilibrium. However, specific computations show that even for extremely small pores the time of attaining a state differing from equilibrium is completely finite. For example, in a column of ground with a height of

Table 2

Dependence of Water Yield Coefficient on Height of Soil Column

Высота колонки, *см* 1	Объем колонки сечением 100 *см*² *см*³ 2	Объем водоотдачи, *см*³ 3	Коэффициент водоотдачи μ 4
190	19000	3338	0,1760
150	15000	2268	0,1460
100	10000	972	0,0972
50	5000	144	0,0288
20	2000	11	0,0055

KEY:
1. Height of column, cm
2. Volume of column with section 100 cm^2/cm^3
3. Water yield volume, cm^3
4. Water yield coefficient

190 cm with h = 190 - 150 = 40 cm the time for attaining h = 35 cm is 16 hours 12.5 minutes and h = 39.9 cm, that is, differing from an equilibrium value by only 1 mm -- 45 hours 25 minutes. However, transition to infinity occurs precisely in this last millimeter.

3. Since the water yield volume (w_i) of the i-th pores at a specific moment in time τ will be equal to

$$w_i = h_i S_i, \tag{6}$$

where S_i is the total cross section of the pores, determined from the equilibrium distribution curve for moisture above the ground water level, then equation (5) makes it possible to calculate the water yield and the distribution of residual moisture in the ground at any moment in time.

Figure 1 shows computed curves of the distribution of moisture for a column of ground with a height of 190 cm and a porosity of 33.6%. In the water yield process curves having a sharply convex (relative to the x and y axes) shape are gradually flattened, then acquire a concave shape, and finally merge with the equilibrium moisture distribution curve. Table 1 gives the total water yield for different moments in time. The water yield rate, maximum at first, decreases rather rapidly. The nature of the change in the rate of water yields is dependent on the composition of the ground, to be more precise, the curve for the size distribution of pores in the particular ground, a reflection of which is the equilibrium moisture curve.

4. The water yield coefficient for each individual pore is characterized by the ratio h/H. However, the h/H ratio will be dependent only on the H value. Accordingly, the water yield coefficient will be dependent not only on the property of the ground, but also the height of the column in the experiment

Table 3

Lag in Decrease in Level in Capillaries of Different Section

H_k см	1 При снижении грунтовой воды 0,12 см/ч: x см	x конца первого часа, см 3	Δ z—x, см	объем водоотдачи, $см^3/см^2$ 4	τ 0,99—время достижения 0,99 x, сек 5	2 z=1,2 см/ч: x см	τ сек 6
10	$0{,}249 \cdot 10^{-3}$	$0{,}249 \cdot 10^{-3}$	0,11975	0,001197	34	$0{,}219 \cdot 10^{-2}$	34
20	$2{,}000 \cdot 10^{-3}$	$2{,}000 \cdot 10^{-3}$	0,1180	0,00165	276	$2{,}00 \cdot 10^{-2}$	276
30	$6{,}777 \cdot 10^{-3}$	$6{,}777 \cdot 10^{-3}$	0,1132	0,00204	936	$6{,}770 \cdot 10^{-2}$	939
40	$1{,}620 \cdot 10^{-2}$	$1{,}620 \cdot 10^{-2}$	0,1038	0,00250	2220	$1{,}66 \cdot 10^{-1}$	2223
50	$3{,}130 \cdot 10^{-2}$	$3{,}03 \cdot 10^{-2}$	0,0897	0,00269	4355	$3{,}15 \cdot 10^{-1}$	4370
60	$5{,}385 \cdot 10^{-2}$	$4{,}94 \cdot 10^{-2}$	0,0806	0,00282	7460	$5{,}43 \cdot 10^{-1}$	7570
70	$8{,}560 \cdot 10^{-2}$	$6{,}48 \cdot 10^{-2}$	0,0552	0,00215	11600	$8{,}66 \cdot 10^{-1}$	12060
80	$1{,}280 \cdot 10^{-1}$	$0{,}78 \cdot 10^{-1}$	0,0420	0,001345	16750	$1{,}297 \cdot 10^{-1}$	18130
90	$1{,}824 \cdot 10^{-1}$	$0{,}810 \cdot 10^{-1}$	0,0330	0,000826	25330	$1{,}858 \cdot 10^{-1}$	26100
100	$2{,}495 \cdot 10^{-1}$	$0{,}960 \cdot 10^{-1}$	0,0240	0,000384	34500	$2{,}552 \cdot 10^{-1}$	35900
110	$3{,}330 \cdot 10^{-1}$	$1{,}005 \cdot 10^{-1}$	0,0195	0,000234	47650	$3{,}405 \cdot 10^{-1}$	48200
120	$4{,}330 \cdot 10^{-1}$	$1{,}025 \cdot 10^{-1}$	0,0175	0,000105	60500	$4{,}475 \cdot 10^{-1}$	63550
130	$5{,}500 \cdot 10^{-1}$	$1{,}030 \cdot 10^{-1}$	0,0170	0,000085	78200	$5{,}73 \cdot 10^{-1}$	81800
140	$6{,}870 \cdot 10^{-1}$	$1{,}100 \cdot 10^{-1}$	0,0100	0,000030	95200	$7{,}18 \cdot 10^{-1}$	103200
150	$8{,}460 \cdot 10^{-1}$	$1{,}130 \cdot 10^{-1}$	0,0070	0,00007	117500	$8{,}92 \cdot 10^{-1}$	129100
160	1,039	$1{,}140 \cdot 10^{-1}$	0,0060	0,000012	143000	$10{,}68 \cdot 10^{-1}$	158700
170	1,254	$1{,}150 \cdot 10^{-1}$	0,0050	0,000010	171000	$13{,}20 \cdot 10^{-1}$	193000
180	1,466	$1{,}170 \cdot 10^{-1}$	0,0030	0,000003	203500	$15{,}82 \cdot 10^{-1}$	233000

$\mu = \frac{0{,}018088}{0{,}12} = 0{,}1507$ $\quad \Sigma = 0{,}018088$

KEY:

1. With decrease in ground water 0.12 cm/hour
2. z = 1.2 cm/hour
3. x -- end of first hour, cm
4. Water yield volume, cm^3/cm^2
5. τ 0.99 -- time of attaining 0.99 x, sec
6. τ sec

Notes: $\Delta z - x$ -- difference between decrease in ground water level Δz and "lag" x, that is, true decrease of water in capillary; 2. Water yield volume $Q = (\Delta z - x)S_i$, where S_i is the section of pores of a particular radius; 3. τ level lag time 0.99 x of limiting value

Table 4

Lag in Rising of Water in Capillaries of Different Section

H_k см	1 При поднятии уровня воды со скоростью 1,2 см/сек: x см	x конца первого часа, см 2	Δ z—x	Объем водоподъема, см³/см² 3	τ 0,99 x, сек 4
10	0,249·10⁻²	0,249·10⁻²	1,19751	0,007185	34,3
20	2,01·10⁻²	2,00·10⁻²	1,1800	0,01652	276
30	6,745·10⁻²	6,745·10⁻²	1,13255	0,02038	930
40	0,1594	0,1594	1,0406	0,02497	2192
50	0,311	0,305	0,8950	0,02685	4265
60	0,532	0,476	0,7240	0,02534	7320
70	0,844	0,642	0,5580	0,021762	11460
80	1,255	0,790	0,4100	0,01312	17550
90	1,785	0,883	0,3170	0,008925	24200
100	2,430	0,960	0,2400	0,00384	32750
110	3,210	0,979	0,221	0,002652	47950
120	4,165	1,041	0,159	0,000954	55850
130	5,260	1,078	0,122	0,000610	70350
140	6,510	1,106	0,094	0,000282	86700
150	7,970	1,115	0,085	0,000085	109900
160	9,100	1,120	0,080	0,000160	128100
170	11,420	1,142	0,058	0,000116	149700
180	13,50	1,180	0,020	0,000020	175200
	μ=0,144			Σ=0,172771	

KEY:

1. With rising of water level at a rate of 1.2 cm/sec
2. x -- end of first hour, cm
3. Volume of water rising cm^3/cm^2
4. τ 0.99 x, sec

or on the decrease in the ground water level in nature and there is certainly no constancy of the water yield coefficient. This coefficient can be constant for ground completely devoid of capillary moisture (except for "cuff" moisture), that is, for gravelly or also for blocky ground, in which at least within blocks there is capillary moisture present, but in such small pores that it is known that in these pores there can be no decrease in the level ($H_k > H$), but the pores between the blocks are so large that there is virtually no capillary rise in them. Table 2 gives the values of the water yield coefficient in dependence on the height of the column for ground with an equilibrium curve of the distribution of capillary moisture, shown in Fig. 1.

Until now we have examined the case of an "instantaneous" decrease in the ground water level by a stipulated value, which is possible only in some cases. We will examine the role of the rate of decrease in the ground water level from a surface with zero (more likely, equal to atmospheric) pressure.

The first position can be formulated in the following way: if the rate of decrease in the ground water level is so small that the entire equilibrium distribution curve for capillary moisture drops down following the ground water without its deformation, then the μ coefficient will be equal to the total porosity minus the quantity of bound (in one form or another) moisture.

In all the pores will the water drop down with such a rate, that is, will all the capillary edge drop down as a whole or will it be deformed? If at the initial moment in time there was an equilibrium distribution of moisture so that movement occurs in the i-th pore, it is necessary that the zero pressure surface drop by some value x and that a piezometric gradient equal to $I_i = x/H_{ki} + x$ develop. Then the rate of water movement in this pore will be

$$V_i = V_i' \frac{x_i}{H_{k_i} + x_i}. \tag{7}$$

We will determine in what pores and with what x values the rate V_i will be equal to the rate of decrease in the ground water level V_z:

$$V_i \frac{x_i}{H_{k_i} + x_i} = V_z. \tag{8}$$

Hence

$$x_i = \frac{V_z H_{k_i}}{V_i - V_z}. \tag{9}$$

In the process of steady motion the height of the column of fluid in the pores will not be H_{ki}, but $H_{ki} + x_i$, where x_i is the lag in the dropping of the capillary meniscus of the i-th pore from the dropping of the ground water surface (the surface with a pressure equal to atmospheric). The rate of this lag will be

$$\frac{dx}{d\tau} = V_z - V_i \frac{x}{H_k + x}. \tag{10}$$

The integration of this equation under the condition x = 0 with $\tau = 0$ and V_z = const gives the following expression:

$$\tau = \frac{1}{V_i - V_z}\left[-x + \frac{H_k V_i}{V_i - V_z} \ln \frac{H_k V_z}{H_k V_z - (V_i - V_z)x}\right]. \tag{11}$$

Equation (11) gives the complex dependence between τ and x, especially since the x value with a definite τ and V_z value must be found by trial and error.

We note the circumstance that the x value tends to its limit with the tendency $\tau \to \infty$. However, as in the case of equation (5) the transition to infinity takes place in the last x fractions. For example, 0.99 x is attained with H_k = 10 cm in the course of 34 sec, when H_k = 50 cm in the course of 4355 sec, etc.

Table 3 gives the x values when the rate of decrease in the ground water level is 0.12 cm/hour, the x value by the end of the first hour of level decrease and also the difference between the decrease in the ground water level and the decrease in the water column in capillaries with different H_k values. Column 5 gives the volume of water yield from different pores.

The cited data show that with a ground water depth of 190 cm the water yield coefficient was less than that obtained experimentally -- 0.1507 instead of 0.176.

Columns 7 and 8 give the limiting x values and the time τ during which 99% of the limiting value is attained in the case of a very great rate of decrease in the ground water level -- 1.2 cm/sec, that is, 10 times greater than in the first case. The limiting x value in large pores is 10 times greater and in small pores is almost 11 times greater than in the case of a lesser rate (0.12 cm/hour). Despite this fact, the time for attaining a state close to the limiting value in general does not differ in the large pores and in small pores differs by only 10-15%.

In all pores with H_k equal to or less than 130 cm, during the first day a state is attained which is close to equilibrium, that is, to that at which the rate of dropping of the water in these capillaries is equal to the rate of drop in the ground water level. In this case the coefficient of water yield from these pores (related to 1 cm) will be equal to 0.266 -- not counting some water release from the smallest pores. However, the limiting value of the water yield coefficient when in all the pores the meniscus drops at the same rate with which the ground water drops will be equal to 0.274.

For extremely small pores with great heights of capillary rising the time of evening out of the rate in the capillary and the ground water is extremely great: with H_k = 200 cm -- 229 500 sec, with H_k = 250 cm -- 554 000 sec and with H_k = 350 cm -- 1 563 000 sec, that is, more than 18 days. With a rate of decrease in ground water of 1.2 cm/hour in pores with H_k = 250 cm we have 155 cm, that is, is commensurable with the variation in the ground water level in the majority of water-bearing layers.

Finally, in particularly small pores, where the rate is $V_1 \leqslant V_2$, the limiting x value is equal to infinity, that is, in these pores no equality is ever established between the rate of dropping of the water in the capillary and the rate of dropping of the ground water level.

Now we will examine the reverse process -- the process of rising of the ground water. In the first stage we will not take into account what is responsible for the rising of the ground water level -- due to the influx of infiltration moisture or due to the influx of ground water from one side. In the latter case the rising of the capillary meniscus and the entire water column in the capillary will also lag behind the rising of the ground water table but will decrease by the lag value x.

Accordingly, the limiting x values will be satisfied from the condition of equality of the rates V_z and

$$V_i \frac{x}{H_k - x},$$

that is

$$x = \frac{V_z H_k}{V_i + V_z}, \tag{12}$$

and the rate of x increase will be equal to

$$\frac{dx}{d\tau} = V_z - V_i \frac{x}{H_k - x}. \tag{13}$$

Integrating this equation under the condition x = 0, τ = 0 and V_z = const, we obtain

$$\tau = \frac{1}{V_z + V_i}\left[x + \frac{H_k V_i}{V_z + V_i} \ln \frac{H_k V_z}{H_k V_z - (V_z + V_i) x}\right]. \tag{14}$$

Table 4 gives the results of the corresponding computations with rates of rising of the ground water 1.2 cm/sec in ground characterized by the equilibrium curve of distribution of capillary moisture shown in Fig. 1 (curve 1).

An analysis of the results of comparison of the rising and falling of the ground water level indicates that with a decrease in the ground water level the lag in the water level in the capillaries is an order of magnitude lower than the lag in the water level during the rising of the ground water.

Thus, the water yield coefficients and the saturation deficit to a considerable degree are dependent on the rate of change in the ground water level, which must be taken into account in a detailed investigation of the water balance of the aeration zone in the case of a shallow position of the ground water and dynamic changes in its levels.

BIBLIOGRAPHY

1. Leybenzon, L. S., DVIZHENIYE PRIRODNYKH ZHIDKOSTEY I GAZOV V PORISTOY REDE (Movement of Natural Fluids and Gases in a Porous Medium), 1947.

2. Popov, O. V., "Water Balance Method in Estimating Ground Water Runoff," TRUDY GGI (Transactions of the State Hydrological Institute), No 139, 1967.

3. Proskurnikov, S. M., "Experimental Data on Study of the Movement of Capillary Water in Sand," TRUDY GGI, No 8(62), 1948.

4. RASCHETY IZMENENIY ZAPASOV PODZEMNYKH VOD PRI GIDROLOGICHESKIKH ISSLEDOVANIYAKH: METODICHESKOYE POSOBIYE (Computations of Changes in Reserves of Ground Water in Hydrological Investigations: Methodological Aid), Leningrad, Gidrometeoizdat, 1974.

5. Romanov, V. V., GIDROFIZIKA BOLOT (Hydrophysics of Swamps), Leningrad, Gidrometeoizdat, 1969.

UDC 556.34

WATER PERMEABILITY OF FROZEN UNCONSOLIDATED SOILS AND ANALYSIS OF THE DYNAMICS OF ITS CHANGE DURING THE PERIOD OF SNOW MELTING AND THAWING

Moscow METEOROLOGIYA I GIDROLOGIYA in Russian No 12, Dec 79 pp 91-98

[Article by Candidate of Technical Sciences V. I. Shtykov, Northern Scientific Research Institute of Hydroengineering and Melioration, submitted for publication 19 April 1979]

Abstract: The author gives dependences for determining the filtration coefficients, rate of advance and position of the absorption front with time in frozen ground as a function of its physicomechanical properties, content of ice and entrapped air. The experimental data on determination of the filtration coefficients for frozen ground agree very satisfactorily with their computed values. Expressions are derived making possible a quantitative evaluation of change in the filtration coefficients for frozen unconsolidated ground with time during the period of snow melting and thawing.

[Text] The carrying out of water balance and hydrological computations in the planning of hydromelioration measures in drained areas and also an evaluation of the effectiveness of drainage during the spring period require a knowledge of water permeability of the ground in a frozen state and the nature of the change during the period of snow melting and thawing of the frozen ground layer and material covering drainage pipes.

The absorption of water in the ground occurs along some filtration paths and therefore in an examination of the above-mentioned problems we will use as a point of departure a filtration model of the ground as a group of capillary tubes with curved axes. Using as a point of departure the Gromeko-Stokes equation [4] and including capillary force among the operative forces, we obtain the following expressions for determining the rate of advance and position of the absorption (percolation) front with time in the case of unconsolidated ground [6]:

$$\frac{dy}{d\tau} = \frac{\gamma d_u^2}{8\pi^2\mu}\left[\frac{4A\sigma\cos\vartheta}{d_u\gamma y} + \left(\frac{h}{y} \pm 1\right)\right], \quad (1)$$

$$\tau = \frac{8\pi^2\mu}{\gamma d_u^2}\left(\frac{4A\sigma\cos\vartheta + d_u\gamma h}{d_u\gamma}\ln\frac{4A\sigma\cos\vartheta + d_u\gamma h}{4A\sigma\cos\vartheta + d_u\gamma h \pm d_u\gamma y} \pm y\right), \quad (2)$$

where y is the distance from the ground water level to the absorption front in a vertical direction (with percolation from above from the surface), cm; τ is time, sec; γ is water density, $g\cdot cm^{-3}$; d_u is the computed diameter of the filtration path, computed from expression (6), cm; μ is the dynamic viscosity coefficient, $g\cdot cm^{-1}\cdot sec^{-1}$;

$$A = -\frac{(n-i-B-\gamma_0 W_H)\left[1-n-\frac{2{,}8(i+B)}{1-0{,}6\sqrt{i+B}}\right]}{(n-i-B)\left[1-n+\gamma_0 W_H+\frac{2{,}8(i+B)}{1-0{,}6\sqrt{i+B}}\right]}$$

is a parameter taking into account the content of nonfreezing water in unconsolidated ground, which with $W_{non} = 0$ is equal to 1; σ is the water surface tension coefficient, $n\cdot cm^{-1}$; ϑ is the wetting angle; h is the water layer on the ground surface with absorption from above (with absorption from below h = 0), cm; n is porosity; i is volumetric ice content; B is the content of entrapped air, whose quantity, in the absence of data, can be assumed equal to 0.04; γ_0 is the density of ground in a dry state, $g\cdot cm^{-3}$; W_{non} is the content of nonfreezing water by mass in fractions.

When $y\to\infty$, and also in the case of contact of the absorption front with the ground water level, the infiltration process undergoes transition into filtration; from (1), by virtue of the expression $dy/d\tau = K_{froz}I/(n - i - B)$, we obtain a dependence for determining the filtration coefficient for unconsolidated ground in a frozen state

$$K_M = \frac{(n-i-B)\,gd_u^2}{8\pi^2\nu}, \quad (3)$$

[M = froz(en)] where g is the acceleration of free falling, $cm\cdot sec^{-2}$; ν is the kinematic viscosity coefficient, $cm^2\cdot sec^{-1}$; I is the head gradient.

The volumetric ice content of the ground i consists of the initial ice content i_0 and the increment of ice content as a result of partial freezing of the water filtering into the ground i'. It is proposed that i' be determined using the formula [8]

$$i' = \frac{(0{,}458\,i_0 + 0{,}17\,\gamma_0 + 1{,}013\,\gamma_0 w_H)\,t}{73{,}2}, \quad (4)$$

[H = non] where t is the mean temperature of the frozen layer (in absolute value).

Having data on the content of nonfreezing water in the ground (Table 1), the initial value of volumetric ice content can be determined using the N. A. Tsytovich formula [9]

$$i_n = \frac{\gamma_M (W - W_H)}{\gamma_л (1 + W)}, \quad (5)$$

[M = froz(en); л = ice; H = non]

where γ_{froz} is the bulk density of frozen ground with an unimpaired structure, $g \cdot cm^{-3}$; W is the total moisture content of the ground by mass in fractions; γ_{ice} is ice density, $g \cdot cm^{-3}$.

Table 1

Content of Nonfreezing Water in Frozen Ground at t = 0°C and in the Absence of Heat Influx

Name of ground with respect to mechanical composition	W_{non} in fractions
Coarse-grained sand	-
Medium-grained sand	0.01
Fine-grained sand	0.02
Sandy loam	0.07
Clayey loam	0.1
Medium clay	0.2

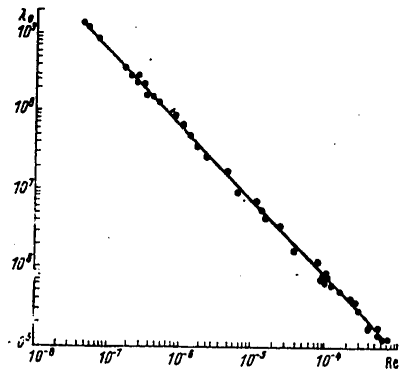

Fig. 1. Theoretical and experimental values of friction coefficient λ_0 accompanying filtration in frozen ground.

A more precise content of nonfreezing water in a particular type of ground can be determined by calorimetric measurements of its samples in a frozen state.

On the basis of numerous experiments for determining the filtration coefficients for sands, from fine- to coarse-grained, in a frozen state with different initial moisture contents, it is possible to obtain a dependence

for determining the computed value of the diameter of the filtration path

$$d_u = 0{,}57 \sqrt[6]{\eta} \frac{(n - i - B)}{1 - n + \frac{2{,}8\,(i + B)}{1 - 0{,}6\sqrt{i + B}}}\, d_{17}, \qquad (6)$$

where η is the coefficient of different granularity of the ground; d_{17} is the diameter of ground particles, the smaller of which in its composition contains 17% of the particles by mass.

Table 2

Experimental Data on Determination of Filtration Coefficient of Sandy Soil in Frozen State

№ опыта	Пористость	Объемная льдистость в долях	Приращение объемной льдистости	Содержание защемленного воздуха	Коэффициент фильтрации мерзлого грунта, *см/сек* (6)	
					опытный (7)	по формуле (3) (8)
1	2	3	4	5		
9 Среднезернистый песок, $W_н$=0,009						
1	0,383		0,020	0,038	0,0080	0,0089
2	0,378	—	0,007	0,010	0,00156	0,00173
3	0,381	0,095	0,006	0,036	0,00220	0,0020
4	0,377	0,061	0,007	0,043	0,0030	0,00310
5	0,377	0,045	0,013	0,047	0,00420	0,00350
6	0,381	0,099	0,009	0,029	0,00140	0,00190
7	0,380	0,135	0,008	0,046	0,00080	0,00065
8	0,381	0,190	0,002	0,060	0,00015	0,000137
9	0,381	0,131	0,002	0,036	0,00130	0,001030
10	0,376	0,164	0,004	0,049	0,00033	0,000310
11	0,366	0,277	—	0,033	0,00001	0,000008
12	0,365	0,288	—	0,018	0,00001	0,000009
13	0,359	0,309	—	—	0,0000061	0,0000055
10 Мелкозернистый песок, $W_н$=0,032						
1	0,423	0,084	0,030	0,056	0,00011	0,00012
2	0,445	0,109	—	0,020	0,00036	0,00036
3	0,381	0,158	0,017	0,053	0,000016	0,000018
4	0,377	0,165	0,031	0,059	0,0000069	0,0000078
5	0,389	0,178	0,011	0,060	0,000017	0,00001
6	0,386	0,248	—	0,051	0,0000024	0,0000022
7	0,363	0,127	—	0,033	0,000060	0,000065
8	0,386	0,168	0,031	0,060	0,000008	0,0000087
9	0,386	0,172	0,031	0,058	0,00001	0,000008
10	0,381	0,158	0,017	0,058	0,000011	0,000013
11	0,397	0,041	—	0,043	0,00055	0,00045

KEY:

1. No of experiment
2. Porosity
3. Volumetric ice content in fractions
4. Increment in volumetric ice content
5. Content of entrapped air
6. Frozen ground filtering coefficient, cm/sec
7. Experimental
8. Using formula (3)
9. Medium-grained sand, W_{non}...
10. Fine-grained sand, W_{non}...

Table 3

Experimental Data on Determination of Filtration Coefficient of Plowed Layer in Frozen State

1 № опыта	Пористость в долях 2	Объемная льдистость в долях 3	Коэффициент фильтрации талого грунта 4: $K_в$ 5	Коэффициент фильтрации талого грунта 4: K_0 см/сек 6	Содержание защемленного воздуха в долях 7	Коэффициент фильтрации мерзлого грунта, см/сек 8: опытный 9	Коэффициент фильтрации мерзлого грунта, см/сек 8: по формуле (8) 10
			$W_в$=0,072				
1	0,514	0,067	0,000098	0,00015	0,016	0,000058	0,000036
2	0,498	0,028	0,000084	0,000093	0,018	0,000047	0,000042
3	0,521	0,113	0,00027	0,00064	0,082	0,000017	0,000022
4	0,512	0,111	0,00017	0,00024	0,033	0,000019	0,000020
5	0,510	0,180	0,00033	0,00039	0,017	0,000014	0,000013
6	0,502	0,177	0,00031	0,00035	0,004	0,000013	0,000015
7	0,502	0,169	0,00018	0,00023	0,025	0,000011	0,000008
8	0,502	0,186	0,00020	0,00025	0,020	0,0000065	0,000007
9	0,506	0,147	0,00013	0,00017	0,027	0,0000060	0,000008
10	0,502	0,243	0,00021	0,00029	0,032	0,0000017	0,0000018
11	0,521	0,268	0,00028	0,000455	0,051	0,0000011	0,0000013
12	0,514	0,316	0,00018	0,00031	0,051	0,00000044	0,00000039

KEY:

1. No of experiment
2. Porosity in fractions
3. Volumetric ice content in fractions
4. Thawed ground filtration coefficient
5. K_w
6. K_0 cm/sec
7. Content of entrapped air in fractions
8. Frozen ground filtration coefficient, cm/sec
9. Experimental
10. Using formula (8)

Table 4

Experimental Data on Determination of Filtration Coefficient for Fill in Frozen State Under Field Conditions

Пористость в долях n 1	Объемная льдистость в долях i_0 2	Коэффициент фильтрации засыпки в талом состоянии, м/сут, K_0 3	Коэффициент фильтрации в мерзлом состоянии 4: опытный 5	Коэффициент фильтрации в мерзлом состоянии 4: по формуле (8) 6
0,40	0,03	40	8,1	8,1
0,42	0,06	63	12,9	10,9
0,42	0,04	51	11,3	12,6

KEY:

1. Porosity in fractions, n
2. Volumetric ice content in fractions
3. Filtration coefficient of fill in thawed state m/day, K_0
4. Filtration coefficient in frozen state
5. Experimental
6. Using formula (8)

With the filtration scheme which we adopted and laminar movement of water the hydraulic friction coefficient λ_0 must be determined by the well-known dependence

$$\lambda_0 = \frac{64}{Re_0}. \tag{7}$$

Figure 1 shows the experimental values λ_0 for frozen sand with four different granularities. The solid line on the graph is a straight line reflecting the dependence (7). This graph shows that the experimental data agree well with the theoretical dependence.

Formula (3) can be given a more universal form if it is expressed through the filtration coefficient for ground in a thawed state at a zero temperature [7]:

$$K_{froz} = K_0 \frac{\left(1 - \frac{i + 0{,}04}{n - \gamma_0 W_н}\right)^3}{\left[1 + \frac{2{,}8\,(i + 0{,}04)}{(1 - n + \gamma_0 W_н)(1 - 0{,}6\sqrt{i + 0{,}04})}\right]^2}. \tag{8}$$

[H = non]

Dependence (8) can be used in the case of consolidated and unconsolidated ground.

The presently existing dependences for determining the filtration coefficient for frozen ground [2, 3] are not sufficiently universal because they do not take into account the entire diversity of the influencing factors: they do not reflect the physical essence [2] or contain parameters which are difficult to determine [3]. In addition, not one of them takes the content of entrapped air into account. The sharpest decrease in the filtration coefficient in dependence on the content of entrapped air is observed in an investigation of the water permeability of frozen ground. In the freezing process air bubbles are formed in the intrapore ice because the ice has no capacity at all for dissolving air, inevitably present in ground water. In addition, there is an additional entrapment of air in the ground pores as a result of closing of the pores communicating with the external air [7].

Tables 2-4 give experimental data on determination of the filtration coefficient of frozen ground which agree very satisfactorily with their computed values.

As is well known, the unfreezing of the ground from above begins only after departure of the snow cover. However, during the period of snow melting the temperature of the water filtering into the ground is about 0°C; therefore, the change in ice content with departure of the snow cover will occur only due to the heat of friction released during water filtration. The heat exchange process in the filtration path is described by the following differential equation [8]:

$$\frac{\gamma^2 r^3}{16\,\mu} I^2 = \Delta\gamma_л \frac{dr}{d\tau}, \tag{9}$$

[Л = ice]

where r is the radius of the filtration path at a particular moment in time, cm; Δ is the specific heat of fusion of ice, $J \cdot g^{-1}$.

Equation (9) was derived on the assumption of a linearity of the filtration paths. However, as indicated by theoretical and experimental investigations, the curvature of the tubes, for example, exerts no influence on the character of the flow and the distribution of temperature in the section of the tubes as long as the motion in them is laminar. Thus, equation (9) is correct only in the case of laminar movement of water in the filtration paths when there is satisfaction of the expression $Re \leqslant Re_{cr}$, where Re is the Reynolds number for the considered filtration flow, related to the infiltration rate; Re_{cr} is the critical Reynolds number.

For the critical Reynolds number, related to the filtration rate and the computed diameter of the filtration path, we have the following dependence [9]:

$$Re_{cr} = 8{,}6\,(n - i - B)\sqrt{\frac{d_{17}}{d_u}}. \tag{10}$$

Taking into account that an impairment of laminar filtration must be expected in ground with large grains, and in particular, in the fill in drainage channels, consisting of this same material, as an example we will compute the critical Reynolds number for a sandy-gravelly mixture characterized by the following parameters: n = 0.42, η = 12, d_{17} = 0.5 mm, i = 0, B = 0.

Relating the critical Reynolds number to d_{17} we find that in the considered case Re_{cr} = 9.2. The critical Reynolds number obtained from experiments according to data from some researchers varies from 1 to 12; according to data from others [1] -- from 7 to 9. It can be seen that the results of computations fully agree with the data in the literature.

In the ground the filtration paths have a curvilinear, periodic configuration of the axes and therefore in the case of infiltration in homogeneous unconsolidated ground the length of the filtration path will be greater than the straight line connecting its ends by a factor of $\pi/2$. Thus, the movement of the water along the computed filtration path in the case of infiltration will occur with $I = 2/\pi$.

Integrating equation (9) and substituting the values of all the constant parameters into the derived expression, we obtain a dependence characterizing the change in the computed diameter of the filtration path with time,

$$d = 2\,d_u \sqrt{\frac{1}{4 - 0{,}766\,a_u^2\,\tau}}. \tag{11}$$

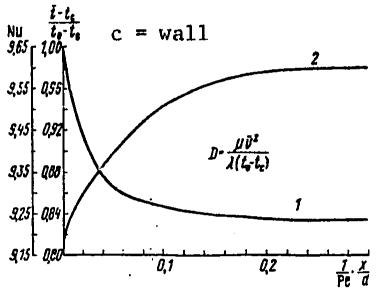

Fig. 2. Change in mean mass water temperature (1) and Nu number (2) along length of computed filtration path with D = 1.0.

In formula (11) d_u must be substituted in mm and τ in days; the d values are obtained in mm. Computations show that the filtration coefficient for frozen fill in a drainage well consisting of a sandy-gravelly mixture, characterized by the parameters d_{17} = 2 mm, η = 1.6, n = 0.42 and i = 0.11, during the 20 days from the moment of onset of snow thawing (under the condition of continuous diversion of water through the drainage well) increases by a factor of 2.9.

Thus, the ice content of coarse-grained ground, and accordingly, the filtration coefficient, can change substantially even before the thawing of the ground.

Now we will examine the change in the filtration coefficient for frozen unconsolidated ground in the process of its thawing. For generality of the discussion we will take a case when the frozen layer has already thawed from above by some depth.

Figure 2 shows graphs characterizing the change in the mean mass temperature of water and the Nusselt number (Nu) along the length of the filtration path.

In the case of sandy-gravelly ground, with a decrease in grain size the 1/Pe d parameter varies from 10^2 to 10^6, where Pe is the Peclet number, and d is the diameter of the computed filtration path.

In this connection it follows from the graphs that already at a distance of several millimeters from the beginning of the filtration path of the frozen zone the mean mass temperature of the water will differ by less than 1% from the mean mass temperature of the water which would be established in the filtration path solely due to the dissipation of energy. The very same thing applies to the Nu number. This leads to the conclusion that virtually all the heat carried by the filtration flow to the upper boundary of the frozen layer is released in it. However, the change in ice

content within the frozen layer occurs for the most part due to the heat of friction released during the filtration of water. The layer with a thickness of several millimeters (in the case of fine-grained sands this will be fractions of a millimeter), in whose extent the filtering water almost completely gives up its heat, reducing its temperature to 0°C, will be called the transitional zone and will be assigned to the thawing part.

Below the transition zone the mean mass temperature of the water and the Nu number will become virtually constant along the length of the filtration path. The mean mass temperature and the Nu number in the filtration path of the frozen layer below the transitional zone are determined with a sufficient degree of accuracy using the following dependences:

$$\bar{t} - t_c = \frac{5}{6} D (t_0 - t_c); \tag{12}$$

[c = wall]

$$\mathrm{Nu} = \frac{\alpha d}{\lambda} = 9{,}6, \tag{13}$$

where α is the heat transfer coefficient, $J \cdot cm^{-2} \cdot sec^{-1}\ °C^{-1}$; λ is the thermal conductivity coefficient, $J \cdot cm^{-1} \cdot sec^{-1}\ °C^{-1}$;

$$D = \frac{\mu \overline{u^2}}{\lambda (t_0 - t_c)}$$

is an aggregate parameter; u is the mean velocity of movement of water in the computed filtration path, $cm \cdot sec^{-1}$; t_0 is water temperature at the entry into the filtration path, °C; t_{wall} is the wall temperature of the filtration path (close to 0°C).

According to the Newton-Richter law the density of the heat flux on the wall of the filtration path is proportional to the temperature head $\bar{t} - t_{wall}$:

$$q = \alpha (\bar{t} - t_c), \tag{14}$$

where $\bar{t}$ is the mean mass water temperature in the considered section of the filtration path.

Due to the quantity of heat released on the wall of the filtration path during the time $d\tau$ an ice layer with the thickness dr melts,

$$q d\tau = \Delta \gamma_л dr. \tag{15}$$

[Л = ice]

As a result, we again arrive at the differential equation (9) [8]:

$$\frac{\gamma^2 r^3}{16 \mu} I^2 = \Delta \gamma_л \frac{dr}{d\tau}.$$

[Л = ice]

However, in this case the value of the head gradient observed within the limits of the frozen layer changes as the ground thaws from above.

Using the equality of the water discharges through the thawing I and frozen layer II, we determine the head gradient in the frozen layer:

$$I_2 = \frac{2K_1H}{\pi[K_2h + K_1(H-h)]}, \quad (16)$$

where H is the thickness of the frozen layer before the beginning of ground thawing, m; h is the depth of thawing, m; K_1, K_2 are the filtration coefficients for ground in the thawed and frozen states respectively, m/day.

Summary

1. The filtration coefficient for frozen unconsolidated ground both during the period of snow thawing and in the process of ground thawing changes solely due to the heat of internal friction of the filtering fluid.

2. The influence of the heat of internal friction on change in the filtration coefficient will be the greater the coarser are the grains of sandy or sandy-gravelly ground.

3. The change in the filtration coefficient in the process of ground thawing occurs more intensively because as thawing proceeds there is an increase in the head gradient in the frozen ground layer.

BIBLIOGRAPHY

1. Aravin, V. I., Numerov, S. N., TEORIYA DVIZHENIYA ZHIDKOSTEY I GAZOV V NEDEFORMIRUYEMOY PORISTOY SREDE (Theory of Movement of Fluids and Gases in a Nondeformable Porous Medium), Moscow, Gosudarstvennoye Izdatel'stvo Tekhniko-Teoreticheskoy Literatury, 1953.

2. Komarov, V. D., "Laboratory Investigation of Water Permeability of Frozen Soil), TRUDY TsIP (Transactions of the Central Institute of Forecasts), No 54, 1957.

3. Kulik, V. Ya., "Dependence of the Filtration Coefficient on the Ice Content of Ground," METEOROLOGIYA I GIDROLOGIYA (Meteorology and Hydrology), No 9, 1969.

4. Patrashev, A. N., GIDROMEKHANIKA (Hydromechanics), Moscow, Voyenmorizdat, 1953.

5. Petukhov, B. S., TEPLOOBMEN I SOPROTIVLENIYE PRI LAMINARNOM TECHENII ZHIDKOSTI V TRUBAKH (Heat Exchange and Resistance in the Laminar Flow of a Fluid in Pipes), Moscow, Energiya, 1967.

6. Shtykov, V. I., "Rate of Advance of the Infiltration Front in Soils," SBORNIK DOKLADOV PO GIDROTEKHNIKE (Collection of Reports on Hydroengineering), No 13, Leningrad, Vsesoyuznyy NII Gidrotekhniki imeni B. Ye. Vedeneyev, Reg. D-409, Informenergo, 1977.

7. Shtykov, V. I., "Influence of Entrapped Air on the Water Permeability of Different Types of Ground," VODNYY REZHIM POCHV I YEGO REGULIROVANIYE V USLOVIYAKH NECHERNOZEMNOY ZONY (Water Regime of Soils and its Regulation Under the Conditions of the Nonchernozem Zone), Leningrad, 1977.

8. Shtykov, V. I., Khrisanov, N. I., "Influence of Freezing on Water Permeability of the Ground in the Operation of Drainage Systems During the Snow Melting Period," MELIORATSIYA I OSVOYENIYE ZEMEL' (Melioration and Exploitation of Lands), Vol 105, 1973.

9. Tsytovich, N. A., MEKHANIKA MERZLYKH GRUNTOV (Mechanics of Frozen Ground), Moscow, Vysshaya Shkola, 1973.

METHOD OF MOIST CONVECTIVE ADAPTATION

Moscow METEOROLOGIYA I GIDROLOGIYA in Russian No 12, Dec 79 pp 99-103

[Article by Candidate of Physical and Mathematical Sciences A. P. Khain, USSR Hydrometeorological Scientific Research Center, submitted for publication 3 April 1979]

Abstract: A new method of moist convective adaptation, conserving the total static energy of a column of the atmosphere, is proposed.

[Text] It is known from an analysis of data from aerological sounding of the atmosphere, averaged over an area of several tens of square kilometers or in time over a period of several hours, that with the exception of the lower kilometer layer the vertical temperature gradient is less than the dry adiabatic gradient ($\partial T/\partial z < \gamma_a$) and as a whole is close to the moist adiabatic gradient. On the other hand, it is known that radiation and other large-scale processes in the atmosphere lead to stratification with a gradient greater than γ_a. Convective movements ensure mixing of atmospheric air in the vertical direction, which brings stratification closer to neutral. This process occurs rather rapidly and bears the name convective adaptation (adjustment).

The authors of [5] proposed a model for taking convective processes into account. This or somewhat modified schemes, called convective adaptation (CA) schemes, have found broad application in models of numerical forecasting and general circulation of the atmosphere [6]. An example of the use of CA in a model of a tropical cyclone is known [4]. Traditionally the CA method is divided into "dry adaptation," applicable to adequately dry air (in any case, the condensation and precipitation processes are not considered) and "moist adaptation" (MCA) for air sufficiently close to saturation. It is necessary to solve two problems when using MCA. The first is determination of the criteria of existence of convection, that is, formulation of the conditions for the beginning and end of MCA. The second is the carrying out of MCA, that is, correction of the temperature field and the mixing ratio with adherence to some conditions.

The theoretical problem of finding the critical temperature gradients in layers of great thickness has not been solved even for a "dry" atmosphere and in particular it has not been solved for an atmosphere close to saturation, when phase transitions are possible. It is therefore not surprising that as a criterion for the onset of MCA different authors make use of different conditions. It is usually assumed that MCA must be used in satisfying the following conditions:

$$-\frac{\partial T}{\partial z} > \gamma_k; \tag{1}$$

$$\langle q \rangle > q_k = k q_s (\langle T \rangle), \tag{2}$$

where T is the mean temperature or the ambient temperature (in contrast to the temperature of a rising particle), $\langle q \rangle$ and $\langle T \rangle$ are the mean weighted mixing ratio and temperature for the layer, γ_k and q_k are some critical values of the temperature gradient and the mixing ratio; q_s is the saturating value of the mixing ratio, computed on the basis of $\langle T \rangle$ and $\langle p \rangle$ in the layer (p is pressure).

In a number of studies the moist adiabatic gradient γ_{ma} is used as the critical temperature gradient.

Frequently as a criterion of the existence of convection in a column of the atmosphere in place of (1) we use the condition

$$\frac{\partial \theta_e}{\partial z} < 0 \tag{3}$$

in some layer, most frequently in the lower layer of the column, θ_e is the equivalent-potential temperature, determined using the expression

$$\theta_e = T \left(\frac{p_0}{p}\right)^{\varkappa} \exp\left(\frac{Lq}{c_p T}\right). \tag{4}$$

It is known that with sufficient accuracy θ_e is conserved in the particle during its ascent both in the absence of condensation and in its presence (with entrainment neglected).

$$T \left(\frac{p_0}{p}\right)^{\varkappa} = \theta$$

is potential temperature. The remaining notations in (4) are those generally employed.

The coefficient k in (2) is dependent on the scale of the considered processes and the interval of the finite-difference meshes in numerical models and is selected from empirical evaluations in the range $0.75 \leqslant k \leqslant 1$. It is usually assumed that as a result of MCA it is possible to establish the temperature profile and the mixing ratio satisfying the condition

$$\frac{\partial \tilde{\theta}_e}{\partial z} = 0. \tag{5}$$

Here and in the text which follows the tilde denotes the values arising as a result of MCA.

Since θ_e is dependent on the two variables T and q, in order to find T and q with known θ_e it is necessary to have still another condition. In virtually all the studies using MCA as this condition we use the following:

$$\tilde{q} = k_1 \tilde{q}_s. \tag{6}$$

The carrying out of MCA is accomplished under the condition of conservation of the full static energy of a column of the atmosphere:

$$\int_0^{p_s} (c_v T + gz + Lq)\, dp = \int_0^{p_s} (c_v \tilde{T} + g\tilde{z} + L\tilde{q})\, dp, \tag{7}$$

where c_v is the heat capacity at a constant volume, p_s is surface pressure.

Condition (7), using the equations of statics and state, can be rewritten as follows:

$$\int_0^{p_s} (c_p T + Lq)\, dp = \int_0^{p_s} (c_p \tilde{T} + L\tilde{q})\, dp = \text{const}. \tag{8}$$

We note that conditions (3) and (5) from the physical point of view are the least sound. In actuality, as indicated by observations [1], condition (3) is always satisfied in the tropics in the lower troposphere to the level 600-800 mb and is not impaired even in regions of powerful convection in clusters [7], ICZ [2] and in typhoons [3], although the curvature of the $\theta_e(z)$ profiles is somewhat decreased during convection. It therefore follows that the conditions (3), (5) cannot serve as a criterion of the onset of convection and the criterion of its completion respectively and therefore in the formulation of the MCA method it is desirable to desist from them.

We introduce into consideration the equivalent-potential temperature of saturated air:

$$\theta_e^* = T\left(\frac{p_0}{p}\right)^{\varkappa} \exp\left(\frac{Lq_s(T)}{c_p T}\right), \tag{9}$$

where q_s is the saturating mixing ratio at the temperature T. It is known that θ_e^* is conserved in the saturated particle during its adiabatic ascent.

We obtain an expression for the difference between particle temperature and ambient temperature, expressed through equivalent-potential temperatures.

$$\theta_{e_l} - \theta_e^* = \left(\frac{p_0}{p}\right)^{\varkappa}\left(T_l \exp\left(\frac{Lq_l}{c_p T_l}\right) - T\exp\left(\frac{Lq_s(T)}{c_p T}\right)\right) \approx$$

$$\approx \left(\frac{p_0}{p}\right)^{\varkappa}\left(T_l - T + \frac{L}{c_p}(q_l - q_s(T)\right).$$

Hence

$$T_l - T = (\theta_{e_l} - \theta_e^*)\left(\frac{p}{p_0}\right)^{\varkappa} - \frac{L}{c_p}(q_l - q_s(T)\Big). \tag{10}$$

With saturation in the particle $q_i = q_s(T_i)$.

Then, since

$$q_s(T_l) \approx q_s(T) + \frac{\partial q_s}{\partial T}(T_l - T),$$

then $\theta_{e_l} - \theta_e^* = \left(\frac{p_0}{p}\right)^{\varkappa}(T_l - T)\left(1 + \frac{L}{c_p}\frac{\partial q_s}{\partial T}\right)$ and

$$T_l - T = \left(\frac{p}{p_0}\right)^{\varkappa}(\theta_{e_l} - \theta_e^*)\left(1 + \frac{L}{c_p}\frac{\partial q_s}{\partial T}\right)^{-1}. \tag{11}$$

The expression for instability energy in the part of the column from the initial level p_{in} to the condensation level p_k (p_c), with (10) taken into account (on the assumption q_i = const), is written as follows:

$$E_1 = -R\int_{p_n}^{p_k}(T_l - T)\,d\ln p = -R\int_{p_n}^{p_k}\left[(\theta_{e_A} - \theta_e^*)\left(\frac{p}{p_0}\right)^{\varkappa} - \right. \tag{12}$$

$$\left. - \frac{L}{c_p}(q_A - q_s)(T)\right]d\ln p.$$

Here θ_{e_A} and q_A are the equivalent-potential temperature and the mixing ratio of the particle at the initial level. Above the condensation level in the layer from p_c to p_2 the instability energy E_2 is equal to:

$$E_2 = -R\int_{p_k}^{p_2}(\theta_{e_A} - \theta_e^*)\left(1 + \frac{L}{c_p}\frac{\partial q_s}{\partial T}\right)^{-1}\left(\frac{p}{p_0}\right)^{\varkappa}d\ln p. \tag{13}$$

In (12)-(13) use is made of the fact that $\theta_{ei} = \theta_{eA}$ due to the conservatism of the equivalent-potential temperature.

It can be seen from (11) that the positive buoyancy of a saturated particle is observed when $\theta_{ei} > \theta_e^*$ or, assuming $\theta_{ei} = \theta_{eA}$, we have $\theta_{eA} > \theta_e^*$.

Assume that θ_e and θ_e^* are dependent on p, as demonstrated in Fig. 1b. An air particle, rising vertically from the point A to the point B, if it lies above the condensation level, becomes warmer than the surroundings and has a positive buoyancy to the point C. We will assume that convection and MCA occur under the condition that the energy of particle instability in the layer from A to C is greater than zero, that is

$$E = E_1 + E_2 > 0. \tag{14}$$

The arising convection must correct the θ_e profile. We will assume that convection at the limit (which, however, is not always attained) tends to straighten the profile θ_e, that is, in some layer from p_{in} to p_B (Fig. 1) establish $\theta_e = \theta_{e\ lim} = \text{const}$. $\theta_{e\ lim}$ can be found from a condition equivalent to (8).

$$\int_{p_B}^{p_H} H(\theta_e)\, dp = \int_{p_B}^{p_H} H_{пред}(\theta_{e_{пред}})\, dp, \tag{15}$$

where $H = c_pT + L_q$; $\theta_{e\ lim}$ satisfies the condition (see Fig. 1)

$$\theta_{e_A} > \theta_{e_{пред}} > \theta_{e_{min}}.$$

[пред = lim]

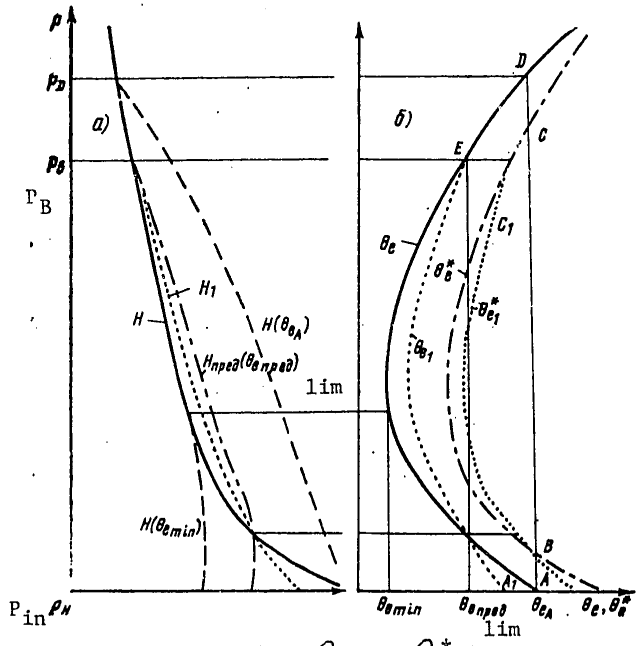

Fig. 1. Dependence of H (a), θ_e and θ_e^* (b) on pressure.

It is easy to show that such $\theta_{e\ lim}$, satisfying condition (15), also exists uniquely. This follows from the monotonic dependence between θ_e and $H = c_p T + Lq$, since

$$\theta_e \approx \left(\frac{p_0}{p}\right)^{\varkappa} T\left(1 + \frac{Lq}{c_p T}\right) = \frac{1}{c_p}\left(\frac{p_0}{p}\right)^{\varkappa}(c_p T + Lq) = \frac{1}{c_p}\left(\frac{p_0}{p}\right)^{\varkappa} H. \tag{16}$$

Thus, $H(\theta_{eA}) > H(\theta_e) > H(\theta_{e\ min})$ for all p. Fig. 1a schematically shows: H, corresponding to θ_e, $H(\theta_{eA})$, $H(\theta_{e\ min})$.

We use the notation

$$F \int_{p_в}^{p_н} H(\theta_e)\, dp.$$

[H = in; B = B]

Then

$$F_1 = \int_{p_в}^{p_н} H(\theta_{e_A})\, dp > F, \quad \text{and} \quad F_2 = \int_{p_в}^{p_н} H(\theta_{e_{min}})\, dp < F.$$

It therefore follows that there is such an $\theta_{e\ lim}$ between $\theta_{e\ min}$ and $\theta_{e\ A}$ at which

$$\int_{p_в}^{p_н} H(\theta_{e_{пред}})\, dp = \int_{p_в}^{p_н} H_{пред}\, dp = F. \tag{17}$$

[H = in; B = B; пред = lim(it)]

H_{lim} is shown schematically in Fig. 1. The areas beneath the H and H_{lim} curves in Fig. 1a are equal. There are two unknown values in (17): $\theta_{e\ lim}$ and p_B. An additional condition for finding both these values is $\theta_{e\ lim} = \theta_e(p = p_B)$. The H_{lim}, $\theta_{e\ lim}$ and p_B values are easy to find by an iteration method.

We note that condition (14) can cease to be satisfied even before the $\theta_{e\ lim}$ value is attained because a change in θ_e leads to a change in θ_e^* and accordingly also the E_1 and E_2 values in (12)-(13).

In the proposed algorithm θ_e changes, gradually after several intervals approaching $\theta_{e\ lim}$ (in this case H tends to H_{lim}). In each interval we check the satisfaction of condition (14). If it is satisfied, the next interval (step) is used. If the inequality (14) is impaired in some interval, the resulting profile θ_e is considered final and MCA ceases.

Each interval from θ_e to $\theta_{e\ lim}$ (or H to H_{lim}) must be taken with satisfaction of condition (8).

The intermediate H_i values in the i-th interval can be determined using the formula

$$H_i = (1 - \alpha_i)\, H + \alpha_i H_{пред}, \tag{18}$$

[пред = lim] where $0 < \alpha < 1$. With $\alpha_i = 0$ $H_i = H$, that is, the initial $H(\theta_e)$ profile with $\alpha_i = 1$ $H_i = H_{lim}$. Therefore

$$\int_{p_в}^{p_н} H_i\, dp = (1 - \alpha_i) \int_{p_в}^{p_н} H\, dp + \alpha_i \int_{p_в}^{p_н} H_{пред}\, dp = (1 - \alpha_i)\, F + \alpha_i F = F,$$

[H = in; B = B; пред = lim] so that in each interval there is satisfaction of condition (8).

Thus, the sequence for carrying out MCA by the first method is as follows:

1. Finding $\theta_{e\ lim}$, H_{lim} (p) and p_B.

2. Computing H_1 from (18), where α_1 is equal, for example, to 0.1 (H_1 is schematically shown in Fig. 1a).

3. Finding θ_{e1} (H_1) (dotted line from point A_1 to E and then the dashed line to point D).

4. Computing $T_1(p)$ and $q_1(p)$ from θ_{e_1} (H_1) with use of condition (6).

5. Computing θ^*_{e1} from the T(p) value obtained in point 4.

6. Checking the conditions for presence of convection (14).

7. If condition (14) is satisfied, H_2 is computed; if it is not satisfied, then $\theta_e(H_1)$, T_1 and q_1 are taken as the MCA result.

In principle it is possible to refine the α_i values until the inequality (14) becomes an equation with the stipulated accuracy.

BIBLIOGRAPHY

1. Pal'men, E., Newton, C., TSIRKULYATSIONNYYE SISTEMY ATMOSFERY (Circulation Systems in the Atmosphere), Leningrad, Gidrometeoizdat, 1973.

2. Fal'kovich, A. I., "Thermodynamic Parameters and Convective Instability in the Tropical Atmosphere," METEOROLOGIYA I GIDROLOGIYA (Meteorology and Hydrology), No 9, 1977.

3. Frank, W. M., "The Structure and Energetics of the Tropical Cyclone. I. Storm Structure," MON. WEATHER REV., Vol 105, No 9, 1977.

4. Kurihara, Y., "A Scheme of Moist Convective Adjustment," MON. WEATHER REV., Vol 101, 1973.

5. Manabe, S., Smagorinsky, J., Strickler, R. F., "Simultaneous Climatology of a General Circulation Model With a Hydrologic Cycle," MON. WEATHER REV., Vol 93, 1965.

6. Manabe, S., Holloway, J. S., Stone, A. M., "Tropical Circulation in a Time Integration of a Global Model of the Atmosphere," J. ATMOS. SCI., Vol 27, No 4, 1970.

7. Ruprecht, E., Gray, W. M., "Analysis for Satellite-Observed Tropical Cloud Clusters," ATMOS. SCI. PAPER No 219, Colorado State Univ., 1974.

UDC 551.(01+465.7:5)

COMPARISON OF MEAN CONDITIONAL ENTROPIES OF TWO COHERENT MODELS OF THE "ATMOSPHERE - OCEAN" SYSTEM

Moscow METEOROLOGIYA I GIDROLOGIYA in Russian No 12, Dec 79 pp 104-106

[Article by Candidate of Physical and Mathematical Sciences V. A. Ryasin, USSR Hydrometeorological Scientific Research Center, submitted for publication 10 April 1979]

Abstract: Mean conditional entropy is a measure of the error in predicting the state of the "atmosphere - ocean" system within the limits of a selected model. It is demonstrated that for two formulated coherent models stipulated in one stochastic space, one of which is embedded in the second, the mean conditional entropy of the external model is greater. The theorem has application in solving the problem of observability of the "atmosphere - ocean" system.

[Text] In the study of problems relating to the observability of the "atmosphere - ocean" system and the adequacy of the network of stations for the monitoring of this system the researcher is forced to deal with discrete models of a system having a finite number of degrees of freedom. The question arises of the justifiability of the conclusions: if any conclusion is drawn using a model of a given dimensionality, it will be correct for a model of greater dimensionality formulated on the same physical principles as for the first model.

In this study we demonstrate the theorem of the relationship of the conditional mean entropies of two coherent models of the "atmosphere - ocean" system of different dimensionality. It follows from the theorem that a positive conclusion of adequacy of the observation system, obtained in the model of lesser dimensionality, may be incorrect for a model of greater dimensionality. In particular, the conclusion formulated in [1] that the existing WWW system is ineffective for precise determination of the altitude of the 500-mb surface is not a conclusion characterizing only the

model of the 500-mb surface (model with few parameters) examined in [1]. It is universal.

Now we will proceed to formulation of the theorem. We will examine determined models of the "atmosphere - ocean" system, that is, those models for which stipulation of the vector of state θ_0 at the initial moment in time t = 0 unambiguously determines the vector of state θ_t of the model at future moments in time t>0. We will assume that measurements having a temporal and spatial tie-in (ξ_i, i = 1, N) made by different measurement systems (satellites, civil aviation aircraft, WWW stations, buoys, etc.) are related in the model by the expression

$$\xi_i = \alpha_i(\theta_0) + \Delta_i,$$

where $\alpha_i(\theta_0)$ is a value, computed in the model, corresponding to the measured Δ_i value with an initial state of the model θ_0, Δ_i is the measurement error.

In the model we will postulate that the vector of its initial state θ_0 and the errors in measuring Δ_i are random. Their properties are determined by some probability distribution function $p(\theta_0, \Delta)$, $\Delta = (\Delta_1, \ldots, \Delta_N)$. With these assumptions it is possible to speak [2] of an entropy $H(\theta_0)$ being a measure of the a priori indeterminancy in the knowledge of the initial state of the "atmosphere - ocean" system, about the quantity of information $I(\xi, \theta_0)$, on θ_0 present in $\xi = (\xi_1, \ldots, \xi_N)$, on the mean conditional entropy $H_\xi(\theta_0)$, being a measure of the a posteriori (after carrying out ξ measurements) indeterminancy in the value of the initial state of the "atmosphere - ocean" system. These parameters are related by the expression

$$H_\xi(\theta_0) = H(\theta_0) - I(\xi, \theta_0).$$

We note that the definition of conditional entropy makes use of the concept of a conditional distribution of probabilities θ_0 with stipulated ξ. Thus, in speaking of mean conditional entropy we will assume that in evaluating the state of the model θ_0 on the basis of data on ξ measurements use is made of the optimum method for processing information on ξ.

Now we will examine two models of the "atmosphere - ocean" system which are coherent in the following way:

1) the components of the vector θ_0^2 of the initial state of the second model include the components of the vector θ_0^1 of the initial state of the first model and the vector θ'_0, containing degrees of freedom of the second model not entering into the first:

$$\theta_0^2 = (\theta_0^1, \theta_0'); \tag{1}$$

2) the ξ_i measurements identical for both models are determined by the expressions

$$\xi_i = \alpha_i^1(\theta_0^1) + \Delta_i^1, \tag{2}$$

$$\xi_i = \alpha_i^2(\theta_0^2) + \Delta_i^2, \tag{3}$$

so that the error in measuring Δ_i^1 of the first, embedded in the second, model consists of the error in measuring Δ_i^2 of the second model and the difference in the values $\alpha_i^2(\theta_0^2)$ and $\alpha_i^1(\theta_0^1)$ computed in the models, corresponding to the ξ_i measurement; point 2) means that everything which is not described by the first model, but which enters into the second model, must, by virtue of the required coherence of the models, be included in the error in measuring the first model.

We will postulate that in the space of values of the parameters θ_0^2 and Δ^2 there is stipulation of the probability density distribution $p(\theta_0^2, \Delta^2)$, which determines the random properties of the θ_0^2, Δ^2 values and the θ_0^1, Δ^1, ξ values, being functions of θ_0^2 and Δ^2. Expressions (1), (2) and (3) and the density $p(\theta_0^2, \Delta^2)$ determine the two coherent models of the "atmosphere - ocean" system stipulated in one stochastic space.

It is obvious that the probability densities $p_1(\theta_0^1, \xi)$ and $p_2(\theta_0^2, \xi)$, obtained from the density $p(\theta_0^2, \Delta^2)$, are coherent:

$$p_1(\theta_0^1, \xi) = \int p_2(\theta_0^2, \xi)\, d\theta_0'. \tag{4}$$

We will say that the second model is a broadening of the first model. We will demonstrate that with such a broadening the mean conditional entropy increases:

$$H_\xi(\theta_0^2) > H_\xi(\theta_0^1). \tag{5}$$

We will introduce the discrete random values $\bar{\theta}_0^1$, $\bar{\theta}_0'$, $\bar{\xi}$ in the following way. We will break down the spaces $\{\theta_0^1\}$, $\{\theta_0'\}$, $\{\xi\}$ respectively into the sets b_i, $i = \overline{1, n_1}$, c_j, $j = \overline{1, n_2}$, d_k, $k = \overline{1, n_3}$. We will say that $\bar{\theta}_0^1$ (similar to $\bar{\theta}_0'$, $\bar{\xi}$) assumes a value $i(j, k)$; if $\theta_0^1 \in b_i$ ($\theta_0' \in c_j$, $\xi \in d_k$). We will demonstrate (5) for discrete values $\bar{\theta}_0^1$, $\bar{\theta}_0'$, $\bar{\xi}$. Since the discretization of the random values θ_0', θ_0', ξ can be made as "fine" as desired, this demonstration will mean the correctness of (5) in a general case.

We will use $P_{\bar{\theta}_0^1 \bar{\xi}}(i, k)$ to denote the probability that $\bar{\theta}_0^1$ and $\bar{\xi}$ assume i and k values and we will use $P_{\bar{\xi}}(k)$ to denote the probability that $\bar{\xi}$ assumes the k value. Then, using the entropy expressions and information from [2], we write the mean conditional entropy in the form

$$H_{\bar{\xi}}(\bar{\theta}_0^1) = -\sum_{i=1}^{n_1}\sum_{k=1}^{n_3} P_{\bar{\xi}}(k)\, f\left(\frac{P_{\bar{\theta}_0^1 \bar{\xi}}(i, k)}{P_{\bar{\xi}}(k)}\right),$$

where $f(x) = x \log x$.

Then, with each i the set of pairs (i, j), j = $\overline{1, n_2}$ can be regarded as the splitting of the i value of the random vector $\overline{\theta}_0^1$ into n_2 values, being values of the random vector $\overline{\theta}_0^2$. In this case

$$H_{\overline{\xi}}(\overline{\theta}_0^2) = -\sum_{i=1}^{n_1}\sum_{j=1}^{n_2}\sum_{k=1}^{n_3} P_{\overline{\xi}}(k)\, f\left(\frac{P_{\overline{\theta}_0^1\,\overline{\theta}_0'\,\overline{\xi}}(i, j, k)}{P_{\overline{\xi}}(k)}\right)$$

and

$$\cdot H_{\overline{\xi}}(\overline{\theta}_0^2) - H_{\overline{\xi}}(\overline{\theta}_0^1) =$$

$$= \sum_{k=1}^{n_3}\sum_{i=1}^{n_1} P_{\overline{\xi}}(k)\left[f\left(\frac{P_{\overline{\theta}_0^1\,\overline{\xi}}(i, k)}{P_{\overline{\xi}}(k)}\right) - \sum_{j=1}^{n_2} f\left(\frac{P_{\overline{\theta}_0^1\,\overline{\theta}_0'\,\overline{\xi}}(i, j, k)}{P_{\overline{\xi}}(k)}\right)\right], \qquad (6)$$

where

$$P_{\overline{\theta}_0^1\,\overline{\theta}_0'\,\overline{\xi}}(i, j, k)$$

is the probability that $\overline{\theta}_0^1$, $\overline{\theta}_0'$, $\overline{\xi}$ assume the values i, j, k.

The coherence condition (4) ensures satisfaction of the equation

$$\sum_{j=1}^{n_2} P_{\overline{\theta}_0^1\,\overline{\theta}_0'\,\overline{\xi}}(i, j, k) = P_{\overline{\theta}_0^1\,\overline{\xi}}(i, k). \qquad (7)$$

We note that the splitting of the i value of the random vector $\overline{\theta}_0^1$ can be carried out successively first into two parts, then into four, etc. In this case in each interval $n_2 = 2$. We use the notation

$$\frac{P_{\overline{\theta}_0^1\,\overline{\xi}}(i, k)}{P_{\overline{\xi}}(k)} = x, \qquad \frac{P_{\overline{\theta}_0^1\,\overline{\theta}_0'\,\overline{\xi}}(i, 1, k)}{P_{\overline{\xi}}(k)} = y.$$

Then, by virtue of (7), the expression in brackets in (6), with $n_2 = 2$, is written in the form

$$g(x, y) = f(x) - f(y) - f(x - y),$$

and here $x \geqslant y$. It is easy to investigate the behavior of the function g(x, y) and we find that $g(x, y) > 0$ when $y < x$.
This means $H_{\xi}(\Theta_0^2) - H_{\xi}(\Theta_0^1) > 0$, which also demonstrates the correctness of the inequality (5).

The entropy $H(\Theta_0)$ serves as a measure of the a priori "trajectories tube" [1] of a model of the "atmosphere - ocean" system, mean conditional entropy $H_{\xi}(\Theta_0)$ is the mean measure of the a posteriori "trajectories tubes" of the model. This means that $H_{\xi}(\Theta_0)$ is also a measure of the error in predicting the state using ξ information within the limits of the adopted model.

The demonstrated theorem means that if some dynamic model of the "atmosphere - ocean" system and model of observations give a small prediction error, an increase in the dimensionality of the dynamic model with

unchanged ξ measurements in general can increase the error in predicting the state to an unacceptable value. On the other hand, if some dynamic model and model of observations give a low prediction accuracy, an increase in the dimensionality of the dynamic model is capable only of worsening the prediction accuracy. In this case the system of ξ measurements must be regarded as not corresponding to the requirements of practical forecasting.

BIBLIOGRAPHY

1. Ryasin, V. A., Sal'nik, V. A., "Maximum Attainable Accuracy of a Forecast in a Class of Models of the 'Atmosphere - Ocean' System," METEOROLOGIYA I GIDROLOGIYA (Meteorology and Hydrology), No 9, 1978.

2. Yaglom, A. M., Yaglom, I. M., VEROYATNOST' I INFORMATSIYA (Probability and Information), Moscow, Fizmatgiz, 1960.

UDC 551.(501+507.362)(73)

METEOROLOGICAL SPACE OBSERVATION SYSTEM IN THE UNITED STATES

Moscow METEOROLOGIYA I GIDROLOGIYA in Russian No 12, Dec 79 pp 107-115

[Article by Corresponding Member USSR Academy of Sciences K. Ya. Kondrat'yev, Main Geophysical Observatory, submitted for publication 25 April 1979]

Abstract: This is a review of the present status and a presentation of concise information on the prospects for the development of a meteorological space observation system in the United States.

[Text] In 1978 in the United States there was a changeover to a third generation of meteorological satellites with the operational designation TIROS-N. An American meteorological space observation system now consists of meteorological satellites in polar orbits (including meteorological satellites of the US Defense Department), and also geostationary satellites. The experimental satellite "Nimbus-7," launched on 24 October 1978, represents the latest advance in the tests of promising instrumentation and methods. It is of interest to examine the experience in developing the United States meteorological space system and the prospects for its further development [8-14].

The principal instrument complex of the two simultaneously functioning TIROS-N satellites (local time of intersection of the equator 0730 and 1500 hours) is a five-channel improved radiometer with a very high resolution IVHRR. This complex makes it possible to obtain information on the following characteristics: 1) ocean surface temperature (OST); 2) albedo of the underlying surface; 3) positions of the boundaries of the snow and ice covers; 4) cloud cover; 5) vegetation cover. In the future a channel 1.6 μm will be added for a more reliable difference between clouds and snow.

A second important instrument complex on the TIROS-N satellites is the operational vertical sounding system (OVS), consisting of three subsystems: tropospheric sounding (TS), stratospheric sounding (SS) and microwave sounding (MS). The OVS instrumentation makes it possible to reconstruct the vertical temperature profiles with an accuracy to 2°C and a relative

humidity 25%. The TIROS-N carried instrumentation for localizing and collecting data from land and sea automatic stations.

In order to meet the needs of programs for the investigation of climate use is also made of: 1) an ultraviolet spectral apparatus (UVSA) for monitoring the exoatmospheric UV solar radiation and the global distribution of ozone; 2) instrumentation for measurement of the earth's radiation balance (RBEA). The UVSA is a 12-channel instrument and ensures a spatial resolution at the nadir of 165 km. The RBEA has two channels (0.2-50μm and 0.2-5.0μm) with the presence of wide-angle (entire visible disk of the planet), intermediate-angle (1000 km) and narrow-angle scanning (87 km) sensors. A channel for measuring the solar constant has been introduced for the purpose of on-board calibration.

Table 1 gives a more detailed characterization of the entire TIROS-N instrument complex [9]. Bearing in mind the necessity for studying the diurnal variation of the radiation balance, plans also call for the installation of RBEA on satellites with a relatively small orbital inclination (about 50°). Combination with the data from two TIROS-N solar-synchronized satellites will make it possible to obtain quite complete information on the radiation balance.

The main range of data obtained using the TIROS-N satellites and transmitted through the global telecommunication system is:

Parameter	Accuracy of determination	Frequency (per day)
1. Thickness (m) and mean temperature (°C) of layers between standard isobaric levels	±1.5°C	4
2. Water vapor content (mm of precipitable water) in layers between standard isobaric levels	±30%	4
3. Temperature (°C) and pressure (mb) at tropopause level	±2.5°C ±50 mb	4
4. Quantity of precipitation in sounding zone	±20%	4
5. Outgoing radiation in clear sky	±2%	8

The "Nimbus-7" was launched into a solar-synchronized orbit with an altitude of about 995 km (with an inclination of 99.1°). It was the first satellite completely intended for monitoring the parameters of environmental quality [10]. The most important tasks in the program for this satellite are: 1) remote sounding of the upper troposphere and stratosphere for the purpose of determining the concentration of a number of small gas and aerosol components, bearing in mind from whence they originate and how they are lost, and also transfer processes; 2) observations of color of the

ocean, surface temperature and ice conditions, especially in the shore zone, taking into account the need for solving the problems involved in detecting contamination in the ocean, clarification of the nature of hydrosols, mapping of zones of bottom sediments and biologically productive regions, study of the interaction between coastal and ocean waters, etc.

In addition to the mentioned, the following are accomplished: 1) remote measurements of the parameters characterizing the conditions near the "underlying surface - atmosphere" discontinuity (soil moisture content, temperature and roughness of the ocean surface, albedo, distribution of the snow and ice covers), which is of great importance for carrying out the objectives of GARP; 2) continuation of observations of components of the earth's radiation balance and the parameters determining them in the interest of the problem of studying climatic changes. The enumerated problems are solved using the complex of instrumentation, consisting of eight instruments, characterized in Table 2.

The six-channel MSZH is supplied with a cryogenic apparatus (using methane and ammonia), maintaining the mercury-cadmium-tellurium radiation sensors at a temperature of 65°K. The basis for the SSM is several radiometers with modulation by pressure by means of cells containing CO_2 (two cells), NO_2, NO, CH_4, CO and H_2O. At the same time, in the receiving telescope there is a mechanical modulator which makes possible the independent measurement of two signals modulated by pressure and mechanically. This makes it possible to exclude the overlapping of the bands of different gases in some spectral intervals.

Altitudinal scanning (with a SSM field of view corresponding to 10 x 100 km) makes it possible to reconstruct the vertical profiles of temperature and the concentration of gases in the layer 10-120 km. Plans also call for the use of observational data on the Doppler shift of emission lines for reconstructing the profile of the zonal wind in the layer 60-120 km. Periodically there is on-board calibration of the SSM using an ideally black body.

The source of information for determining the vertical profile of the aerosol concentration on the basis of SAI data is measurements of the attenuation of solar radiation at a wavelength of 1μm at sunrise and sunset relative to the satellite. The measurement data for three months ensure the coverage of a latitude zone of 64-80° in both hemispheres. The altitudinal resolution is about 1 km.

The UVS, directed to the nadir, has 12 channels in the interval 250-340 nm (spatial resolution at the nadir 200 x 200 km); these are intended for reconstruction of the ozone profile, but will also alternatively measure the spectral distribution of the exoatmospheric solar radiation or the earth's spectral brightness in the range 160-400 nm. In order to determine the reflectivity of the lower boundary of the atmosphere within the limits of the coinciding field of view the UVS is supplied with a photometer at a

Table 1

Complex of Scientific Instrumentation Aboard TIROS-N Satellite

Instrument	Channels	Spatial resolution, km	Width of scanning band, km	Measured climatic parameters
UVSA	12 channels in range 255-344 nm	165	Only nadir	Vertical profile of concentration and total ozone content
UROVR	0.58-0.68 μm 0.725-1.0 1.53-1.73 3.55-3.93 10.3-11.3 11.5-12.5	1	30000	Temperature of ocean surface, snow and ice cover, albedo, cloud cover, vegetation cover
OVS TS	20 channels in range from visible region to 15 μm	30	1000	Vertical profiles of temperature and humidity
SS	3 channels in band 15 μm CO_2	147	1450	Vertical profile of temperature in stratosphere
MS	4 channels in band 5.5 mm O_2	100	1700	Vertical temperature profile

Table 2

General Characteristics of Scientific Instrumentation Carried on "Nimbus-7"

Instrument	Type of measurements	Parameters determined
1. IR monitor of stratosphere in horizon zone (MSZH)	Scanning atmosphere in horizon zone	Vertical temperature profile; H_2O, HNO_3, NO_2 concentration
2. Sounding of stratosphere and mesosphere (SSM)	Scanning atmosphere in horizon zone	Vertical temperature profile; CH_4, CO, H_2O, NO, N_2O concentration
3. Instrument for measuring stratospheric aerosol (SAI)	Measurements of attenuation of solar radiation in eclipse	Vertical profile of aerosol concentration
4. Spectrometers for measuring UV solar scattered radiation and mapping ozone (UVS/OMS)	Measurements of direct solar and outgoing UV radiation	UV solar constant, vertical profile and total content of ozone
5. Radiometer for the earth's radiation balance (RRBE)	Spectrometers for solar and outgoing radiation	Solar constant, short-wave and long-wave outgoing radiation
6. Scanning multichannel microwave radiometer (SMMR)	Scanning under satellite	Ice-snow cover, temperature ocean, wind speed, moisture-water content of air, rainfall intensity
7. Scanning colorimeter for shore zone (SCSZ)	Scanning under satellite	Chlorophyll, hydrosol and yellow matter content (as salinity indicator), currents, bottom sediments
8. IR radiometer for temperature and humidity (RTH)	Scanning under satellite	Auxiliary images for other experiments, structure of temperature field of ocean surface

wavelength of 380 nm. The UVS is calibrated against the sun.

The parallely operating system for the mapping of the total ozone content (OMS) operates in a regime of stepped spatial scanning and has six channels in the interval 310-340 nm and also at a wavelength of 800 nm. The OMS has a spatial resolution of 50 x 50 km. The 20-channel RRBE contains both wide- and narrow-angle scanning sensors intended for measurements: 1) exoatmospheric solar radiation in the range 0.2-40 μm (10 channels); 2) integral

fluxes of short-wave (0.2-4.0μm) and long-wave (4.0-40μm) radiation, and also spectral albedo at wavelengths less than 0.7μm (4 channels); 3) angular distribution of the intensity of outgoing radiation (solid angle 0.25 x 5.12°) in the short-wave and long-wave ranges (8 channels).

The instrumentation carried aboard the "Seasat-1" satellite made it possible to obtain important meteorological and climatological information [8, 14]. Much useful data, from the point of view of the problems of weather and climate, is contained in the observations made from the natural resources satellite "Landsat-3" [12].

The fundamental prospects for development of the American meteorological space observation system are related to the task of monitoring different climatic parameters and factors. This applies, in particular, to the atmospheric content of ozone, small gas contaminating components and aerosol [1-5, 9, 10]. Satellites with a small inclination were mentioned above. These satellites will also be used for aerosol measurements by the method of sounding on slant ("eclipsed") paths. Such satellites are called stratospheric, aerosol and gas sounding satellites (SAGSS). In the future instrumentation for measuring aerosol and the radiation balance should be installed jointly on these satellites.

During 1979 plans call for carrying out the launching of the small specialized satellite "Applications Explorer-B (AE-B)," fully intended for determining the content of aerosol and ozone in the stratosphere at altitudes from the level of the upper boundary of the clouds to 60 km [11]. The satellite will carry a four-channel photometer for measurements of the attenuation of solar radiation by the atmosphere during sunrise and sunset relative to the satellite. Each two weeks this will make it possible to obtain data on the vertical profiles of attenuation for the latitude zone 72°N-72°S. It is assumed that the use of these data in combination with the results of ground measurements at some points will make it possible to solve the following problems: 1) mapping of the vertical profiles of attenuation caused by aerosol and ozone in the mentioned latitude zone; 2) determination of the optical properties of stratospheric aerosol; 3) determination of the global three-dimensional fields of the concentration of aerosol and ozone; 4) study of the spatial-temporal variability of the fields of concentration of aerosol and ozone; 5) investigation of exchange between the troposphere and stratosphere; 6) evaluation of the effects of stratospheric aerosol and ozone from the point of view of their influence on global climate.

AE-B data will be used jointly with similar aerosol measurements from the "Nimbus-7" satellite. Plans call for putting the AE-B into an orbit with an inclination 50° and an altitude of 600 km. The "ozone" channel of the photometer was centered at 0.6μm (maximum of the Chappuis band) and the "aerosol" channels were centered at wavelengths 0.385, 0.45 and 1.0μm. Plans call for determination of aerosol attenuation by means of excluding Rayleigh scattering with the use of density data obtained on the basis of

the measured values of atmospheric pressure and temperature. The field of view for the photometer is about 0.5 minute of angle. This will ensure an altitudinal resolution of 0.5 km. The dynamic range for each of the photometer channels in this photometer is approximately 1000 and the measurement errors do not exceed 0.1% relative to the exoatmospheric intensity of solar radiation.

An evaluation of the accuracy in determining the coefficients of attenuation of solar radiation by aerosol and ozone gives values of about 10 and 50% respectively. The accuracies are considerably higher near the maxima of the aerosol and ozone concentrations. Plans call for an extensive program of surface, aircraft and balloon measurements both by means of the taking of samples and by means of remote (particularly lidar) measurements. In this connection plans call for carrying out international cooperation.

The specific purposes of the "Climsat" polar satellites are measurements of the ice and snow cover, topography of the surface of the polar ice, precipitation, humidity, surface ground layer, topography of the ocean surface, liquid water content of clouds and moisture content of the stratosphere [9]. The instrument complex aboard these satellites includes a microwave ground moisture content radiometer (MGMCR), multichannel microwave scanning radiometer (MMSR), radioaltimeter (RA), multichannel radiometer for measuring IR radiation of the atmosphere near the limb of the planetary disk (RLPD), two-channel scanning instrument for obtaining images (TSI), whose characteristics are given in Table 3. The MGMCR ensures an adequately high resolution as a result of use of a large antenna (10 x 10 m) with electric scanning. The moisture contents of the upper ground layer obtained using this radiometer, with a thickness of several centimeters, will be used taking into account the corresponding parameterization and data from ground measurements at individual points for evaluating the moisture content of the deep layers of ground.

The MMSR is supplied with a mechanical scanning system and makes it possible to measure outgoing radiothermal emission at both polarizations. The radioaltimeter has an antenna with a diameter of 1 m and makes possible measurements of satellite altitude with an accuracy to about 10 cm. This instrument will be used primarily in the very high latitudes for investigations of the ice cover.

The considered instrument complex must be installed on standard (modular) NASA satellites. The altitude of the polar orbit of the satellite (plans call for putting it into an initial orbit with an inclination of 57° using a transport spaceship) is about 725 km. The plan is to adjust the orbit for the purpose of a uniform coverage of the earth's surface. The total weight of the satellite is 1745 kg. In the future it is proposed that the scientific instrumentation aboard the "Climsat" satellites be improved and extended by the incorporation of instruments for measuring stratospheric aerosol (evidently, in the latter case laser sounding is the most suited).

Table 3

Scientific Instrumentation Complex on "Climsat" Satellite

Прибор 1	Каналы 2	Пространственное разрешение, км 3	Ширина полосы сканирования, км 4	Измеряемые параметры климата 5
6 ВРВГ	21 см	30	1000	Влажность грунта 13
7 СММР	0,8; 1,4; 1,7; 2,8; 4,6 см	18—100	500	Процент открытой воды, снежный покров, водность облаков, осадки, ТПО 14
8 ДСА	0,55—0,75; 10—12 мкм 11	10	100	Облачный покров 15
9 РКДП	6,2; 6,3; 9,6; 11,3; 15(2) мкм 12	200	1000	Вертикальные профили водяного пара и озона в стратосфере 16
10 РВ	13,5 Ггц 12	1—2	Только в надир 18	Топография поверхности океана и ледяного покрова 17

KEY:

1. Instrument
2. Channels
3. Spatial resolution, km
4. Width of scanning zone, km
5. Measured climatic parameters
6. MGMCR
7. MMSR
8. TSI
9. RLPD
10. RA
11. μm
12. GHz
13. Ground moisture content
14. Percentage of open water, snow cover, liquid water content of clouds, precipitation, temperature of ocean surface
15. Cloud cover
16. Vertical profiles of water vapor and ozone in stratosphere
17. Topography of ocean surface and ice cover
18. Only at nadir

Plans call for the launching of the first "Climsat" satellite in 1983, and the second -- in 1985.

Part of the scientific instrumentation aboard "Climsat" will undergo testing aboard the "Spacelab" orbiting station in the early 1980's. The improvement in the instrumentation will be directed to increasing the accuracy in reconstructing the temperature of the ocean surface (better than 1°C) and the vertical profile of air temperature (up to 0.5-1°C), obtaining data on the moisture content of the deeper ground layers (measurements at a wavelength of 1 m) and more reliable aerosol data. In order to reconstruct the profile of the concentration of stratospheric aerosol work is proceeding on methods based on observations of star occultations and atmospheric brightness at the horizon.

D. Atlas, et al. [13] have described a system of operational meteorological satellites (OMSS) planned in the United States for the 1990's, the basis for which is eight low-orbit (500 km) non-solarly synchronized satellites (NSSS) in four strictly polar orbits (inclination 90°), displaced by 45°, which will ensure obtaining global information each 3 hours (the NSSS will pass over the poles each 11.8 minutes) and three environmental geostationary satellites (EGS) over the western hemisphere (separated by a distance of 30-45°with a central longitude of 95°W), making it possible to carry out synchronous observations of a number of regions, which will in turn make possible a stereographic analysis of images of the cloud cover. The most important changes in the purposes of the observation system in comparison with those now existing are a broadening of oceanographic and climatological observations and also the obtaining of quantitative information necessary for numerical mesometeorological forecasts (such information must, in particular, have high spatial-temporal resolution). The OMSS data must also find application for solving different problems in the interests of agriculture, hydrology, aviation, industry and tourism.

Fundamentally new characteristics of functioning of NSSS are: 1) use of transport spaceships for the delivery of satellites and (if necessary) repair of vehicles in orbit; 2) use of an on-board system for the global coordinate tie-in of observational data (SGCTI), reception and processing of quantitative information on geographically tied-in physical parameters at a ground center; 3) use of a data transmission scheme "NSSS - EGS - GC," reflecting, in particular, the unity and interrelationship of all the OMSS components. In addition, there will also be a system for the direct transmission of NSSS data.

The presence of a system of non-solarly synchronized NSSS will make it possible in the course of a year to accumulate a mass of observational data relating to any moment local solar time in the limits ±1.5 hours. Servicing by means of a transport spaceship ensures a lifetime of the NSSS of more than 10 years.

The low orbital altitude of the NSSS affords broad prospects for the use of active (lidar and radar) sounding. An important function of these NSSS is interrogation (each three hours) of automatic platforms (ground stations, sea buoys, balloons) with subsequent geographical tie-in and transmission of the collected data to the GC [ground center] via the EGS (this causes a lag in obtaining data constituting only 59 minutes). The communication functions performed by the EGS (also including the transmission of the processed information from the GC to the regional centers and other users) are regarded as important as obtaining observational data.

Table 4 contains a comparison of a list of additional scientific instrumentation used on the OMSS satellites with the instrument complex on the TIROS-N, constituting the basis of the OMSS (I -- improved apparatus, N -- instrumentation absent on the TIROS-N).

The low resolution of the vertical temperature profiles, reconstructed on the basis of IR data, led to the development of the LSTH instrument for the purpose of obtaining altitudinal resolution (2 km) and accuracy (IR) corresponding to GARP requirements. The two-channel LSTH has one channel coinciding with the resonance absorption line and a closely positioned channel at the frequency of minimum attenuation. The problem of increasing the vertical resolution must also be solved by the IRSSHR, the developed variant of which provides for a spectral resolution of 2 cm^{-1}, and in the long run -- to 0.2 cm^{-1} in the band 4.2 μm of CO_2 with broader channels in the bands 15 μm, 3.7 μm and 5.7 μm. The possibilities of the use of a spectrometer with a diffraction grating supplied with a "comb" of sensors, a Michelson interferometer and Fabry-Perot standards are analyzed.

The LPS ensures a determination of surface pressure with the necessary accuracy (0.3% or 3 mb) with a high resolution and also determination of the vertical pressure profile.

The pulsed LPS is based on the use of "impact" line broadening; its frequency was selected in the region of the wing of the oxygen line (in such a case the measured signal is proportional to the square of pressure). Another possibility for determining this parameter is the use of a multiwave radar for the oxygen band 60 GHz (RSSF). The LWS is a coherent pulsed lidar in the band 15 μm of CO_2. The wind indicator is the drift of atmospheric aerosol traced using data on measurements of the Doppler shift of with two or three sighting angles with a stipulated accuracy during motion of the satellite. The ten-channel scanning IMS has already been tested on the satellites "Seasat-1" and "Nimbus-7." It functions at horizontal and vertical polarizations at frequencies 37, 21, 18, 10.69 and 6.6 GHz.

The data from the IMS allow determination of the following parameters: temperature of the ocean surface and precipitation over the ocean, wind shearing stress, continuity of the ice cover, snow water content, moisture content (and possibly, microstructure) of clouds, moisture content of the ground (rough estimate). The addition of the channels 1.4 and 94 GHz, as well as three channels in the oxygen band 55 GHz and the water vapor bands 21 and 183 GHz will considerably broaden the possibilities for obtaining information. The use of an antenna of about 10 m will make it possible to increase the resolution to 3-50 km with a width of the scanning zone of about 2000 km.

The two-channel MR in the range 1-2 cm will be used in determining the intensity of precipitation: 1-10 mm/hour (channel 35 GHz) and up to 200 mm/hour (16 GHz). The principal purpose of the scatter meter used on the "Seasat-1" is determination of wind velocity at the ocean surface, but in combination with the IMS it will also be used for evaluating the ice cover, waves, temperature of the ocean surface and ground moisture content. A radioaltimeter operating at a wavelength of 2.2 cm, of the type carried aboard the "Seasat-1," will make it possible to determine the level (the height) of the ocean surface with an accuracy to ±10 cm, the velocity of

Table 4

Comparison of Additional Complex of OMSS Scientific Instrumentation and Instrumentation Duplicating That Used on the TIROS-N Satellites

Parameters	Instrumentation	
	TIROS-N	OMSS
Weather		
Vertical temperature and humidity profiles	Filter IR sensor	Lidar temperature and humidity sensor LSTH
	IR sensor with modulation by pressure	Passive IR sensor with superhigh resolution IRSSHR
	Microwave sensor	Improved passive microwave sensor IMS
Surface pressure	N	Lidar pressure sensor LPS
	N	Radar sensor of surface pressure RSSF
Wind profile	Monitoring of clouds. I	Lidar wind sensor LWS
Ocean surface temperature	Two-channel scanning radiometer (TSR)	Active-passive system for obtaining microwave images APSMWI
Cloud cover	Same	Same
Precipitation	N	Same
		Meteorological radar (MR)
Climate (Ocean)		
Wind shearing stress	N	APSMWI Scatter meter SM
Ocean surface level	N	Radioaltimeter RA
Temperature of ocean surface and wind speed	Sea buoys (data collection)	

Table 4 (continued)

Parameters	Instrumentation		
	TIROS-N		OMSS
Climate (radiation balance)	Instrumentation for measuring earth's radiation balance (ERBI)		
Surface albedo	TSR		
Solar constant	Band radiometer BR		
UV solar radiation	UV monochromator (UVM) for measuring outgoing radiation		
Climate (land, hydrology, plant cover)			
Moisture content of surface ground layer		N	APSMWI
Plant cover	TSR		
Climate (cryosphere)			
Sea ice (continuous)		N	APSMWI
Snow cover	TSR		
Moisture content of snow		N	APSMWI
Level of ice surface		N	RA Side-scanning radar
Boundaries of continental ice cover			
Atmospheric contamination and small components			
Stratospheric aerosol		N	Instrumentation for eclipse measurements of attenuation of solar radiation IEMASR
Tropospheric aerosol		N	Aerosol lidar AL

Table 4 (continued)

Parameters	Instrumentation	
	TIROS-N	OMSS
Ozone	UVM	
Stratospheric water vapor	N	Limb sensor LS
N_2O, NO_x, CH_4, freons and others	N	Differential correlation radiometer -- DCR (troposphere) and LS (stratosphere)
Parameters of circumterrestrial space		
Fluxes of solar protons and electrons		
Total fluxes in near space	Sensors for monitoring the parameters of circumterrestrial space	

******

sea currents to minimum values 30-50 cm/sec and the height of sea waves in the range 1-20 m with an accuracy ±10% and to map relief and the physical characteristics of the ice cover. The presence of a side-scanning radar, operating at a wavelength of 22 cm, similar to that in the instrument complex on the "Seasat-1," will make it possible, in particular, to obtain information on the parameters of sea waves and the ice cover with a spatial resolution of 25 m and with a width of the scanning zone of 100 km. The IEMASR has already been tested on the "Nimbus-7" satellite.

The AL instrument affords the sole possibility for determining the profile of tropospheric aerosol concentration. The combination of multispectral data from measurements of backscattering and attenuation will make it possible to determine the mean size and refractive index of aerosol particles. LS and DCR data are intended for determining the profiles of the concentration of small gas components with an accuracy to about 1 ppb.

A characteristic of a global satellite observation system of the future is the collection of images not only from the entire visible disk of the earth, but also images measuring 2000 x 2000 km or less for monitoring processes at regional scales. The resolution of the images in the visible and IR spectral regions will attain 300 and 1000 m respectively with a frequency up to 2 minutes. Spectral measurements of outgoing radiation in the CO_2 bands 4.3 μm and (or) 15 μm will make it possible to determine the vertical profiles of temperature and humidity with a spatial resolution of about 5-10 km. In order to increase the altitudinal resolution it is possible to use a higher spectral resolution (0.5-2 cm^{-1}) or an interferometer method with partial scanning.

The possibilities of microwave remote sensing from the global satellite observation system are being discussed. For example, a radiometer at a frequency of 94 or 140 GHz can be used for virtually continuous monitoring of the dynamics of the intensity of precipitation. A factor of great importance for increasing the spatial resolution is the use of large antennas with a diameter up to 100 m. It is possible that technical progress will make it possible, in the future, to employ active sounding apparatus as well in the global satellite observation system. Critically it is of great importance to solve the problems involved in the processing and dissemination of data, an important component of which is the primary processing of information aboard a satellite.

As noted in [6], considering the present-day diversity of space instrumentation for monitoring of the environment the optimum planning of observation systems is assuming particular importance. The inadequate accuracy in determining the sought-for parameters is requiring solution of the problem of four-dimensional assimilation of data from ordinary and satellite observations [7].

BIBLIOGRAPHY

1. Kondrat'yev, K. Ya., "Possibility of Studying Atmospheric Contamination Using Satellites," METEOROLOGIYA I GIDROLOGIYA (Meteorology and Hydrology), No 9, 1970.

2. Kondrat'yev, K. Ya., SPUTNIKOVAYA KLIMATOLOGIYA (Satellite Climatology), Leningrad, Gidrometeoizdat, 1971.

3. Kondrat'yev, K. Ya., SPUTNIKOVYY MONITORING KLIMATA: OBZOR. METEOROLOGIYA (Satellite Monitoring of Climate: Review. Meteorology), Obninsk, Inform. Tsentr, 1978.

4. Kondrat'yev, K. Ya., Pokrovskiy, O. M., SPUTNIKOVAYA METEOROLOGIYA (Satellite Meteorology), USPEKHI SSSR V ISSLED. KOSMICH. PROSTRANSTVA (USSR Successes in Space Exploration), VTOROYE KOSMICH DESYATILETIYE 1967-1977 (Second Space Decade 1967-1977), Moscow, Nauka, 1978.

5. Kondrat'yev, K. Ya., Timofeyev, Yu. M., METEOROLOGICHESKOYE ZONDIROVANIYE ATMOSFERY IZ KOSMOSA (Meteorological Sounding of the Atmosphere from Space), Leningrad, Gidrometeoizdat, 1978.

6. Kondrat'yev, K. Ya., Pokrovskiy, O. M., "Planning of Multipurpose Experiments With Remote Sensing of Environmental Parameters and Natural Resources," IZV. AN SSSR, SERIYA GEOGRAF. (News of the USSR Academy of Sciences, Geography Series), No 3, 1978.

7. Pokrovskiy, O. M., Ivanykin, Ye. Ye., Kaygorodtsev, A. Ye., "Numerical Modeling of Systems for Observing and Analyzing the Ozone Field," METEOROLOGIYA I GIDROLOGIYA, No 1, 1979.

8. Cutting, E., Born, G. H., Frautnick, R. A., McLaughlin, W. I., Neilson, R. A., "Mission Design for Seasat-A, an Oceanographic Satellite," AIAA 15th AEROSPACE SCIENCES MEETING, Los Angeles, California, January 24-26, 1977.

9. PROPOSED NASA CONTRIBUTION TO THE CLIMATE PROGRAM, Goddard Space Flight Center, Greenbelt, Maryland, November 1977.

10. Schiffer, R. A., "Satellite Global Monitoring of Environmental Quality," PROC. OF THE TENTH INT. SYMPOSIUM ON REMOTE SENSING OF ENVIRONMENT, 6-10 October 1975, Ann Arbor, Vol 1, 1977.

11. Science Support for the Applications Explorer Mission-B/Stratospheric Aerosol and Gas Experiment Sensor," ANNOUNCEMENT OF OPPORTUNITY, Washington, D. C., June 21, 1976.

12. "The New Landsat," SPACEFLIGHT, Vol 20, No 8, 1978.

13. Atlas, D., Bandeen, W. R., Shenk, W., Gatlin, J. A., Maxwell, M., VISIONS OF THE FUTURE OPERATIONAL METEOROLOGICAL SATELLITE SYSTEM, Preprint, EASCON'78 Electronics and Aerospace Systems Conference, September 25-27, Arlington, Virginia, 1978.

14. Williams, F. L., McCandless, S. W., Jr., "'Seasat-A' - Ocean Observation Satellite," PROC. OF THE SYMP. ON METEOROL. OBSERV. FROM SPACE: THEIR CONTRIBUTION TO THE FGGE, June 8-10, Philadelphia, 1976.

SIXTIETH BIRTHDAY OF MIKHAIL ARAMAISOVICH PETROSYANTS

Moscow METEOROLOGIYA I GIDROLOGIYA in Russian No 12, Dec 79 p 116

[Article by members of the Board of the USSR State Committee on Hydrometeorology and Environmental Monitoring]

Professor Mikhail Aramaisovich Petrosyants, Doctor of Geographical Sciences, marked his 60th birthday on 4 December. He is a member of the Board of the USSR State Committee on Hydrometeorology and Environmental Monitoring, Director of the USSR Hydrometeorological Center, a member of the Joint Organizing Committee of GARP, was director of two major interdepartmental

expeditions TROPEKS-72 and TROPEKS-74, is Deputy Chairman of the Problems Council on Weather Forecasting, is the author of a series of profound and original investigations in the field of regional meteorology and general circulation of the atmosphere and is a member of the editorial board of the journal METEOROLOGIYA I GIDROLOGIYA (Meteorology and Hydrology).

In sincerely congratulating M. A. Petrosyants on this noteworthy date, we wish him good health, personal happiness and long years of productive creative work for the well-being of Soviet science.

SIXTIETH BIRTHDAY OF VASILIY NIKIFOROVICH BABCHENKO

Moscow METEOROLOGIYA I GIDROLOGIYA in Russian No 12, Dec 79 p 117

[Article by the Board of the USSR State Committee on Hydrometeorology and Environmental Monitoring]

[Text] Vasiliy Nikiforovich Babchenko, head of the Ural Territorial Administration of Hydrometeorology and Environmental Monitoring, marked his 60th birthday on 25 December 1979.

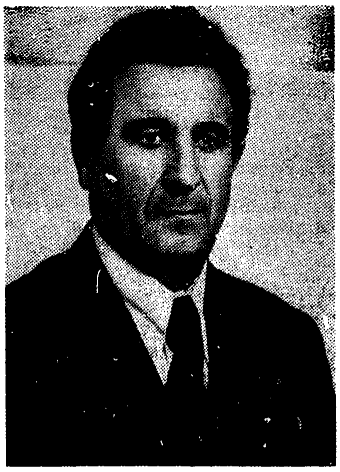

Vasiliy Nikiforovich was born in a family of rural workers in Kustanayskaya Oblast in 1919. In 1945 he graduated from the Higher Military Hydrometeorological Institute of the Red Army.

After demobilization from the army in 1947 he worked in Moscow at the "Giproredmet"(State Institute for the Design and Planning of Rare Metals Industry Establishments) until February 1948, then moved to the Hydrometeorological Service and since that time has been living and working

in the Urals, first as a senior hydrological engineer of the Sverdlovsk Administration of the Hydrometeorological Service and then as head of the scientific research section of the Sverdlovsk Geophysical Observatory, and since 1954 he has continuously headed the territorial administration of the Hydrometeorological Service (at the present time this is the Ural Territorial Administration of Hydrometeorology and Environmental Monitoring).

During the past quarter-century there have been many changes and much growth of the hydrometeorological service in this highly important region of our country. There has been an augmentation of personnel, a strengthening of the material and technical base and an improvement in the work quality of absolutely all subdivisions. The hydrometeorological study of the Ural region has become deeper and broader.

In the Urals V. N. Babchenko is known not only as a director and organizer, but also as an experienced engineer. He is the editor of numerous publications of the Administration on Hydrometeorology and Environmental Monitoring, the author and co-author of individual published works.

The Communist V. N. Babchenko capably combines a great volume of work on directing the administration with active public and pedagogic activity. Over a period of 12 years he has presented lectures to student hydrometeorologists at Perm State University.

Having high special training and great experience in organizational work, Vasiliy Nikiforovich is successfully ensuring the direction of the body of Ural hydrometeorologists and is enjoying the leadership and respect not only of the workers of the service, but also all those who know him in the scientific, planning and production organizations of the Urals.

For his organizational work in the hydrometeorological servicing of the national economy V. N. Babchenko has been awarded the order "Emblem of Honor," an award "Distinguished Worker of the Hydrometeorological Service," and a silver medal of the USSR All-Union Exhibition of Attainments in the National Economy.

In congratulating Vasiliy Nikiforovich on his 60th birthday, we sincerely wish him undiminished energy, enjoyment of life and health and many years of productive work.

CONFERENCES, MEETINGS AND SEMINARS

Moscow METEOROLOGIYA I GIDROLOGIYA in Russian No 12, Dec 79 pp 117-119

[Article by A. P. Zhilyayev, Yu. G. Slatinskiy and G. V. Gruza]

[Text] A session of the Scientific-Technical Council of the Special Committee of the Administration of Hydrometeorology and Environmental Monitoring was held in Rostov-na-Don on 25 May. The conferees examined the problem of the state of operation of sea hydrometeorological stations and posts in the Sea of Azov-Black Sea basin and in the northern Caspian region. A report was presented by I. P. Bryanov, Deputy Director of the Rostov Hydrometeorological Observatory.

It was noted in the report and in the addresses of the participants in the session that during recent years in the Special Committee much work has been carried out for rationalization of the sea network and types of observations, an increase in the quality of information arriving for the servicing of national economic organizations and prognostic agencies of the State Committee on Hydrometeorology.

At the present time the sea network include 25 subdivisions, including two river mouth stations (Donskaya and Kubanskaya), to which is joined a network of posts in the deltas of the Don and Kuban'.

According to the results of work during 1978 the overwhelming majority of stations and posts had only "excellent" and "good" evaluations both with respect to implementation of the plan and the quality of observations, as well as respect to the quality of data punching. All the sea subdivisions are supplied with punchers of the T-56 or T-63 variants. Preventive maintenance of the punchers is carried out regularly in accordance with a special schedule with the assistance of local communication divisions, which makes it possible for stations to maintain the quality of punching stably at a high level.

In the sea network the Special Committee is carrying out construction of new and reconstruction of operating post facilities. During recent years new SUM apparatus has been introduced at the Gelendzhik marine hydrometeorological station and the Tuapse hydrometeorological bureau. Plans have been

developed for the construction of SUM apparatus with remote control for the hydrometeorological bureau at Novorossiysk. In 1979 new water gages of the GM-3 type were installed at the Dolzhanskaya marine hydrometeorological station and at the marine hydrometeorological post at the Yasenskaya crossing.

The subdivisions of the marine network operating under the Special Committee are participating in carrying out scientific research work and special observations. The Donskaya and Kubanskaya mouth stations and the Astrakhanskaya Hydrometeorological Observatory have collected a great volume of information for developing a forecast of the influence of water management measures on the hydrological and hydrochemical regimes of the mouth regions of rivers and the adjacent regions of the Sea of Azov and the Caspian Sea. During the last two years alone the river mouth stations under the Special Committee operating in the Sea of Azov, in collaboration with the river mouths laboratory of the Sevastopol' Division of the State Oceanographic Institute, have carried out several major expeditions with a total duration of 118 days, during which about a thousand stations were occupied and extensive experimental data was collected for an analysis of the trends in further development of mouth regions under conditions of increasing removal of runoff for economic needs.

The marine network under the Special Committee has been taking an active part in carrying out a number of experiments having great national economic importance. For example, the Donskaya mouth station already for a number of years has been participating in the patroling of the Sea of Azov during the entire navigation season. The Astrakhanskaya Hydrometeorological Observatory is carrying out investigations for clarifying the possibility of year-round navigation on the Lower Volga and in the Northern Caspian. The Tuapse and Novorossiysk Hydrometeorological Bureaus are developing a method for predicting dangerous phenomena (bora, sudden gales, etc.).

An important place in the work of the marine network operating under the Special Committee is occupied by the preparation of materials for the published part of the hydrological yearbook. In this respect a particularly great amount of work falls to the lot of the river mouth subdivisions which prepare the sections for their regions. In 1979 Volume XIII (Black Sea) and Volume XIV (Sea of Azov) of these yearbooks for 1976 were published. Similar materials for 1977 are being prepared for the press.

At the session there was a detailed examination of the problems involved in operation of the shipboard network. It was noted that during 1979 the Special Committee had under its jurisdiction a total of 64 shipboard stations with navigators. During 1978 about 30,000 hydrometeorological observations were made in different regions of the world ocean. Shipboard inspectors carried out 70 inspections and 156 visits to shipboard stations, did much work on the introduction of new KN-09-S codes and KGM-15A logs at all shipboard stations, and improved the quality of the incoming data.

While noting the unquestionable attainments in the organization of operation of the sea network, the scientific and technical council of the Special Committee brought attention to a number of unsolved problems.

A resolution which was adopted formulated a number of fundamental tasks for further improvement in the activity of the sea network of the Special Committee, intensification of coordination of actions for direction of the network between the Special Committee and the Sevastopol' Division of the State Oceanographic Institute, and an increase in the responsibility of all links in the hydrometeorological service in implementation of the approved tasks in the plan.

A. P. Zhilyayev and Yu. G. Slatinskiy

In accordance with a resolution of the Executive Committee of the WMO, plans have been laid for holding an international symposium "Stochastic and Statistical Methods in Weather Forecasting" during the period 8-12 September 1980 in Nice. The symposium is being organized by the WMO with the support of the French Meteorological Institute and the American Meteorological Society. The purpose of the symposium is to bring together meteorologists, statisticians and other specialists engaged in the development and application of stochastic and statistical methods in the prediction of weather in order to examine and discuss the latest scientific and practical attainments in this field of meteorology.

The attention of participants in the symposium will be directed to the use of stochastic and statistical methods in the prediction of large-scale processes and weather phenomena for all time scales. In addition, one or two sessions will be devoted to the possibilities of the stochastic and statistical prediction of small-scale (that is, local) weather.

At the symposium there will be presentation of solicited reports by leading researchers in these fields and voluntarily submitted reports on the themes of the symposium.

The following themes are highly encouraged for inclusion in the volunteered reports:
-- Stochastic and statistical predictions of large-scale meteorological processes;
-- Development of the techniques of stochastic and statistical forecasting;
-- Stochastic-dynamic forecasts;
-- Use of stochastic and statistical methods for study of increase in errors in dynamic models;
-- Stochastic and statistical methods for long-range weather forecasting;
-- Statistical modification of large-scale dynamic forecasts.

The Organizing Committee for the symposium began its work with the following members: Doctor A. Murphy (United States) -- Chairman, Doctor L. Bengston (European Center for Medium-Range Forecasts), Doctor R. Boykov (WMO), Doctor

G. V. Gruza (USSR), Doctor G. Lepas (France), Doctor R. Miller (United States), Doctor D. Russo (France).

In the Soviet Union there have been three all-union symposia on the use of statistical methods in meteorology at Leningrad at the Main Geophysical Observatory and at Obninsk at the All-Union Scientific Research Institute of Hydrometeorological Information - World Data Center.

The impending international WMO symposium will make it possible to generalize the results of use of stochastic and statistical methods in meteorology primarily for solution of problems in weather forecasting.

G. V. Gruza

NOTES FROM ABROAD

Moscow METEOROLOGIYA I GIDROLOGIYA in Russian No 12, Dec 79 p 119

[Article by B. I. Silkin]

[Text] As reported in SCIENCE NEWS, Vol 114, No 25, p 425, 1978, E. J. Weinheimer, a scientific specialist at Rice University (Houston, Texas), speaking at a conference of the American Geophysical Union, held in December 1978 at San Francisco, reported on investigations of atmospheric electricity undertaken using a system of instruments called "BEEPS" (a system for obtaining profiles of the electric environment using balloons).

A peculiarity of this system is that the instruments included in it are not, as usual, suspended to the balloon, but are placed within it. In addition, the surface of the balloon itself, covered by aluminum (its diameter is 4 m), in essence is itself a part of the instrument; the static electricity excited by the plastic envelope of other balloons in many cases distorts the instrument readings.

The balloons are intended for ascent to 14 km. Their instrumentation measures the intensity and direction of the electric field in the atmosphere, its conductivity and the electric currents directed from the atmosphere to the earth.

The first two launchings of such balloons coincided with the moment of intersection of the boundary of a sector of the sun's magnetic field, that is, with the time of a change in its polarity. An analysis of these data enabled the speaker to establish that conductivity is the atmospheric characteristic most dependent on change in polarity of the sun's magnetic field.

Positive ion conductivity (the capacity of positive ions to create conductivity) is evidently higher during the period before a change in polarity of the earth's magnetic field than after it.

Further experiments of specialists at Rice University are directed to tracing, by means of the "BEEPS" system, all such atmospheric characteristics in the course of a full rotation of the sun about its axis, that is, in the course of 27 terrestrial days.

OBITUARY OF VYACHESLAV VYACHESLAVOVICH BYKOV (1921-1979)

Moscow METEOROLOGIYA I GIDROLOGIYA in Russian No 12, Dec 79 pp 119-120

[Article by a group of comrades]

[Text] Candidate of Physical and Mathematical Sciences Vyacheslav Vyacheslavovich Bykov, a leading specialist in the field of numerical forecasting methods and dynamic meteorology, died prematurely on 23 August 1979.

V. V. Bykov belongs to that generation of Soviet meteorologists the beginning of whose work in their selected field fell during the years of the Great Fatherland War.

In 1941 V. V. Bykov, a student in the fourth year in the Physics and Mathematics Faculty of the Moscow Pedagogic Institute, was sent to continue his training at the Higher Military Hydrometeorological Institute of the Red Army. After successful graduation from the institute in 1944, V. V. Bykov participated in the meteorological support of combat and transport aviation.

Beginning in 1947 V. V. Bykov worked at the Central Institute of Forecasts, first in the Synoptic Research Section, and then from 1951 -- in the Dynamic Meteorology Section, at that time headed by USSR Academy of Sciences Corresponding Member I. A. Kibel'. It was his work in this section that established V. V. Bykov as a scientist. His knowledge of mathematics and meteorology, as well as his great experience as a weatherman, enabled him to be included quickly in the active research and operational work in the field of dynamic meteorology and numerical forecasting methods.

During the 1950's he carried out a series of studies concerning allowance for the influence of orography in hydrodynamic forecasting models. These studies of his, like all which followed, were characterized by unusual thoroughness and great care in working through the problem to be solved. On the basis of this cycle of studies Vyacheslav Vyacheslavovich prepared and in 1955 successfully defended his dissertation for award of the academic degree of Candidate of Physical and Mathematical Sciences.

In the years which followed he worked successfully in creating and refining different elements of prognostic models. He proposed and investigated some approaches to the development of methods for determining wind fields from the geopotential field applicable to their use in prognostic models. He proposed a multilevel model for predicting meteorological fields on the basis of solution of "full" equations characterized by the inclusion of some principles from synoptic forecasting practice. V. V. Bykov has devoted much attention to developing an objective analysis method. The analytical scheme which he created (in collaboration with G. P. Kurbatkin) accelerated the practical introduction of the first Soviet prognostic models on the basis of solution of "full" equations. V. V. Bykov successfully applied his synoptic experience in constructing and further developing this scheme.

In 1965, in connection with the holding of a regional academic seminar of the WMO at the USSR Hydrometeorological Center, which was devoted to numerical forecasting, V. V. Bykov did much scientific-organizational work for ensuring the uncompromising implementation of the extensive seminar program. He presented a series of lectures in which he successfully propagandized the attainments of the Soviet school of dynamic meteorology, and in particular, the experience in formulating and using the first operational forecasting models on the basis of solution of "full" equations in hydrodynamics.

Since 1970 V. V. Bykov has headed the Section on Hydrodynamic Short-Range Forecasts and Mesometeorology at the USSR Hydrometeorological Center, created earlier by I. A. Kibel', where at that time a number of prognostic schemes were developed, improved and introduced into practice.

V. V. Bykov over a period of years has participated in the activity of the WMO Working Group on the Global System for Data Processing, where our science and practice have been successfully represented.

The many-sided and productive activity of V. V. Bykov has been recognized by the entry of his name into the Book of Honor of the USSR Hydrometeorological Center and his receipt of the title "Distinguished Worker of the USSR Hydrometeorological Service."

V. V. Bykov has been a member of the CPSU since 1965. He has invariably combined scientific-productive and organizational activity with public work. Over a period of years he was a propagandist and was elected to the Party Bureau of the USSR Hydrometeorological Center.

A severe illness suddenly interrupted the productive scientific and scientific-organizational work of Vyacheslav Vyacheslavovich. The 47 studies which he wrote remain as a heritage for researchers and practical workers and the bright memory of him as a work-loving, highly erudite, self-demanding and dedicated specialist and leader, responsive and good person will remain in the hearts of all who have had the opportunity to know and work with him.

5303 -END-
CSO: 1864